Adaptive Assistance method of Gait Training Robot for Improving Ability of Toe Control

人のつま先制御能力を向上させる歩行訓練ロボットの適応的な介入手法の提案

February 2020

Tamon MIYAKE

三宅　太文

Adaptive Assistance method of Gait Training Robot for Improving Ability of Toe Control

人のつま先制御能力を向上させる歩行訓練ロボットの適応的な介入手法の提案

February 2020

Waseda University

Graduate School of Creative Science and Engineering,

Departent of Modern Mechanical Engineering,

Research on Bio-Mechanical System

Tamon MIYAKE

三宅　太文

Abstract

Walking is important for promoting active aging, which contributes to the health and longevity of societies. Frequent walking in daily life helps keep physical functions and reduces lifestyle-related diseases. However, the risk of falling during walking inhibits walking in daily life. In particular, tripping, or unintentional contact of the toe against ground or obstacles, is one of the main causes of falling. Prevent tripping promotes walking as a daily safe activity. Therefore, it is important to develop equipment that can reduce tripping risk during walking.

Robotic technology has the potential to encourage humans to walk with a low risk of tripping. Gait assistance robots aim to assist with the walking motion in older people during their outdoor activities. The gait assistance robots are designed to be used in daily life and assist the gait motion by directly moving the lower limbs. In contrast, gait training robots aim to maintain or improve the ability of people to walk by themselves. People can rely on robotic assistance and reduce their own exertion when the robot moves human legs. Gait training is required for promoting the improvement of gait, which declines with age and maximizing the user ability in their daily lives.

Robot-aided gait training has been researched for improving motor control ability without depending on daily robotic assistance. Adaptive control is important in gait training robots as they are required to encourage people to walk actively. Specifically, an approach of the assistance as needed has been researched. Control of the interaction force between a robot and a human allows the user to walk in a different manner from the desired predetermined trajectory using force-field control. As the trajectory-based control is mainly targeted at severely affected patients, multiple degrees of freedom are used to recover motor function for joint-angular trajectory generation. Another adaptive approach of assistive technology is torque optimization by using a cable-driven robot based on the estimation of metabolic cost for improving human's energy efficiency while walking. The cable-driven mechanism is mainly used for people who can walk by themselves. The conventional algorithms are adaptive to human ability and involve the evaluation of the human state after human action. Conversely, no conventional gait training robots can adjust control parameters based on tripping avoidance ability.

Tripping occurs if the toe approaches the ground at an arbitrary point among gait cycles. Minimum toe clearance (MTC) in the mid-swing phase is a clinical parameter to avoid tripping. The human sensory-motor system controls the MTC to avoid its reduction. Toe height is controlled corresponding to the environment with conscious function. However, there is a possibility that people are not aware of small steps, such as those over a carpet or a rug, thus

causing tripping. Modification of the control ability to avoid MTC reduction is necessary for reducing the tripping risk.

The objective of this study is to present a control system for gait training robots with intermittent force application based on the prediction of MTC to improve human toe control ability during walking. To avoid the MTC reduction and, thus, to encourage people to walk, the MTC needs to be previously predicted and, when the value is lower, modified. It is necessary to apply a force to the human body to modify the MTC only in case of reduction. Therefore, a system to switch the assistance-mode and non-assistance-mode was necessary. Moreover, the author assumed that the kinematic information of lower limb joints in the same phase among gait cycles was related to future toe clearance. Therefore, the techniques for the detection of phase and pattern classification were proposed and combined as the prediction algorithm. Moreover, the gait phase detection technique is needed for robotic control. Prediction should be performed sufficiently early to assist the swing motion.

Chapter 1 introduces the background of the thesis in terms of aged-society and the importance of walking for establishing society's health and longevity. Moreover, the author describes the purpose and originality of this study after summarizing the state-of-the-art robotic technologies that encourage people to walk and neurophysiological mechanisms of human locomotion.

Chapter 2 introduces a hardware system of the robot with a cable-driven system that increases toe height. To establish the force application method, it is necessary to clarify the relationship between the timing of the applied force and the change in toe trajectory during walking. The author designed the system to apply the force to a part of the shank and the force direction was longitudinal along the shank toward the knee. The robot controls the motor rotation and transmits the cable tensile force to the lower leg. This actuator system was designed to ensure safety: the motor does not pull the cable when it is not activated and almost all the pulleys are located far away from the body so that the cable tensile force is transmitted only to a frame which people wore. The cable tensile force was measured by the loadcell attached between the frame and the cable-spring component. First, the effect of force application timings on the joints and the toe was investigated in younger people. Four-time points of force application were considered based on knee flexion motion, i.e., condition 1, time when the knee joint started flexing in pre-swing phase; condition 2, time when the toe was lifted by knee flexion motion; condition 3: time when the knee joint was flexing after toe-off; and condition 4: time when knee joint was about to finish flexing. The increase in the maximum knee flexion angle caused the increase of the maximum toe clearance in the swing phase. Changes in the ratio of the hip angle to the knee angle after maximum toe clearance can be considered as the cause of increased minimum toe clearance. The force application in the later swing phase might inhibit older people from extending the knee and contacting the ground. Next, the effect of force application at toe-off was investigated in older

people. MTC could be increased by the force application around toe-off even in older people. Consequently, the author concludes that the force application around toe-off was effective as assistance to increase MTC.

Chapter 3 introduces the proposed novel gait event detection algorithm. For precise timing control of force application and prediction of MTC, a more precise algorithm for gait event detection than the method mentioned in chapter 2 was needed. The author proposed the algorithm using the plantar structure between lower limb joint angles that are different among phases. In chapter 2, the timing of force application to increase the MTC was toe-off or later. Therefore, the author aimed at ensuring the algorithm to detect the toe-off phase. First, the algorithm derives the four planes, which are related to swing motion, motion for preparing foot–ground contact, loading response motion, and support the motion for the body, in the angular space of hip, knee, and ankle joints without supervised learning. Next, the switching points of the planes related to toe-off were detected by calculating the measured angular coordinates and the planes. The results of the experiment involving seven subjects show the change in the planes reflected the change in gait phases. The error was less than 0.035 s when the gait events were detected after calculating planes using the first gait datum. Moreover, although the data were analyzed offline, the results show that the heel contact and toe-off could be detected as soon as the angles were sensed once the planes were derived.

Chapter 4 introduces a novel toe clearance prediction algorithm with a radial basis function network using the angles, angular velocities, and angular accelerations of the hip, knee, and ankle joints in the sagittal plane. The calculation timing of the proposed algorithm was the start of the swing phase, and the MTC predicted appeared in the same swing phase. The input data could be extracted with the algorithm based on the method established in Chapter 3. The author performed experiments where six subjects walked on a treadmill for 360 s. For each subject, gait data with 20-200 gait cycles were used for training the radial basis function and 100 gait cycles data were used for evaluation in each person. The root mean square error between the measured MTC and the predicted MTC was 2.34 mm. Moreover, the error was 2.88 mm when the walking velocity was changed. The errors of the MTC are smaller compared with those of previous methods. The probability of detecting a value lower than the median toe clearance was higher than 68%, that is, the probability was higher than the probability of random detection. Although the accuracy can still be improved, the author concludes that this algorithm is able to influence the distribution of minimum toe clearance because the error was smaller than the original standard deviation of minimum toe clearance.

Chapter 5 introduces the evaluation of the system that intermittently applies force based on the MTC prediction algorithm to encourage people to walk by avoiding MTC reduction. The algorithms of Chapters 3 and 4 were implemented on the hardware system of Chapter 2. Eight

participants were asked to walk on a treadmill, and we tested the effect of the system on the participant's MTC distribution. First, the radial basis function network was trained with approximately 200 gait cycle data in each person. Next, the data of MTC before, during, and after the assistance phase were analyzed for 120 s. The force-application and non-force-application modes were switched based on the prediction result. The results showed that the minimum and first quartile values of MTC could be increased during and after the assistance phase. If the participants were fully moved by the robot, the after-effect did not alter the guided motion. Therefore, the author assumes that the proposed intermittent force application based on prediction involved modification by encouraging the participants to try to avoid MTC reduction consciously through proprioceptive stimulation.

Chapter 6 describes the conclusion and limitations of the study as well as proposes the research scope. In future studies, the long-term investigation of gait training effects with the proposed system would be beneficial. The author assumes that the automatic calibration method of angular sensors would be required for long-term use in the case where the sensors shift.

The contribution of this study is the establishment of an intermittent force application method in gait training robots based on the prediction of MTC and the modification of the MTC distribution. The proposed system allows people to freely move and can be combined with various training systems for reproducing environments such as obstacles. Moreover, the proposed prediction-based assistance method can be used in other training systems to improve the precision of the motion and device control ability.

Table of contents

Symbol tables

F	Force
τ	Torque
θ	Joint angle
L	Length of a segment of body
V	Voltage
Φ	Polar angle
$\boldsymbol{S, U}$	Switching coordinates of phases in angular space
K	Proportional gain
$\boldsymbol{P}$	Coordinates in angular space
$\boldsymbol{Q}$	Projected coordinates to plane
$\boldsymbol{R}$	Coordinates on the plane
$\boldsymbol{w}$	An eigenvector constituting a plane in angular space
α	Coefficients of the eigenvectors
$\boldsymbol{O}$	Orthogonal vector of the normal vector of a section plane in angular space
a, b, c	Parameters of $\boldsymbol{O}$
$\boldsymbol{W}$	Weight vector of the radial basis function network
$\boldsymbol{x}$	Input vector of the radial basis function network
$\boldsymbol{y}$	Output vector of the radial basis function network
$\boldsymbol{c}$	Centroid vector of the radial basis function network
$\boldsymbol{N}$	Number of the radial basis function units
σ	Standard deviation of the Gaussian function
$\boldsymbol{m}$	Data dimension of the radial basis function network
γ	A variable coefficient of the radial basis function network
$\boldsymbol{d_{max}}$	The maximum distance amongst the data
$\boldsymbol{T_d}$	Time constant
ΔT	Sampling time

List of tables

Chapter 1

Chapter 2

Chapter 3

List of figures

Chapter 1

Chapter 2

Chapter 3

Chapter 4

Chapter 5

Chapter 5

Chapter 1 Introduction

1.1 Importance of health and longevity in a society

1.1.1 Aging society

Japan is a super-aged society in which people aged 65-year-old or more corresponds to over 25% of the total population [1.1]. This number is expected to increase to 38.4% by 2065. Figure 1.1 shows the transition of Japanese population from 1950 to 2018, and the forecasted transition from 2018 to 2065. The ratio of caregivers to care recipients is decreasing. Furthermore, increase in aging population causes increase in social security and medical expenses [1.2].

Healthcare activity draws increasing attention regarding economic efficiency. The global market size of the healthcare industry is growing [1.3]. Currently, companies focus on health and productivity management to enhance the well-being of employees and improve the quality of work [1.4]. One-dollar investment leads to an investment return of approximately three dollars [1.5]. The Japanese government selected Japanese companies that engaged in an effort to promote health and productivity management and provided them with a health and productivity stock selection [1.4]. Additionally, the total amount of medical expenses can be reduced by promoting the healthcare activity, as approximately 30% of the expenses (the total is approximately 40 trillion yen) is related to lifestyle diseases [1.6].

Despite the promoted healthcare activity, the rate of unhealthy duration still does not decrease (keeps approximately 10%), while the average life expectancy has been increasing [1.7]. Therefore, reduction in the rate of unhealthy duration is the necessary challenge. In this respect, active aging is proposed to solve the social problems of the aging society.

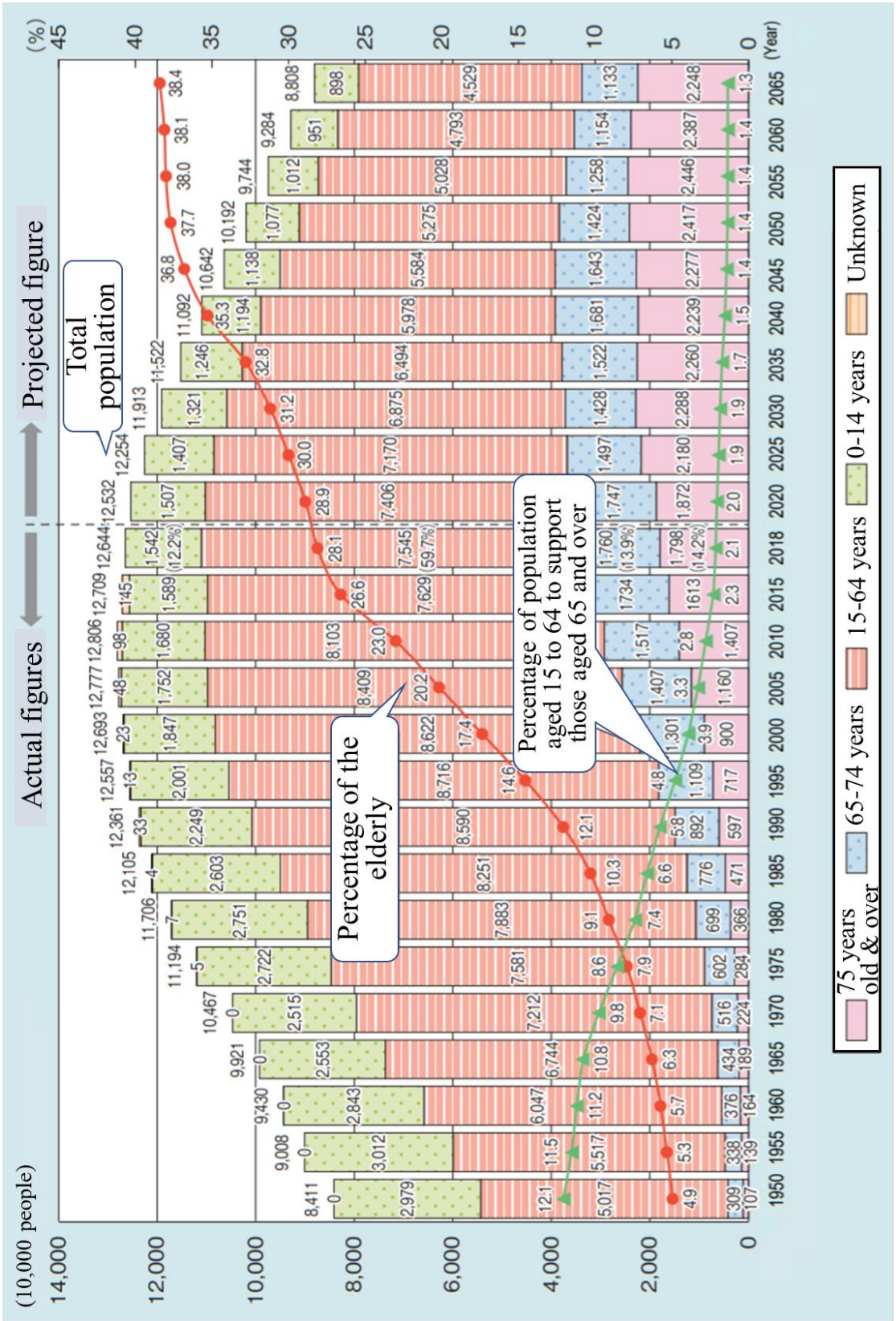

Fig. 1.1 Demographics of Japan [1.1].

According to the World Health Organization, active aging means the maximization of opportunities for maintaining health and participation in society to improve the quality of life (QOL) [1.8]. Generally, as we become older, there is a decline in motor ability and physiological functions [1.9]. Finally, care is required when the physical ability declines. To achieve active aging, it is important to implement initiatives that enable older people to live independently. In particular, walking is important for longevity because it is effective in maintaining health and avoiding health-related problems for older people.

1.1.2 Disuse syndrome

Disuse syndrome is one of the factors that inhibit active aging [1.10]. It refers to the decline in mind-body functions due to the decrease in the amount of activity in daily life. Specific symptoms of this syndrome are muscle and bone atrophy, reduced cardiopulmonary and digestive function, and decreased mental and cognitive functions. Older people fall into a vicious circle that causes the disuse syndrome because the decline in mind-body function with age causes a decrease in activity. The process of the vicious circle is explained by the life function that hierarchically evaluates the life represented by the International Classification of Functioning, Disability and Health (ICF) (Fig. 1.2) [1.11]. The vicious cycle of the syndrome constitutes (1) social participation, (2) life activity, and (3) mind-body function across all three levels. The decline in the mind-body function restricts daily activities, reduces the will and opportunity to participate in society, and reduces the frequency of activities in daily life, such as shopping and exercise, which results in “inactivation of life”. Moreover, further decline in mind and body function is induced.

If the older people fall into the vicious circle of disuse syndrome, they will eventually be forced to stay bedridden. If one spends an entire day in bed in a state of absolute rest, the muscles of the entire body atrophy by 3% [1.12]. Resting due to illness also promotes the inactivation of life. Therefore, it is important to increase the activity opportunities of the older and prevent the disuse syndrome. The performance of aerobic exercises on a daily basis is effective for the prevention of the disuse syndrome. Walking is the most

frequent aerobic exercise performed in daily life. Therefore, efforts to encourage the older to walk are important for them to maintain an independent life and prevent disuse syndrome.

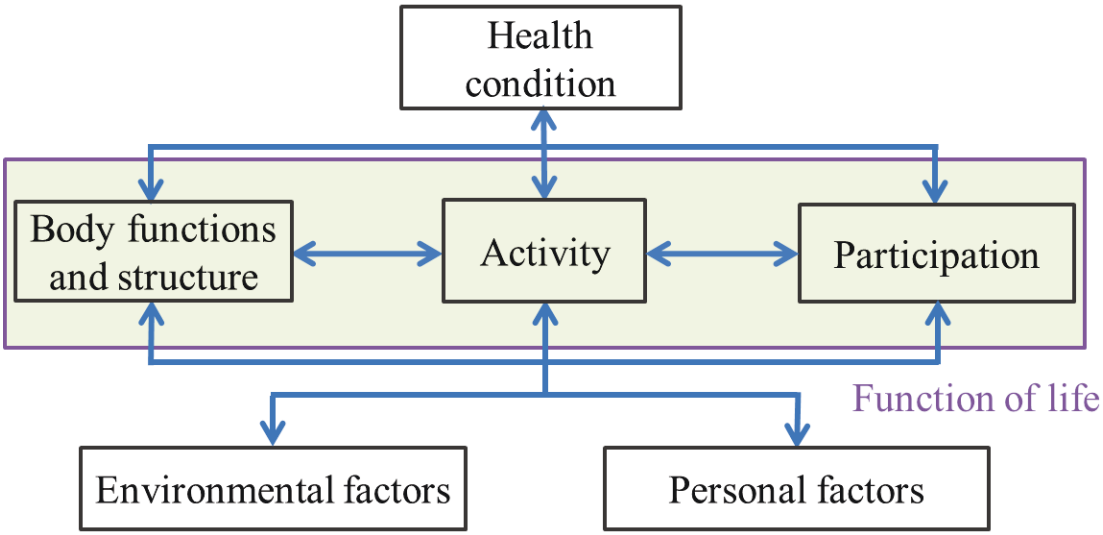

Fig. 1.2 The model of ICF [1.11].

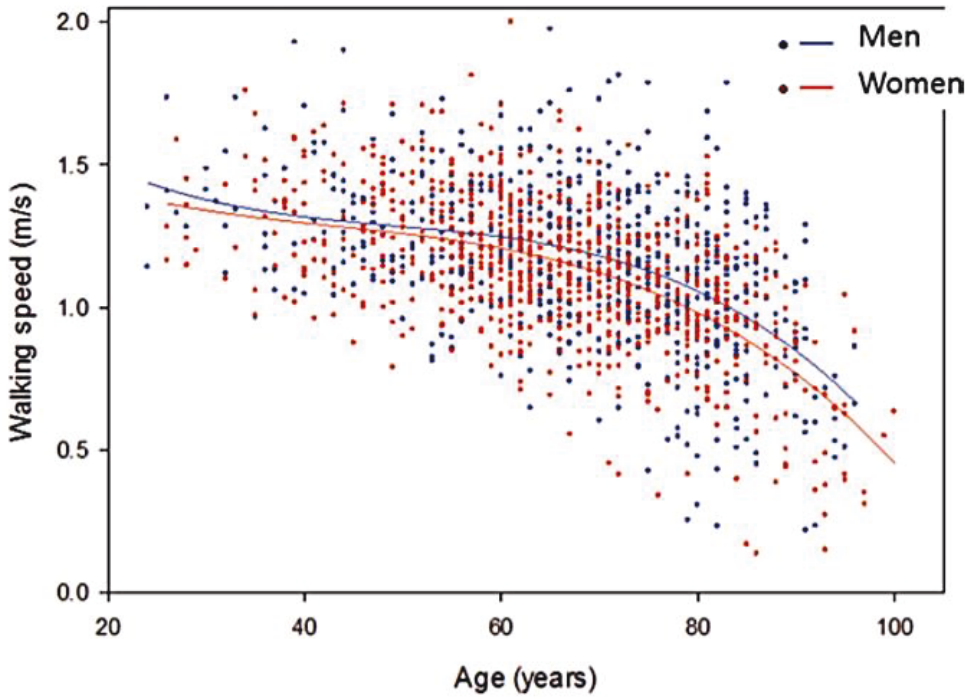

Fig. 1.3 Relationship between age and walking speed [1.13].

The frequency of hospitalization after orthopedic surgery dramatically increases for people who are older than 50 years [1.14]. As shown in Fig. 1.3, decline in gait velocity tends to accelerate from 60–70 years [1.13]. Although the starting time of decline differs in individuals, it was reported that this decline starts in early adulthood and accelerates in or just after the end of middle age. Prevention treatment is beneficial even when people are middle aged, before being certified as Needed Support/Long-Term Care.

1.1.3 Problems while walking

In older people, the risk of falling during walking increases due to the deterioration of the mind and body functions with age. Falling is a serious problem for the older people, as approximately 80% of the causes of accidents in older people are due to falling, and approximately 20% of the older people fall annually [1.15]. Therefore, older people are more likely to stay home and walk less frequently due to the thought that they can live in relief at home, where they feel peace of mind, rather than going out with the risk of falling [1.16]. To encourage older people with impaired mental and physical functions to walk by themselves, it is necessary to reduce the risk of falling during walking.

Falling is caused by an unexpected loss of balance due to tripping and slipping. Tripping, which is usually caused by unintentional contact of the swinging foot against an obstacle (e.g., carpet) is the main cause of falling [1.17, 1.18]. Therefore, it is necessary to prevent falling due to tripping. To promote active aging, it is important to develop equipment to support and train older people to walk with less risk of tripping. In the next section, the gait mechanism is explained to clarify how to control the motion to avoid tripping.

1.2 Gait mechanism

1.2.1 Gait phase

Walking is a cyclical movement that moves the body forward by repeating a series of

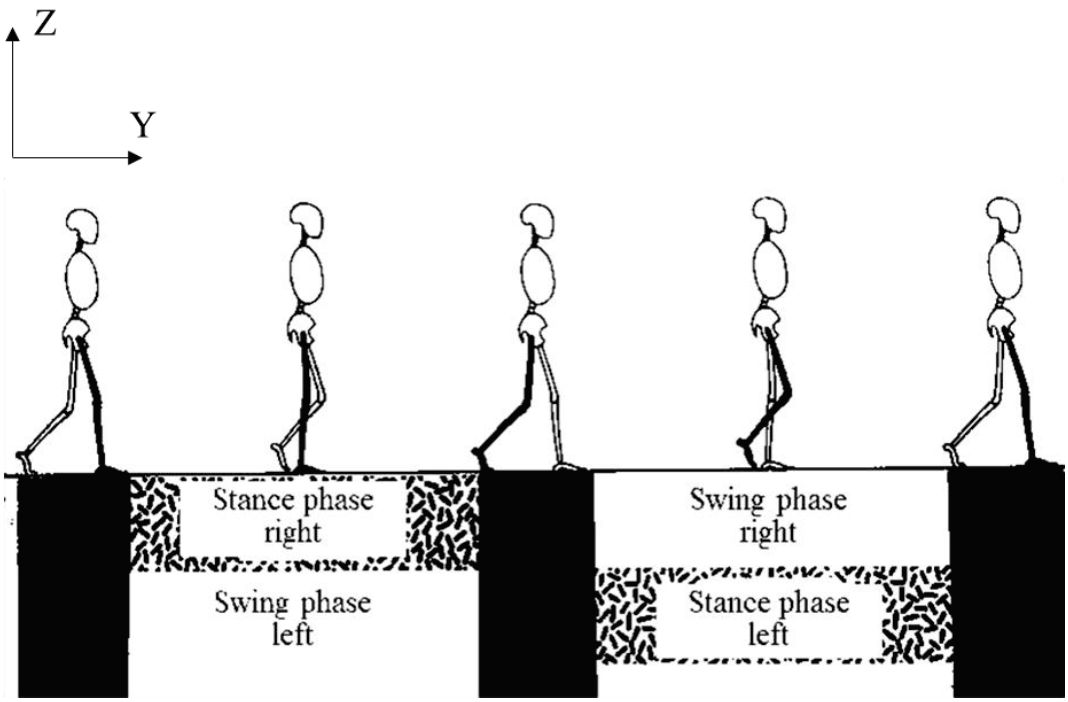

Fig. 1.4 Gait cycle (in planar plane) [1.19].

movements of the lower legs, supporting the body and swinging forward while maintaining a stable posture [1.19]. The cycle of a series of movements of the lower limbs during walking is called gait cycle. The gait cycle is divided into a stance phase, in which the lower legs are in contact with the ground, and a swing phase, in which the lower legs are separated from the ground (Fig. 1.4). The gait cycle is further functionally divided into eight gait phases, and the task required to walk in each phase is achieved as follows [1.19]. First, shock absorption and forward movement of the body are achieved in the initial contact and loading response phase. Next, single leg support is performed from the middle stance phase to terminal stance phase. After supporting both legs in the pre-swing phase, the swinging leg moves forward through initial, middle, and terminal swing phases. By advancing while controlling the position of the center of gravity in each walking phase, the stability of walking is enhanced. The position of the center of gravity while walking is controlled within the support base [1.20]. The support base means the area of the foot the case of one-foot contact, and the area of the feet and between them in the case of two contacts.

1.2.2 Neuro-system for locomotion

There are conscious and unconscious movements, and walking has both characteristics. In the central nervous system, upper centers located at the upper level, such as basal ganglia, have the function of consciously generating motion, and lower centers located in lower levels, such as brainstem and spinal cord, have the function of unconsciously moving (Fig. 1.5) [1.21-1.23]. Once humans start walking, they can continue walking without being conscious of the rhythmic movement of lower extremity muscles. Automated gait is realized because lower layers, such as the spinal cord among the central nervous system, considerably contribute to the gait generation [1.24]. Periodic movements of flexor and extensor muscles are performed by a central pattern generator (CPG) located in the spinal cord [1.25]. The midbrain gait evoked area, which is also in the brainstem of the lower center, determines the start and end of walking based on the commands from the upper center, and is important to issue an instruction to start the exercise [1.21]. In contrast, the upper center controls the activities of the lower centers that generate gait patterns based on senses and cognition, but does not control the walking rhythm and stride sequentially. The cerebellum acts in coordinated movements between limbs in real time based on information from the midbrain gait evoked areas and somatosensory feedback information from the limbs. The cerebellum also acts in constructing an internal model that calculates and outputs a movement command to a muscle so that it reaches the target lower-limb trajectory when feedforward control is performed on gait. The basal ganglia, which are multiple nuclei located near the center of the brain, output to the midbrain gait evoked areas and acts regulating gait expression and muscle tone. The cerebral cortex acts in planning and cognitive aspects of movement and contributes to the correction of movement by the appearance of walking and the feedback of external environmental information. As described, gait is not controlled by top-down with the upper central brain but controlled by the central nerves in each hierarchy.

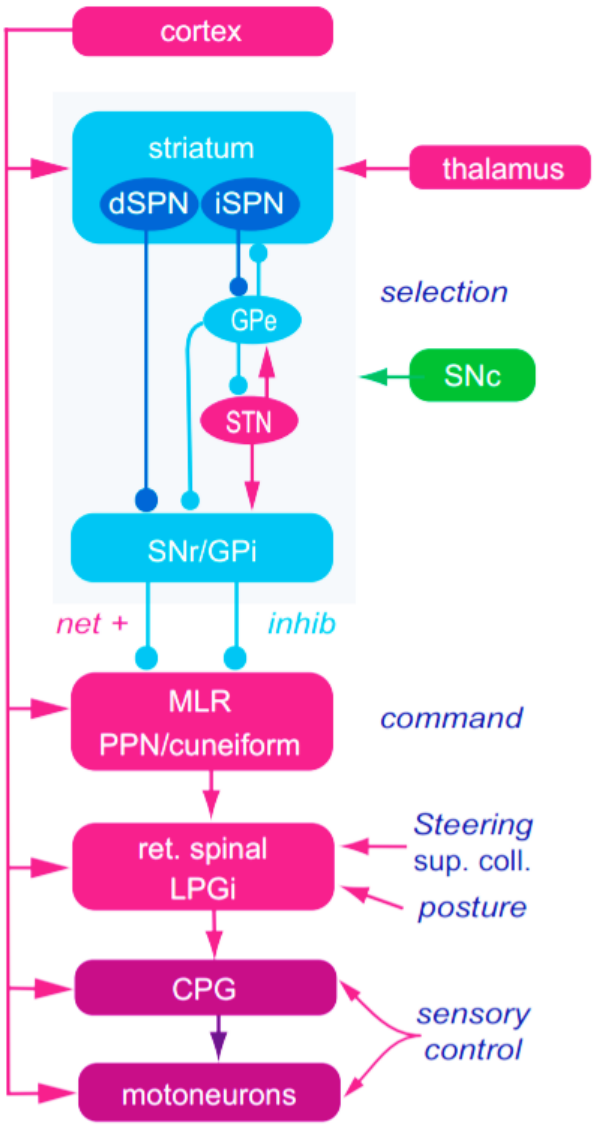

Fig. 1.5 Diagram of the different components from cortex and basal ganglia to spinal central pattern generators (CPGs) regulating basic aspects of locomotor propulsion [1.22]

The cerebellum can relearn the gait motion thorough repetitive training [1.26]. People adapt to external interference during walking as a reactive adjustment with lower level of the central nervous system. The reactive adjustment is not controlled by the cerebellum. The modified proprioceptive information of the legs is passed to the vermis of cerebellum via dorsal spinocerebellar tract [1.27]. The cerebellum restores the patterns of the movement as an internal model and modifies the ones generated by the spinal cord after

trial and error learning. There are two types of motor learning processes: explicit learning and implicit learning. The explicit learning is the learning with the cognitive feedback and working memory while the implicit learning is without cognitive process [1.28, 1.29]. For fast gait learning, the implicit learning is effective because it is processed by the cerebellum involved in predictive adjustment for gait adaptation [1.30].

1.2.3 Human control strategy for avoiding tripping

Causes of tripping can be divided into problems of cognitive and non-cognitive functions. Gait motion is controlled by changing joints kinematic pattern adapting to the environment. If there is an obstacle in front of walkers, they recognize it with visual information and raise their foot as a predictive adjustment [1.31]. People do not take the strategy of gait motion using excessive energy. As shown in Fig. 1.6, it takes excessive energy cost to lift the toe (foot scuff also takes excessive cost) [1.32]. Therefore, it is beneficial to avoid excessive lifting toe during walking in terms of energy efficiency. However, because it is difficult to perceive small steps (such as carpets or rugs) visually, it is necessary to be able to avoid tripping at small steps without recognition. In fact, the main situation of tripping is at home with carpets or rugs [1.33].

Proprioceptive information of end point is the most important for controlling the body [1.34, 1.35]. Minimum toe clearance (MTC) that is the minimum value of toe clearance at the mid-swing phase is a critical parameter related to tripping [1.17, 1.36-1.38]. Median of variability of MTC have been reported to be determined by individuals' attitudes regarding the control of toe clearance [1.39]. Specifically, a low variability of MTC suggests better neuromuscular control of toe motion [1.37. 1.40, 1.41] while a lower average MTC reflects increased both attention and cognitive workload during the performance of the task [1.39, 1.42]. The MTC variability can be reduced by improving an ability to control the MTC. Even older people do not trip every gait cycle. The possibility of tripping increases when the toe approaches the ground or hidden small steps at an arbitrary point among gait cycles. Therefore, it is necessary to control MTC and avoid lowering it during walking for tripping avoidance.

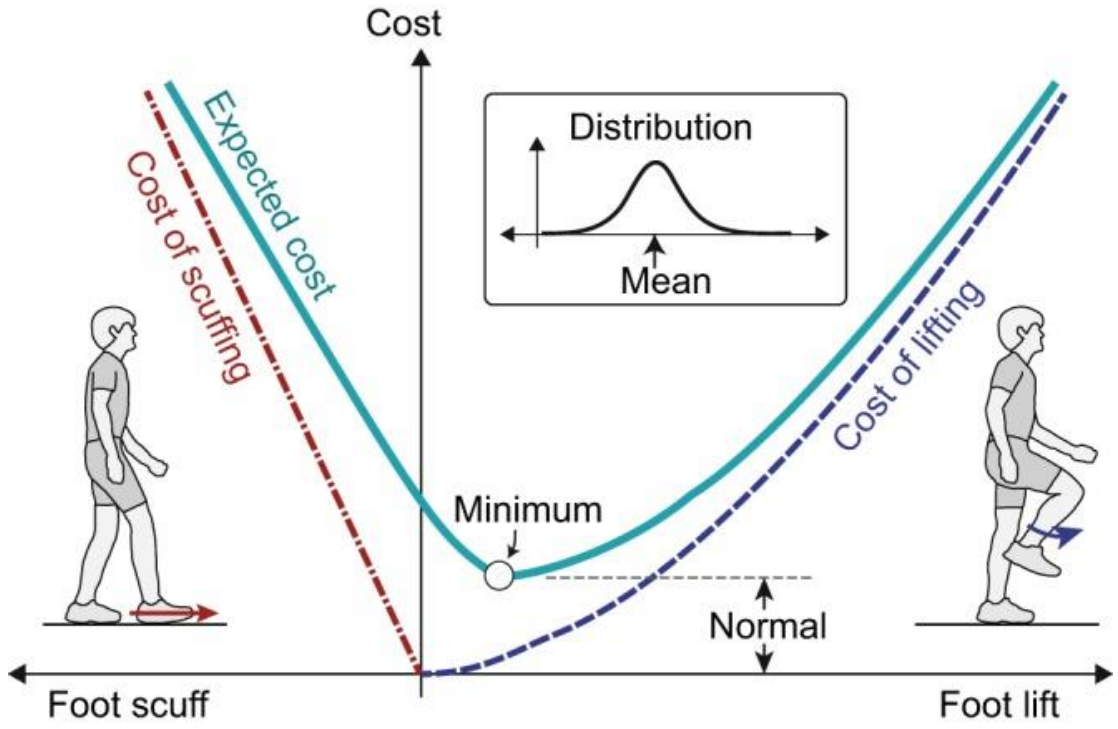

Fig. 1.6 Relationship between energy cost and foot height [1.32].

In the next section, the development situation of robots that are not limited to fall prevention, in terms of promoting walking, and the issues involved in fall prevention are explained.

1.3 Role of robotics for encouraging people to walk

Many devices have been researched and developed for improving QOL. In particular, many walking assistance and gait training devices have been developed in order to realize independent walking for the older. Robotic technology is used to deal with the diversity of the surrounding environment when walking and individual differences in the psychosomatic function level of the older. In the following sections, the gait assistance and the gait training robots as well as the significance of the gait training robot for the older people and its current approach are explained.

1.3.1 Importance of gait training robots

The strategy of encouraging older people to walk independently with a robotic technology can be separated into two methods: a gait assistance robot and a gait training robot. The gait assistance robot aims to assist the walking motion of older people when they try to go out. These robots are designed to be used in daily life and assist the gait motion by directly moving the lower limbs. The gait training robot aims to maintain or improve the ability of people to walk by themselves. The gait training promotes the improvement of mental and physical functions that decline with age, leading to maximization of the ability of the older. Perturbation-based gait training could promote motor adaptation following unexpected balance loss [1.43-1.47]. However, this method has a risk of injuring patients with a resistance force. Therefore, this study focused on the assistance-based method.

The gait assistance robot is designed so that it can be used in various situations in daily life. Rhythm walking assist developed by HONDA Robotics (Fig. 1.7) senses the hip joint angle during walking, assists the amount of leg swing by operating the motor in coordination with the movement of the hip joint, and increases the movement range of the hip joint [1.48]. The walking assistance cart (Fig. 1.8) developed by RT. Works Co., Ltd. has the functions of monitoring and sensing older people with network technology in addition to support them with a motor [1.49]. Older people can walk with less risk of falling by using a gait assistance robot. However, it does not improve physical functions that have declined because people start relying on the device. In order to prevent disuse syndrome, it is important to maximize the ability of the older people. Older people who have problems such as disability and difficulty in standing should always have a support when moving, but in older people who can walk on their own, practicing this activity is desirable.

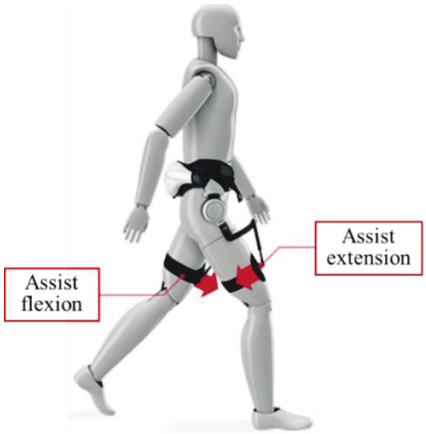

Fig. 1.7 Walking Assist [1.48].

Fig. 1.8 Walking assist cart [1.49].

1.3.2 Classification of gait training robot

Gait training robots have been designed to improve physical functions. By using robotic technology for gait training, load adjustment and leg trajectory generation can be realized in real time. The use of robotic technology is also beneficial to reduce the burden on the physical therapists and allows the user to exercise alone. Furthermore, the system was designed to improve user's motivation and efficiency of gait training by providing virtual reality and gait information. The target of gait training robots includes not only older people but also postoperative and paralyzed patients. There are differences in the type and design of the device depending on the purpose. The movement of the gait training robots can be classified into robots that do and do not generate lower limb trajectories. Each feature is listed below.

1.3.2.1 Non-assistance-based Gait Training Robot

This type of gait training robots does not directly guide the lower limb trajectory for the user but supports the user to walk autonomously. A typical example of a gait training robot for older people is the 2-belt senior trainer PW-21 (Fig. 1.9) developed by Hitachi [1.50]. The left and right belts operate independently, and the load mode can be set separately for the left and right sides. In addition, it is possible to conduct a fall prevention training by suddenly starting and stopping one of the belts as a perturbation, leading to the acquisition of a gait with enhanced fall avoidance ability. An unconstrained gait training robot (Fig. 1.10) was developed by Ritsumeikan University for fully restraining people by controlling the fall of a pedestrian. It is possible to perform gait training without any changes [1.51].

Even though these robots do not interact with a human physically, it is possible to encourage people to perform actions adapting to perturbation that causes a fall or user's internal factors, and improve gait ability. However, the motion of the lower limb cannot be guided to obtain a gait with less risk of tripping. The tripping is caused by insufficient clearance from the ground, so motion guidance is required by a training robot that generates trajectories to change the motion of the lower limbs.

1.3.2.2 Assistance-based Gait Training Robot

The robot attached to the lower limbs generates movements of the lower limb joints to improve the user's gait. In addition, by adjusting the amount of load on the lower limbs, it is possible to voluntarily encourage the lower limbs to move and improve kicking power and walking speed. The design of the gait training robot that generates the trajectory of the lower limbs can be divided into an end effector type and an exoskeleton type. As end effector type gait training robots, Gait Trainer GTI (Fig. 1.11) developed by Reha-Stim (Germany) [1.52], 4-axis redundant parallel robot (Fig. 1.12) [1.53], there is a pelvic holding robot developed by Waseda University [1.54]. Gait Trainer GTI controls the foot plate on which the foot is placed, thereby encouraging the movement of the foot in multiple gait phases [1.52]. A four-axis redundant parallel robot rehabilitates the movement of the ankle joint by moving a platform that fixes the tip of the foot with a pneumatic actuator [1.53]. In the pelvis holding robot (Fig. 1.13), the end effector holds the pelvis and simulates the pelvic handling operation performed by the physical therapist [1.54].

Fig. 1.9 PW-21 [1.50].

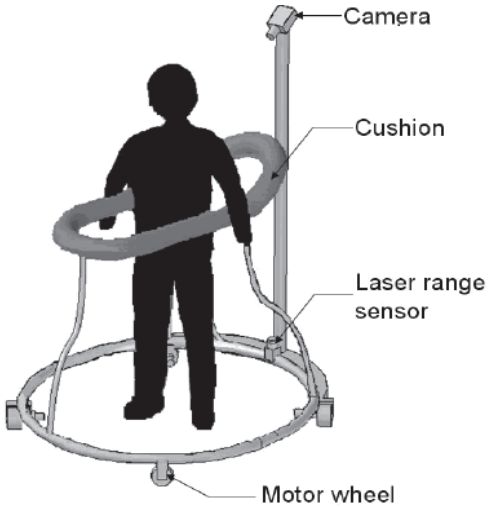

Fig. 1.10 Unrestraint support robot [1.51].

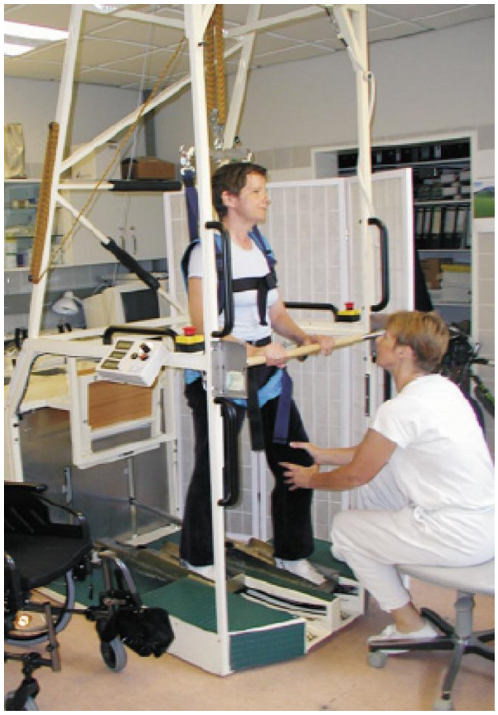

Fig. 1.11 Gait Trainer GTI [1.52].

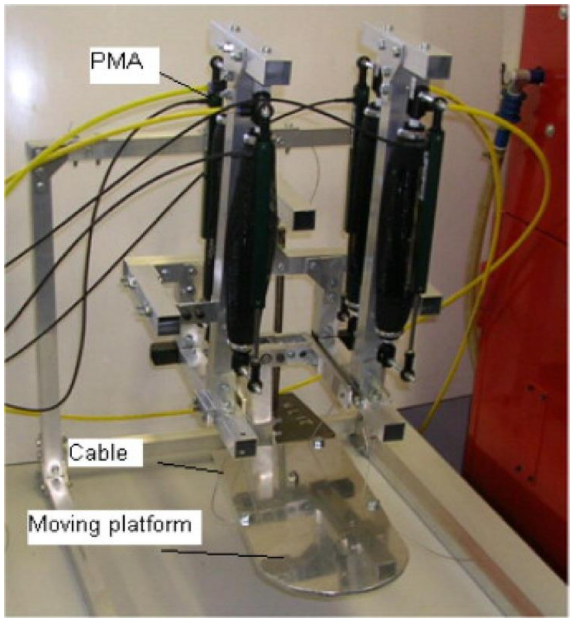

Fig. 1.12 4-axis redundant parallel robot [1.53].

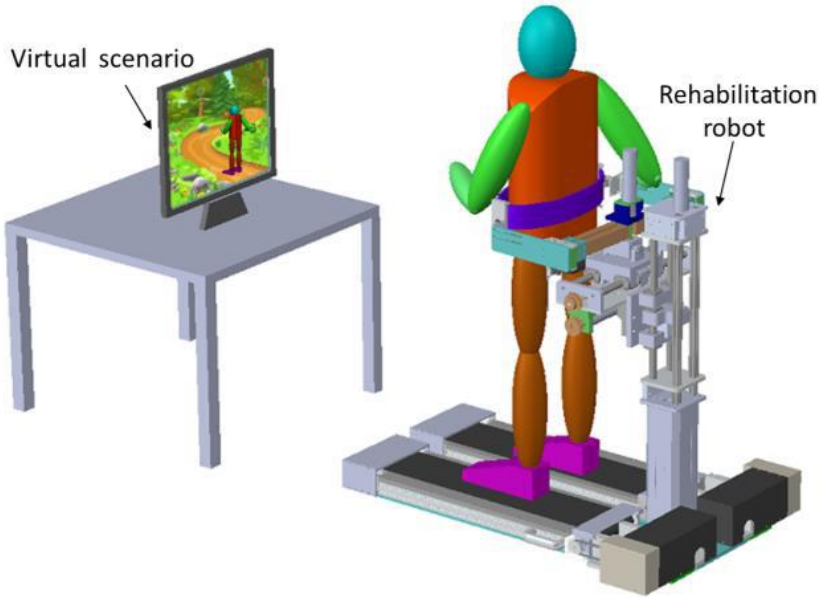

Fig. 1.13 Gait rehabilitation robot assisting pelvic motion [1.54].

Representative examples of exoskeleton-type gait training robots combined with treadmills are the Lokomat (Fig. 1.14) developed by Hokoma [1.55], ALEX developed

by the University of Delaware [1.56], and LOPES developed by the University of Twente [1.57]. Lokomat consists of a robotic device that generates a trajectory, a weight loader, and a treadmill [1.55]. The user is able to perform passive walking that automatically generates a gait with a robot brace attached to the lower limbs on a treadmill. ALEX (Fig. 1.15) has a mechanism to move the hip and knee joints with linear actuators [1.56]. LOPES (Fig. 1.16) has a mechanism with two degrees of freedom in the hip joint and one degree of freedom in the knee joint, and it uses a series elastic element to mitigate obstruction of the user and the exoskeleton [1.57]. There is a walking support robot (Fig. 1.17) developed by Yasukawa Electric as an exoskeleton robot combined with biofeedback [1.58]. The user's kicking force can be evaluated during walking by visual feedback of the plantar pressure. By presenting the target value to the user through feedback, the user can voluntarily exert a kicking force and improve the kicking motion of the ground. In addition, there is a robot suit HAL welfare (Fig. 1.18) developed by CYBERDYNE as a robot that uses biological signals [1.59]. The thigh and crus have drive, control, and sensor functions that support walking motion by measuring myoelectric and joint angles.

Fig. 1.14 Lokomat [1.55].

Fig. 1.15 ALEX [1.56].

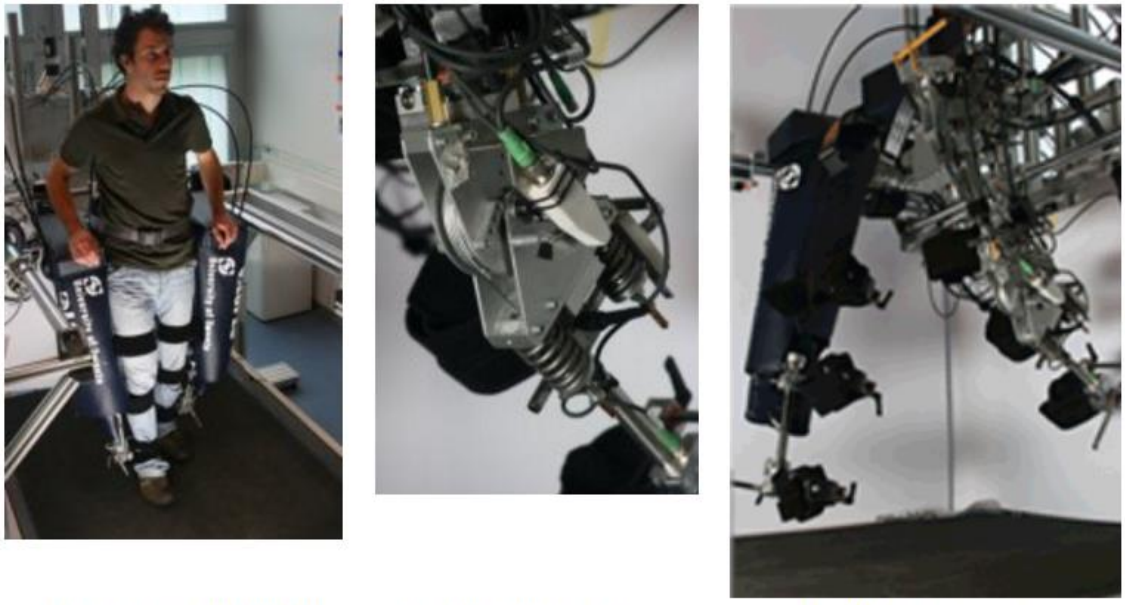

Fig. 1.16 LOPES [1.57].

Fig. 1.17 Gait assist robot [1.58].

Fig. 1.18 HAL [1.59].

LOPES II is the exoskeleton type robot applying an assistance of end-effector approach based on admittance control with the eight degrees of freedom [1.60]. Bio-inspired reflex-based control of the LOPES II resulted in reduction of metabolic cost and muscle

activation of humans (Fig. 1.19) [1.61]. Toyota Motor Corporation developed the novel gait training robot named Welwalk WW-2000, which assists the knee flexion and extension motion (Fig. 1.20) [1.62]. The RE-Gait [1.63] is an ankle motion assistive device for rehabilitation, which activates the muscles related to the knee and hip joints (Fig. 1.20). Because it is important for assistive robots not to inhibit the natural gait motion of humans, light-weight devices were developed, such as Harvard University's soft exosuit, which is assisting ankle motion (Fig. 1.21) [1.64].

Fig. 1.19 LOPES II [1.61]

Fig. 1.20 Welwalk WW-2000 [1.62]

Fig. 1.21 RE-Gait [1.63]

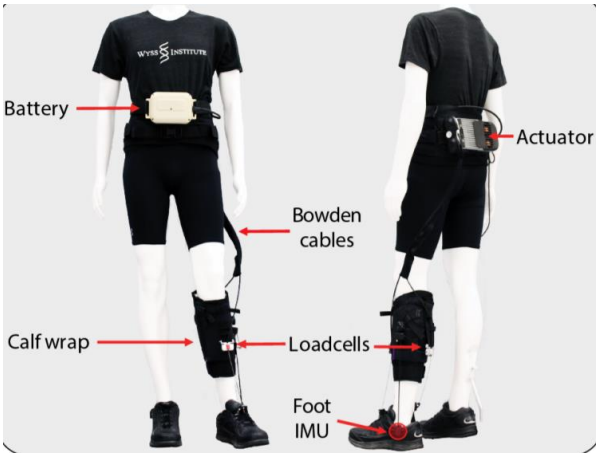

Fig. 1.22 A soft exosuit developed by Harvard University [1.64].

1.3.3 Control method

In this section, the control method of the exoskeleton type of gait training robots that generates the trajectory of the lower limbs is explained. Although there are differences in the control methods required by the patient's gait function, the final goal of using a gait training robot is to enable the user to walk independently. Therefore, research on control methods has been developed to encourage more voluntary movements during gait training. Below, the author classifies the control methods of exoskeleton type gait training robots that generate trajectories of the lower limbs in an organized framework based on [1.65].

1.3.3.1 Positional control

Positional control is a technique for controlling a gait training robot using the lower limb joint angle as a target value. The user of the robot passively walks with the lower limbs being continuously moved by the gait training robot [1.57, 1.66-1.68]. The main purpose is to provide training support for paralyzed patients in the early stages of rehabilitation. The robot ARTHuR generated a trajectory with “teach-and-replay” technique [1.66]. In LOPES, there is a method for controlling hemiplegic patients by position control that generates a trajectory that moves the lower limb of the paralyzed side from the trajectory of the lower side of the healthy side [1.57]. In trajectory generation by position control, the gait is fixed to the reference trajectory, and it is difficult to change the leg trajectory according to the ability of the user. In addition, it is difficult to encourage active walking because the user is forced to follow a fixed reference trajectory.

1.3.3.2 Electromyography (EMG) based control

EMG control is a control technique that moves the lower limb frame of the robot based on muscle activity [1.69-1.74]. The robot assists the movements based on detection of human’s intention by predicting how much the lower limbs move with myoelectric potential. HAL determines the assisting torque by estimating the torque that the wearer is

going to exert from the myoelectric potential [1.72]. If the wearer is a paralyzed patient, the pattern of the myoelectric potential cannot be measured normally; thus, the myoelectric potential is used as a trigger to generate a pre-programmed action. Daniel et al. at the University of Michigan developed a control method that drives a pneumatic actuator by performing proportional control within the upper and lower limits set in advance using myoelectric potential as feedback information [1.73]. In EMG strategy, there is still a problem in obtaining an accurate control signal due to the displacement of the position where the electrode is attached and the influence of the different target muscles.

1.3.3.3 Impedance control

Impedance control in a gait training robot adjusts the lower limb joint angle, the interaction force generated between a person and the robot, and the lower limb trajectory by controlling its impedance as a target value [1.57, 1.75-1.79]. The interaction force generated between a person and a robot is the torque that the robot applies to the human joint or the torque that occurs when the person resists the movement of the robot. The larger the interaction force, the higher the difference between the active human walking motion and the robot motion. In impedance control, as the deviation from the trajectory generated by the robot increases, the guidance force to the trajectory increases. As the degree to which the force to guide the trajectory increases can be adjusted, by using impedance control, Lokomat and LOPES allow the patient to walk with a gait that varies from the reference trajectory [1.78, 1.79]. However, since there are individual differences in the appropriate impedance value, there remains a problem in encouraging active walking.

(4) Adaptive control

Adaptive control is a control method in which the robot adapts to human movements and changes control parameters for assistance. In adaptive control, it is expected to

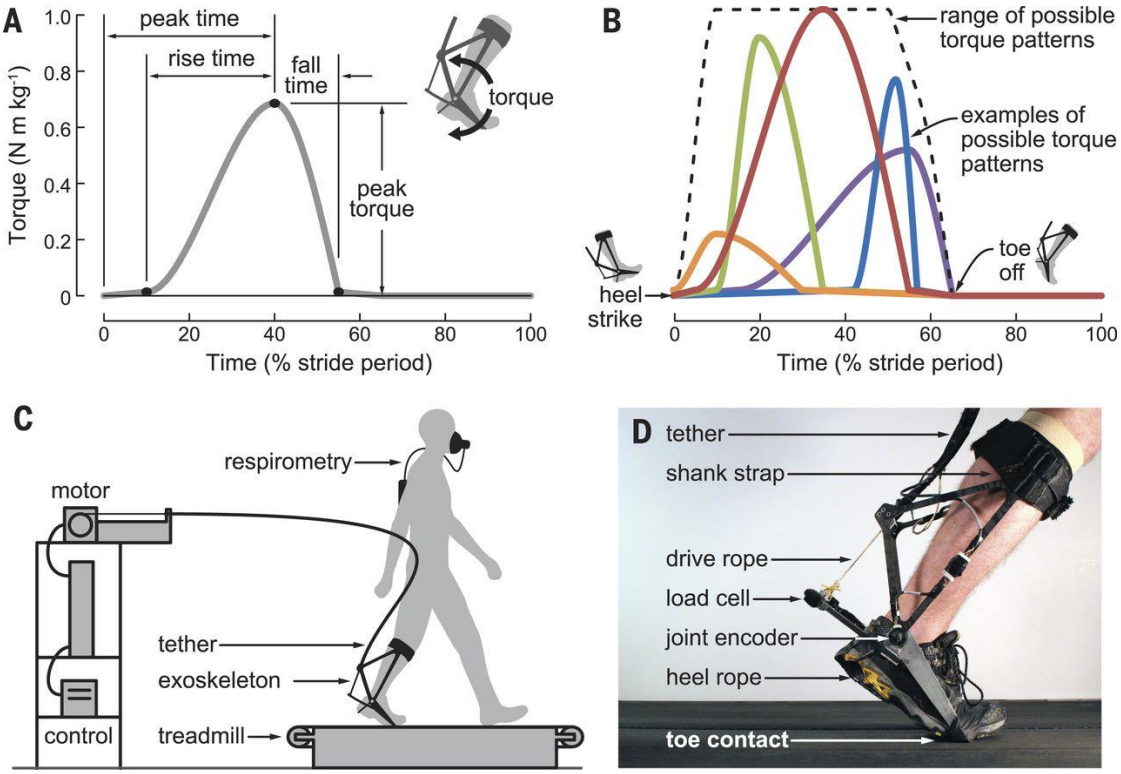

Fig. 1.23 Human-in-the-loop optimization of hip assistance with a soft exosuit [1.89].

increase the efficiency of gait training to encourage people to actively participate in training. Adaptive method is realized based on evaluation of human motion or bio signals. The parameter of impedance controller was adjusted based on EMG or interaction force between human and machine in previous researches. In order to increase patient's motivation, providing assistance only when needed is required comparing to the strategy of imposing an inflexible control [1.65]. Assistance-as-needed control strategy of the gait-training robots is being actively studied to adjust the assistance level or mechanical impedance modes based on a human ability [1.56, 1.61, 1.80-1.85]. Control of the interaction force between a robot and human allows the user to walk in a different manner from the desired predetermined trajectory using force-field control. As the trajectory-based control is mainly targeted at severely affected patients, multiple degrees of freedom are used to recover motor function for joint-angular trajectory generation. In a study [1.86], the assistance-as-needed strategy was performed by reducing the assistance force when the patient's tracking errors were small. This strategy could achieve both assistance

to help the patient complete movement tasks and optimization of compliance to allow the patients to actively move [1.65]. Duschau-Wicke et al. proposed a method in which the robot does not assist when walking within a certain error range with respect to the reference trajectory, and assists when it deviates from the error range [1.79]. Krishnan et al. also reported that walking time and other parameters related to walking ability were improved by shortening the time to guide the robot to the trajectory compared to the case without shortening [1.87].

Another adaptive approach of assistive technology is torque optimization using a cable-driven robot based on the estimation of metabolic cost for improving human's energy efficiency while walking [1.88, 1.89], as shown in Fig. 1.23. The cable-driven mechanism is suitable mainly for people who can walk by themselves. The conventional algorithms are adaptive based on human ability by evaluating the state after human action.

Conversely, assistance-based methods that decide the robotic parameters by predicting the gait motion beforehand have not yet been established. Although the bio-feedback method could increase mean MTC [1.90], it could not modify MTC distribution (increase in only lower values of MTC). The robot based on an evaluation of a human motion after human action cannot modify the motion in real-time. Prediction of MTC is important for modifying the toe motion in real-time to encourage people to walk with more precise MTC control. Therefore, an assistance-as-needed approach based on MTC prediction is necessary.

1.4 Objective of the Thesis

The objective of this thesis is presenting a control system of gait training robot with intermittent force application based on prediction of MTC in order to improve human toe control ability during walking. Our hypothesis is that robotic assistance along with the MTC prediction algorithm can modify human control to inhibit the reduction of MTC. No research has yet investigated the effect of robotic assistance using MTC prediction on the modification of MTC control. We assumed that people could modify their MTC

control through training, in which a robot detects the lower values of MTC distribution beforehand and increases it.

To encourage people to walk by avoiding MTC reduction, the MTC needs to be predicted previously and modified only when the value is lower. It is necessary to apply the force to the human for modifying the MTC only in case of reduction. Therefore, the system had to be designed to switch assistance-mode and non-assistance-mode. Moreover, the author assumed that the kinematic information of lower limb joints in the same phase between gait cycles was related to the future toe clearance. Thus, the techniques of detection of phase and pattern classification were proposed and combined as the prediction algorithm. Moreover, gait phase detection technique was needed for robotic control. Prediction should be performed sufficiently early to assist the swing motion.

A hardware that can switch between force-application and non-force-application modes, gait event detection algorithm, and MTC prediction algorithm were developed. The increase in the lower values of MTC distribution with robotic assistance using the proposed prediction algorithm was investigated. Moreover, it was evaluated whether a person can modify his/her MTC distribution even after the assistance is withdrawn. Angular information was beneficial for the physical human-robot interaction. Therefore, a system was proposed using only angles as human biological information to assist

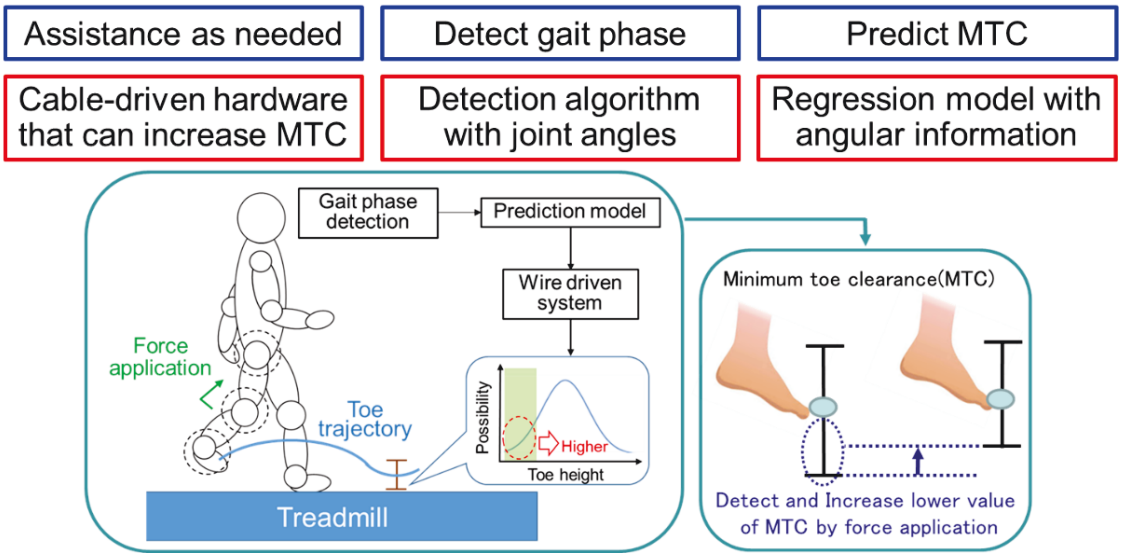

Fig. 1.24 System overview of the proposal.

Table 1.1 Comparison of adaptive gait assistive methods.

	Exoskeleton	Soft exosuit	This research
Objective	Improve ability of motor generation	Minimize human energy cost	Improve ability of toe control
Assistive method	Impedance control based on reference angular trajectory	Apply wire tensile force	Apply wire tensile force
Measured bio-signal	Angles, EMG	Indirect calorimeter	Angles
Adaptation method	Adjust interaction force to guide the reference trajectory	Evaluation of metabolic cost	Adjust an assistance timing based on toe height
Final target	Affected patients (Rehabilitation)	Able-bodied people	Able-bodied older people

humans in walking, detect gait phase, predict MTC, and evaluate the after-effect.

The novelty of this study is the establishment of an intermittent force application method of gait training robot based on prediction of MTC and modification of the MTC distribution. The proposed system can allow people to freely move and can be combined with the training system to reproduce environments such as obstacles. Moreover, the proposed prediction-based assistance method can be used for other training systems to improve the precision of the motion and improve the control ability in the future.

1.5 Structure of this thesis

This thesis consists of 6 chapters (Fig. 1.25).

- **Chapter 1**

  This chapter introduces the background of the thesis in terms of aged-society, importance of walking, and state-of-the-art of robotic technologies encouraging people to walk. Tripping is one of the main causes of falling that seriously inhibit walking especially for older people. MTC control that inhibits it from lowering is

important to avoid tripping during walking. However, there is no study for gait training robot to improve ability of MTC control. Therefore, this study aims at establishing the control strategy of assistance as needed based on MTC value. Angular information was beneficial for the physical human-robot interaction. Therefore, the author proposed the system using only angles as human biological information to assist human, detect gait phase, predict MTC, and evaluate after-effect.

- **Chapter 2**

  Hardware system using cable-driven system is explained in this chapter. The system was designed to switch force application and non-force application modes. Moreover, the system aims at increasing MTC when the force is applied. Cable-driven system was applied because the cable-tension control can achieve both the force and non-force applications. To establish the cable-driven system to assist human toe motion as needed, it was needed to analyze the effect of force application timings on the changes of the toe trajectory and the lower limb joint angles. The force was applied to a part of the shank and the force direction was longitudinal along the shank toward the knee. The author investigated the effect of force application timing on toe trajectories and the angles of the lower-limb joints in the experiments in which the force was applied to participants while they walked. The application of the force when participants lifted their toe from the ground and maintained knee flexion just after toe-off, increased the maximum toe clearance. The toe clearance in the later swing phase increased when the force was applied at toe-off or after toe-off because of a change in the ratio of the hip angle to the knee angle.

- **Chapter 3**

  Gait event detection algorithm is explained in this chapter. For precise timing control of force application and prediction of MTC, a more precise algorithm of gait event detection than the method mentioned in chapter 2 was needed. The author focused on the plantar structure between lower limb joint angles that are different among phases. The proposal is a novel algorithm for the gait event detection using the inter-joint coordination of the hip, knee, and ankle joints that have a lower-dimensional structure.

The proposed algorithm derives the four planes in the angular space and finds the switching points of the planes. The results of the experiment involving seven subjects show that the change in the planes reflected in the change in gait phases. Moreover, although the data were calculated offline, the results show that the heel contact and toe-off could be detected as soon as the angles were sensed once the planes were derived.

- **Chapter 4**

Prediction algorithm of MTC is explained in this chapter. The author proposed a novel method for predicting toe clearance that uses a radial basis function network. The input data were the angles, angular velocities, and angular accelerations of the hip, knee, and ankle joints in the sagittal plane at toe-off. Toe-off was detected by the algorithm based on the proposal in Chapter 3. In the experiments, seven subjects walked on a treadmill for 360 s. The radial basis function network was trained with gait data ranging from 20 to 200 data points and tested with 100 data points. The root mean square error between the true and predicted values was 3.28 mm for the maximum toe clearance in the earlier swing phase and 2.30 mm for the minimum toe clearance MTC in the later swing phase. Moreover, using gait data of other five subjects, the root mean square error between the true and predicted values was 4.04 mm for the maximum toe clearance and 2.88 mm for the MTC when the walking velocity changed. This provided higher prediction accuracy compared with existing methods. The proposed algorithm used the information of joint movements at the start of the swing phase and could predict both the future maximum and minimum toe clearances within the same swing phase.

- **Chapter 5**

Effect of prediction-based assistance on MTC distribution is explained in this chapter. In this thesis, the author implemented the gait event detection algorithm and the MTC prediction algorithm on the developed hardware system to encourage people to walk by avoiding lowering the MTC reduction. Eight participants were asked to walk on a treadmill, and the effect of the system on MTC was evaluated. The MTC data before,

during, and after the assistance phase were analyzed for 120 s. The results showed that the minimum and first quartile values of MTC could be increased during and after the assistance phase.

- **Chapter 6**

In this chapter, the summary and limitations of this study are explained, and research scope is proposed.

Chap. 1 Introduction

・Risk of tripping in older people

・Sate of the art: Control strategy of gait training robot

Chap. 2 Gait Assistance Method

・Decide timing of force application with Cable-driven system

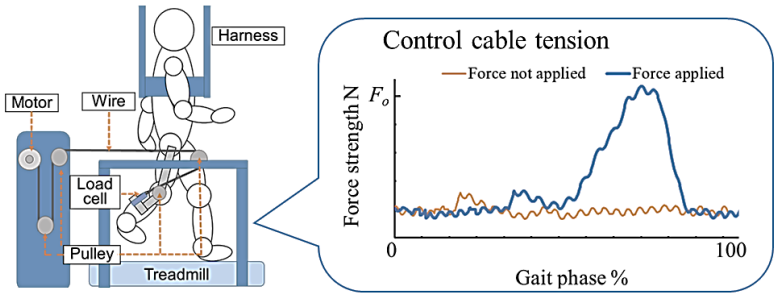

Chap. 3 Gait Event Detection Algorithm

・Establish detection algorithm using only angles

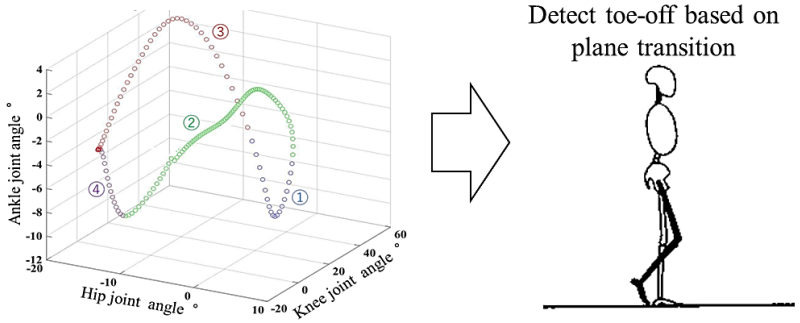

Chap. 4 Prediction Algorithm of MTC

・Establish prediction algorithm of toe clearance

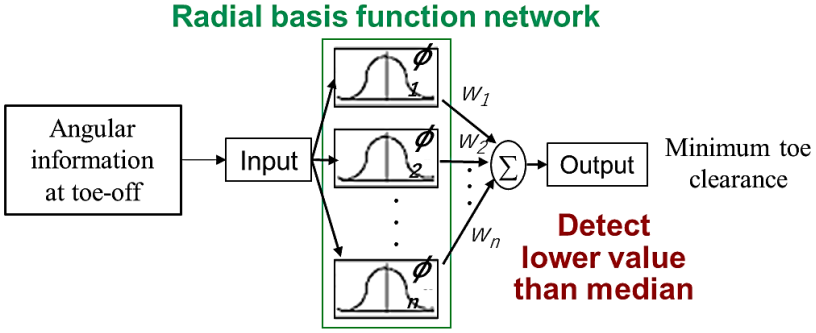

Chap. 5 Evaluation of Prediction-based assistance

・Robot control based on prediction to reduce variance

Chap. 6 Conclusion

Fig. 1.25 Structure of the thesis.

Chapter 2 Gait Assistance Method

2.1 Background

The appropriate timings of assistance and non-assistance are unclear for assisting toe swing motion. Joint motions are controlled during walking and their combination generates the toe trajectory. It is necessary to analyze the changes of the toe trajectory and the lower limb joint angles for determining the force application timing.

In this chapter, the author investigated the effect of timing of the force application on the increase of toe clearance. The toe clearance in the entire swing phase was analyzed when the force was applied in some timings. Moreover, the changes in joint angles of hip, knee, and ankle joints were analyzed because these joints generate the toe swing motion [2.1]. The author aimed at ensuring one degree of freedom of the force application to simplify the robotic system and reduce intervention.

Joint motions at the start of the swing phase are the knee joint flexion and ankle joint plantar flexion that lift the shank and foot. The foot is moved forward by the hip joint that maintains flexion during the swing phase. The toe clearance is ensured by the knee joint flexion in the early swing phase. The knee joint extends from the middle swing phase to prepare foot contact on the ground. The knee joint flexion is generated by the hamstring muscle contraction and the shank acceleration. The toe trajectory in the swing phase has maximum and minimum values.

The hypothesis is that the application of the fore at toe-off is effective for increasing MTC. The force is applied to assist the shank movement and generate mainly knee flexion torque, because the shank movement has the largest contribution to ensuring the toe clearance [2.2]. The author assumed that the increased knee flexion angle in the early swing phase causes the increase in maximum toe clearance. If the maximum knee flexion angle increases, the knee flexion angle during knee extension increases, although the knee

maximum extension angle does not change. The author assumed that the increased knee flexion angle in the late swing phase (during knee extension) causes the increase in MTC and does not disturb the knee extension.

2.2 Robotic system

2.2.1 Design and configuration

A cable-driven system was designed to apply the force application to the human. The point where the force was applied was a middle part of the shank. The direction of the applied force was longitudinal along the shank toward the knee joint, as shown in Fig. 2.1. The knee assistive flexion torque was generated by pulling the cable as the product of the cable tension and moment arm. This force causes the additional acceleration of the shank and the assistive effect on the thigh that assists hip flexion motion. The applied knee flexion torque is:

$$\tau_{knee} = F\mathrm{R}, \tag{2.1}$$

where τ_{knee} indicates the applied knee flexion torque, F indicates the force strength, and R indicates a moment arm. The force is transmitted to the thigh and moves the thigh because the force direction from the point of force application at the shank was parallel with the longitudinal direction of the shank. This force can generate the hip flexion torque as:

$$\tau_{hip} = FL_1 \sin\theta_{knee}, \tag{2.2}$$

where τ_{hip} is the applied hip flexion torque that is generated by the force application, L_1 is the length of thigh (from the knee joint to the hip joint), and θ_{knee} is the angle between the shank and the thigh in sagittal plane.

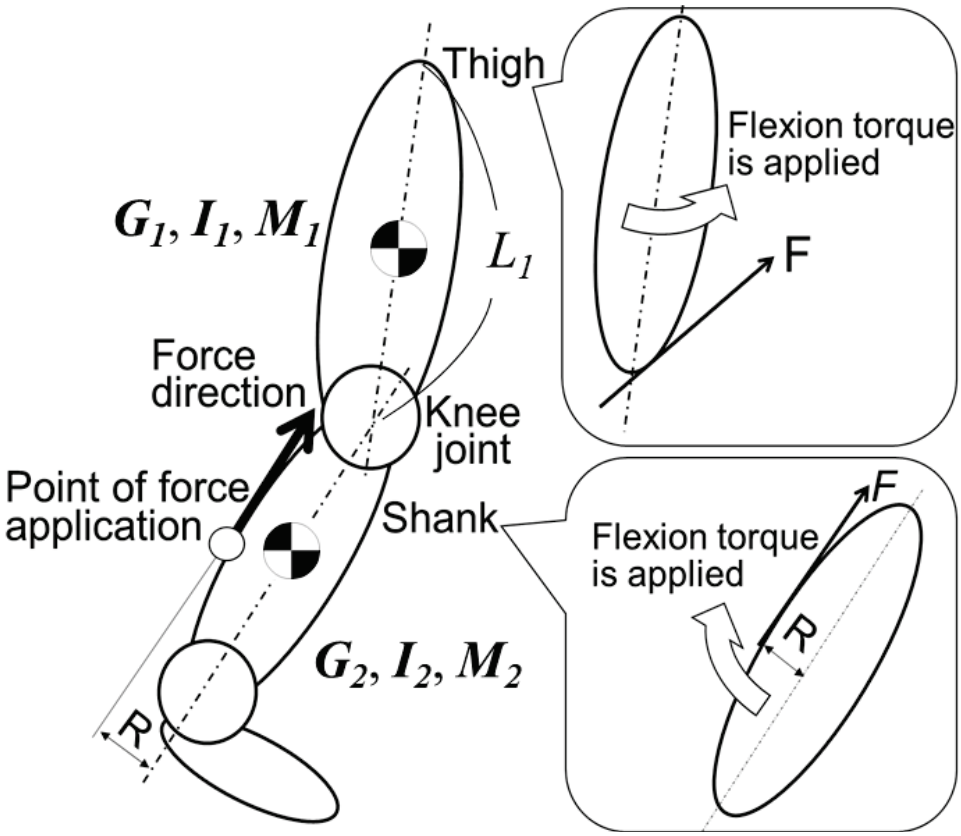

Fig. 2.1 Point and direction of force application.

Figures 2.2 and 2.3 shows the constitution of the hardware system. AC servomotor (NX610MA-PS25; Oriental Motor Co., Tokyo, Japan) was put away from the body. The motor pulled a nylon cable and applied the force to a frame that people wore with their thigh and shank using elastic bands. A spring (E659; stiffness of 0.040 N/mm) and loadcell (LUX-B-200N-ID; Kyowa Electronic Instruments Co., Tokyo, Japan) was between the cable and the frame for enabling the system to stably control the cable tension. The load cell was attached to a point 0.05 m distance from the center of the frame. The weight of the frame was approximately 100 g. The size is shown in Fig 2.4. Goniometers (SG110, SG150, Biometrics Ltd., Newport, UK) were attached to the leg under the frame with a tape for sensing the hip, knee, and ankle joints angles. Three pulleys supported the cable and one movable pulley compensated the cable length. Foot was pulled toward the pulley located around the hip (Fig. 2.5) when people were keeping swing motion. The

movable pulley was located between the frame and the motor and compensated the length of the cable. The movable pulley was used to reduce the cable tension as much as possible when the motor was not activated (Fig. 2.6). In preliminary experiment, the author confirmed that cable length varied within 0.10 m during walking. Therefore, the range of the movable pulley was designed to be 0.05 m considering the change in the cable length as a result of movement of the movable pulley as shown in Fig. 2.3. A servomotor (S03N/2BBMG, Grand Wing Servo-Tech Co., Ltd., Taipei, Taiwan) and a rachet gear were used as a locking system for the movable pully in case where the cable was winded. A timing belt which was connected with a plate supporting the movable pulley rotated the rachet gear corresponding to its movement. The robot controlled the servomotor rotational position to move the pawl of the ratchet for locking and unlocking the movable pulley movement. A pulley cover was used to avoid the fall of the cable from the pulley. The Windows system was included for force control the tensile of the cable.

Figure 2.7 shows the overall hardware configuration of the robotic control system. The system consisted of AC motor, motor driver, load cell, load cell conditioner, goniometer, goniometer amplifier, moving pulley stop mechanism, Arudino, analog I / O board, counter board, and computer. The main controller was the computer of the Windows system. The counter board (CNT-3208M-PE, CONTEC, Osaka, Japan) and the analog I/O board (ADA16-32/2(PCI)F, CONTEC, Osaka, Japan) were connected to the main controller via the PCI Express bus. The goniometer and load cell values were processed by the analog I/O boards. The goniometer data were transmitted via K800 Amplifier. The tensile force was sensed by the load cell and committed to the controller via an amplifier (WGA-670B, Kyowa, Tokyo, Japan). The load cell had output with a voltage of 0 [V] to 10 [V] in response to an input of 0 [N] to 20 [N]. The conversion from the voltage V of the goniometer to the angle θ is given by the flowing formula:

$$\theta = 90V - 180, \tag{2.3}$$

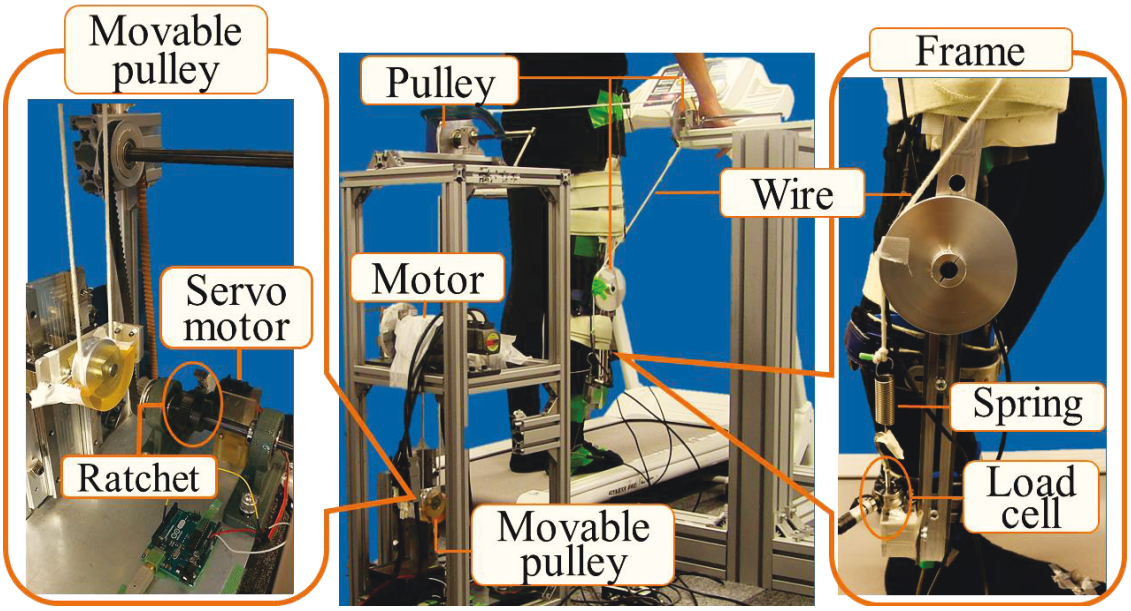

Fig. 2.2 Appearance of the cable-driven robot.

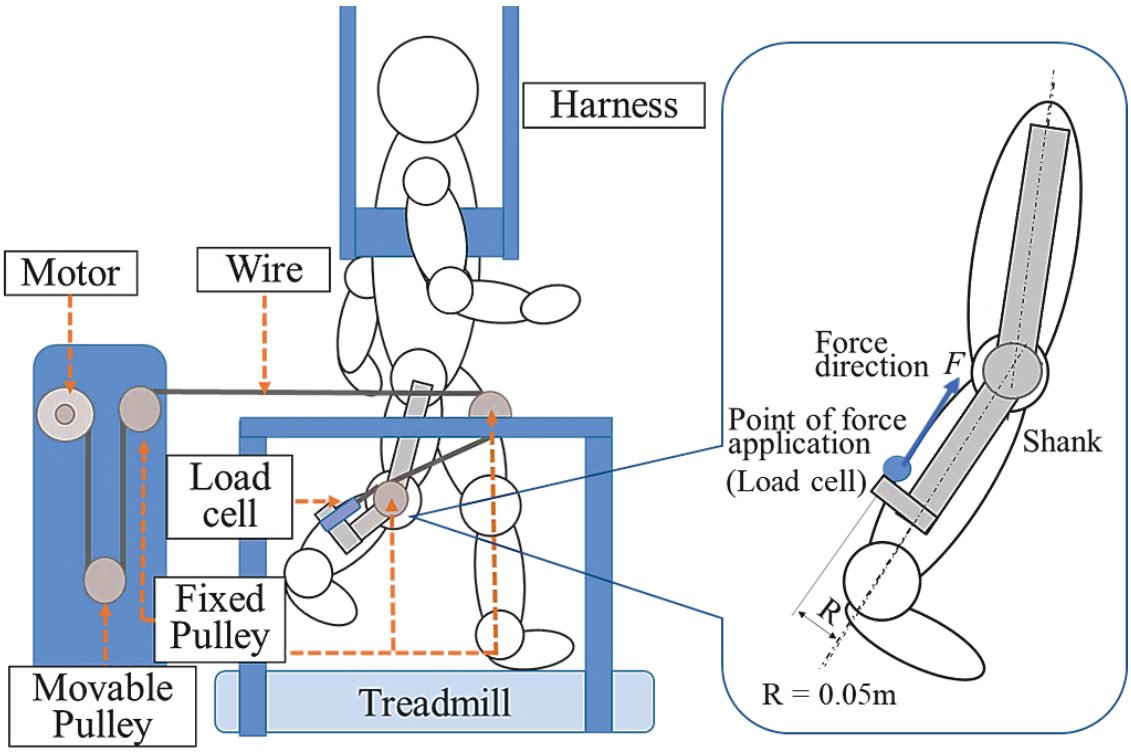

Fig. 2.3 Mechanism of the cable-driven robot.

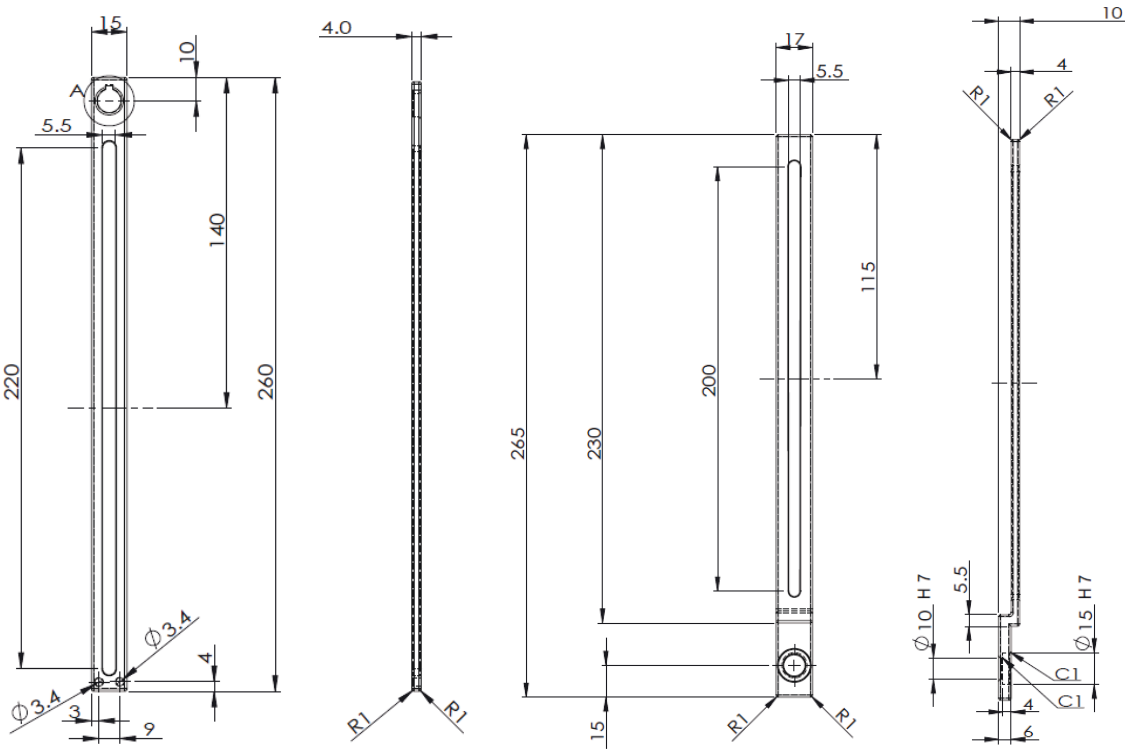

(a) Frame for shank (b) Frame for thigh

Fig. 2.4 Design of the frames.

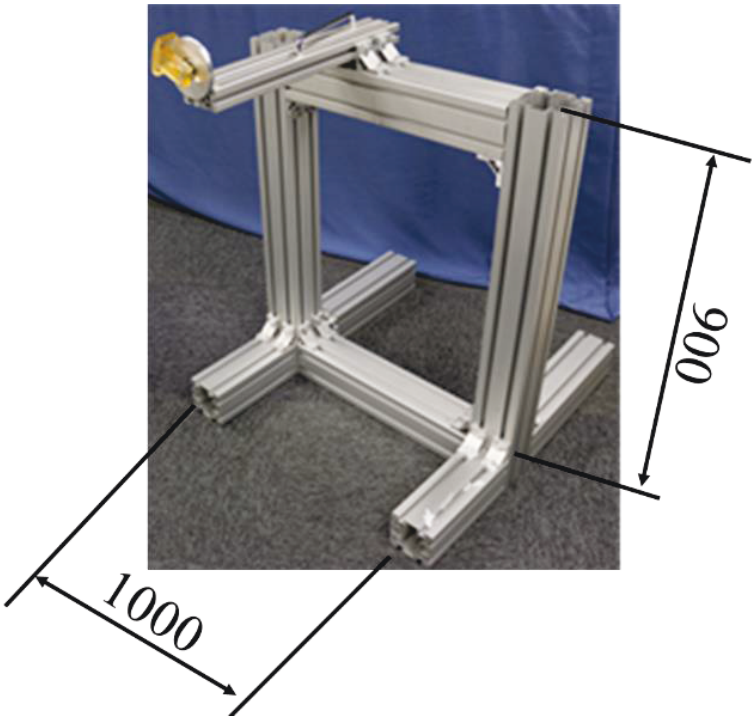

Fig. 2.5 Pulley for supporting cable.

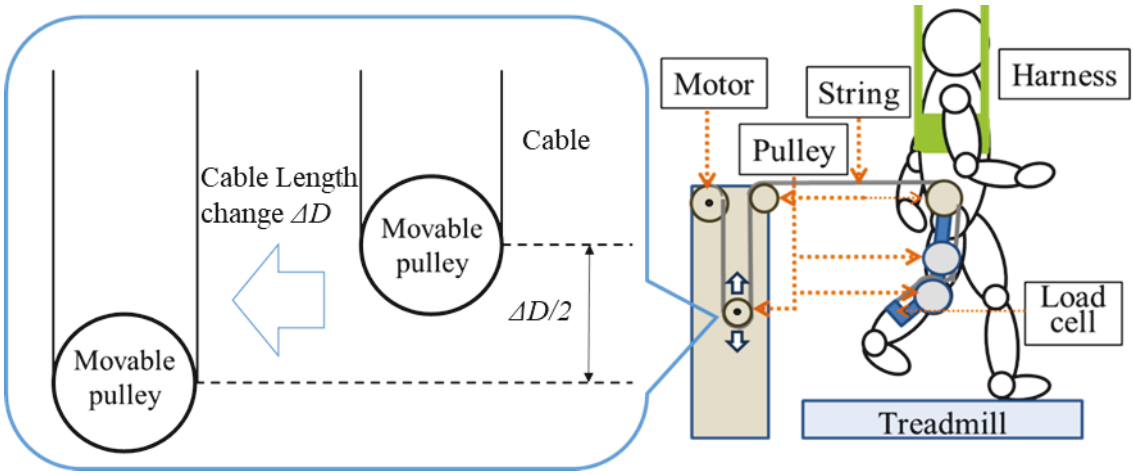

Fig. 2.6 Compensation of cable length change with movable pulley.

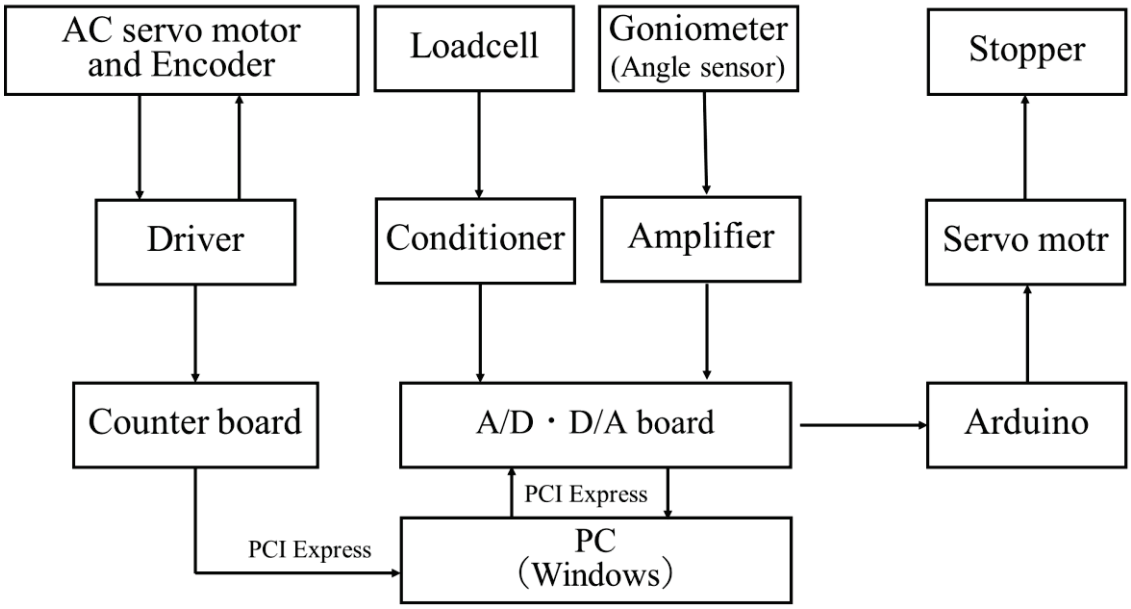

Fig. 2.7 System arrangement.

Tables 2.1, 2.2, 2.3, 2.4, 2.5, 2.6, 2.7, and 2.8 show the specifications of NX610MA-PS25, spring E659, goniometer SG150, goniometer SG110, Load cell LUX-B-200N-ID, servomotor S19CLN / 2BBMG / JR, K800 Amplifier, and the amplifiers WGA-670B, respectively.

Table 2.1 Specifications of NX610MA-PS25.

Item		Characteristic value
Type		AC servo motor
Declared torque	N・m	6.44
Item		Characteristic value
Max rotational speed	r/min	3000
Rated current	A	2.9
Power supply	V	100-115
Reduction ratio		25
Backlash	arcmin	15
Declared power	W	100
Moment of inertia	$kg・m^2$	0.0436
Detector		Absolute encoder 20 bits per rotation
Mass	Kg	1.55
Resolution		100~100000 (default 1000)

Table 2.2 Specification of spring E659.

Item		Characteristic value
Name		E659
Material		SUS304WPB
Outside diameter	mm	8
Wire diameter	mm	0.9
Free length	mm	50.1
Total number of turns		39.5
Spring constant	N/mm	0.393
Length during usage	mm	67.8
Allowable length	mm	85.3
Max load	N	18.34
Initial tension	N	4.511

Table 2.3 Specifications of goniometer SG150 (No.1).

Item		Characteristic value
Accuracy	°	± 2
Measuring range	°	± 150

Table 2.3 Specifications of goniometer SG150 (No.2).

Weight	g	17
Input resistance	kΩ	0.23
Operating temperature range	℃	10–40

Table 2.4 Specifications of goniometer SG110.

Item		Characteristic value
Accuracy	°	± 2
Measuring range	°	± 150
Weight	g	19
Input resistance	kΩ	0.23
Operating temperature range	℃	10–40

Table 2.5 Specification of Load cell LUX-B-200N-ID.

Item		Characteristic value
Rated capacity	N	± 200N
Nonlinearity		Within ± 0.15%
Hysteresis		Within ± 0.15%
Repeatability		Within 0.05%
Rated output	mV/V	± 0.9
Safe temperature range	℃	-20–80
Compensated temperature range	℃	-10–70
Temperature effect on zero balance	/℃	Within ± 0.03%
Temperature effect on output	/℃	Within ± 0.005%
Safe excitation voltage	V	10
Recommended excitation voltage	V	1–5
Input resistance		375 Ω ± 1.5%
Output resistance		350 Ω ± 1%
Safe overload		150%
Natural frequency	KHz	14
Recommended tightening torque	Nm	3
Weight	g	50
Material		SUS metallic finish

Table 2.6 Specifications of S19CLN / 2BBMG / JR.

Item	Characteristic value
Connector Type	JR
Torque Nm (4.8 V)	6
Speed s/60°	0.1

Table 2.7 Specifications of K800 Amplifier.

Item	Characteristic value
Dimensions mm	Subject unit: 100 x 50 x 25 Base unit: 180 x 170 x 48
Mass g	Subject unit: 150 Base unit: 550
Analogue channels	8
Digital channels	5
Communication from subject unit to base unit	RS 422
Input voltage differential bridge mode mV	± 12
Input voltage single ended high level mode mV	± 4
Output (full scale) V	Analog +0.0 to +4.0
Analog channel input impedance M Ohm	1
Power supply per channel V	+ 5.0 V
Power supply per channel tolerance %	± 1
Accuracy %	Better than ± 0.5
Maximum common node V	+3.5 to -2.5
General bandwidth KHz	5

Table 2.8 Specification of instrumentation amplifiers WGA-670B (No.1).

Item	Characteristic value
Applicable transducers	Strain gage transducers
Applicable bridge resistance Ω	87.5 to 10000
Measuring range mV/V	± 3.2
Bridge excitation V	10
Digital zero adjustment range	Same as measuring range
Display	± 19999
Update times/s	15.6
Sampling rate times/s	2000

Table 2.8 Specification of instrumentation amplifiers WGA-670B (No.2).

Nonlinearity	Within ± 0.03%
Zero stability μVRTI/℃	± 0.25
Sensitivity stability /℃	± 0.01%
Conversion rate times/s	500
Setting parameters	Indication for 10 V output (± 19999)
Operating temperature/humidity range ℃	-10 to 50
Power supply V	AC 100–240 ± 10% (50/60 Hz)

2.2.2 Force application method

The positional control of the motor position was performed for controlling the applying force of the cable-driven robot. Initially, the robot detects the force application timing. It was used angular information for the timing detection as an experimental protocol. After detecting the timing, the robot activated the motor system and applied the force to a human for a short time.

2.2.1 Decision of assistance timing

The timing was detected based on a phase of the angular trajectory as shown in Fig. 2.8. The phase of the trajectory in an angular space of three joint angles could be derived by watching a plane from one point of view. If the angle information is used for detection of robotic assistance, the change of gait can be easily and automatically analyzed because the angle change reflects the gait change. Although the joint movement is cyclical during walking, it is difficult to detect the maximum and minimum values of angle parameters in real-time because of the noise and variability of the angle range between gait cycles. In contrast, the angular space has a lower-dimensional structure and the angular trajectory is on planes [2.3]. Polar angle of the angular trajectory can be derived as the phase if the initial point is decided after projecting angular point onto the plane.

To calculate the polar angle, the basis vectors and mean angle data of the plane are needed. The coordinates $\boldsymbol{P}$ on the plane are expressed by

$$\boldsymbol{P} = \alpha 1\boldsymbol{w1} + \alpha 2\boldsymbol{w2} + \boldsymbol{R}, \tag{2.4}$$

where ***w1*** and ***w2*** indicate basis vectors, $\alpha 1$ and $\alpha 2$ are coefficients of the basis vectors, and ***R*** indicates the coordinates of the mean angle data in the swing phase. The basis vectors cab be derived using principal component analysis.

The vectors from the coordinates before projection to the coordinates after projection and the two eigenvectors ***w1*** and ***w2*** are perpendicular to each other. Therefore, α and β were calculated using the inner product as

$$\alpha 1 = \boldsymbol{Q}\,\boldsymbol{w1} - \mathbf{G}w1, \tag{2.5}$$

$$\alpha 2 = \boldsymbol{Q}\,\boldsymbol{w2} - \boldsymbol{G}\,\boldsymbol{w2}, \tag{2.6}$$

where ***Q*** denotes the coordinates of the lower-limb joint angle space before projection.

Parts of angular data were extracted based on the hip joint angle. The planar structure is different between the swing and stance phases [2.4]. Therefore, a part of data were extracted as the swing phase data if the hip joint is flexing angle changed from a minimum flexion angle to a maximum flexion angle while a part of data were extracted as the stance phase data if the hip joint is extending from a maximum flexion angle to a minimum flexion angle. First the switching point from the plane related to the stance phase to the plane related to the swing phase was derived by detecting time point where the hip joint started flexing and finding the point where the sum of the projection distances from a sensed angular point to points projected onto two planes related to the swing and stance phases was minimum because the two planes intersect at the points. Next, a polar angle of the joint's angular trajectory which was projected onto the plane of the swing phase was calculated. The formula to calculate polar angle φ was

$$\varphi = \cos^{-1}\left(\frac{(\boldsymbol{U}-\boldsymbol{R})\cdot(\boldsymbol{S}-\boldsymbol{R})}{\|\boldsymbol{U}\cdot\boldsymbol{R}\|\|\boldsymbol{S}\cdot\boldsymbol{R}\|}\right) \tag{2.7}$$

where ***S*** indicates a switching point from the stance phase to the swing phase and ***U*** indicates the point of sensed angles in real time.

2.2.2.2 Force control method

The robot switched the force-application and non-force-application modes. The plane for deriving the polar angle (phase) was calculated using several gait cycles. After detection of the phase of the angular trajectory that was decided as a timing to apply the force for the experiment, the motor system was activated. The servo motor and rachet stopped the movement of the moving pulley to inhibit it from compensating the cable length when the force was applied.

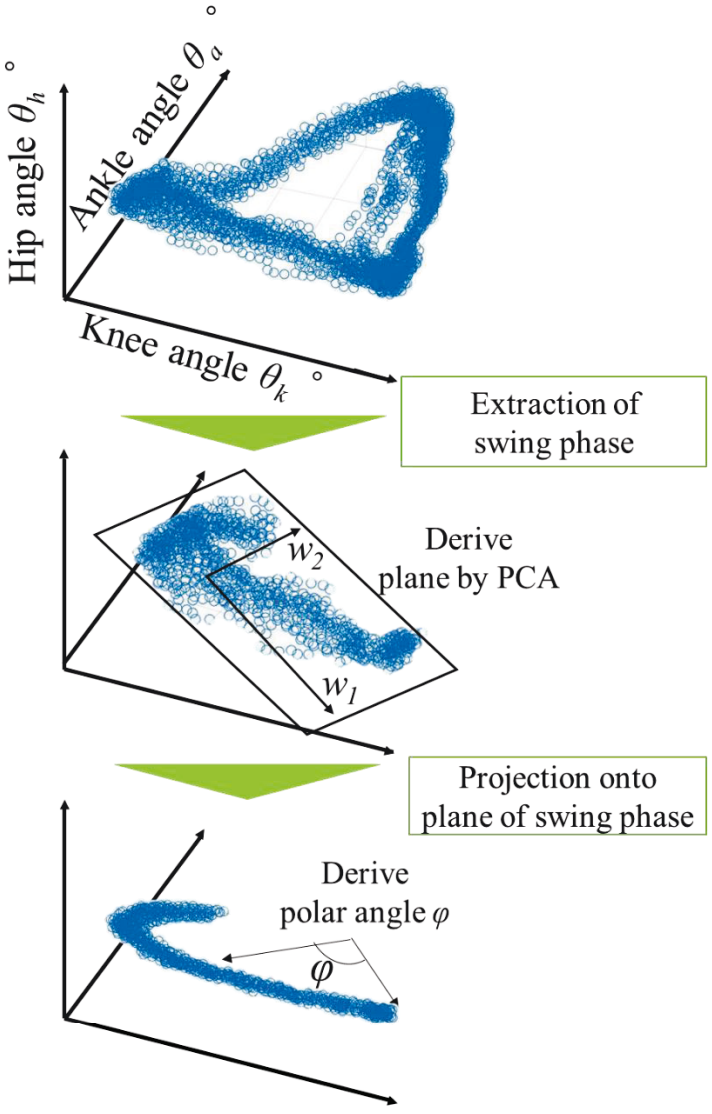

Fig. 2.8 Timing detection method by deriving a plane.

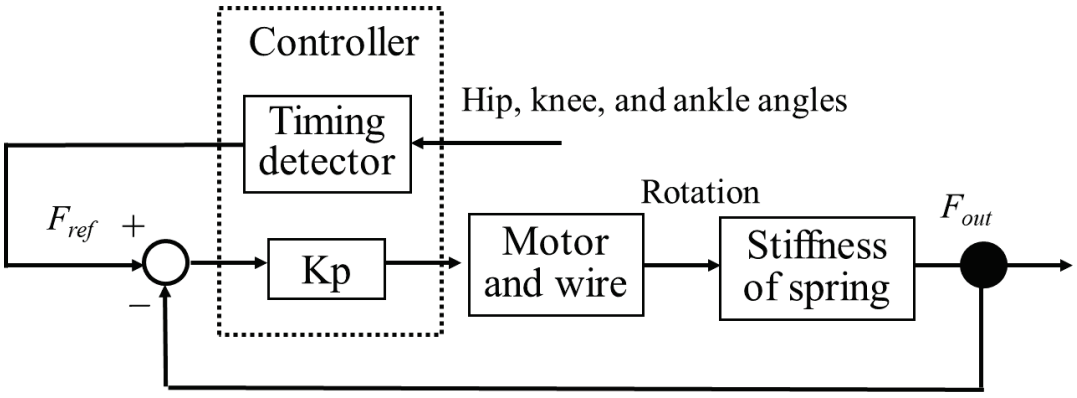

Fig. 2.9 Block diagram of force control in the system.

As shown in Fig 2.9, when the motor system was activated, the controller controlled the motor angular speed and tensile cable force based on feedback from the load cell with PID control as:

$$F_{out\_new} = K_p(F_{out\_old} - F_{ref}), \tag{2.8}$$

where K_p denotes the proportional gain, F_{out} denotes the output of the tensile force, and F_{ref} denotes the desired tensile force. The flexion torque applied to the knee joint was determined solely by determining the cable tension because the moment arm was constant (0.05 m). The controller returns the motor rotational position to the initial position for stopping the force application after the short-term force application was finished. If the robot tried not to apply the force when the force application timing was not detected, the robot stopped the motor rotation.

2.3. Experiment in younger people

2.3.1 Experimental procedure

Experimental protocol consisted on walking on a treadmill during non-force and force-application phases. Participants held a handrail when they walked in this experiment. Walking speed was constant (2.5 km/h) to reduce the error in detecting the timings to apply the force among participants. Moreover, because the walking speed was

slower than the usual walking speed in young people, the experimental force application could be performed safely. To investigate the effect of timing difference of the force application, there was a possibility that the applied force would disturb human walking.

Five healthy adults (one female and four males; age 24 ± 2 years, height 166 ± 15 cm, body weight 56 ± 12 kg) who have no neurological injuries or gait disorders were recruited in this experiment. Function of adapting to a new gait pattern in older people is same as younger people [2.5]. Therefore, younger people were recruited to decrease the risk of falling and to conduct many trials during experiment. This experiment follows the principles of the institutional review board of Waseda University. The author gave the participants detailed the experimental objectives and explained that they were able to withdraw from the experiment whenever they desired. The experiment was conducted after the obtainment of their consents.

Evaluation of gait change was made with the goniometers and a motion capture system (Raptor-E; Motion Analysis, Santa Rosa, CA, USA) that could measure the toe clearance. A marker was attached on the first metatarsophalangeal joint of the right foot. Fig. 2.10 shows the Raptor-E and Fig. 2.11 shows the position of marker. Table 2.9 shows the specification of the Raptor-E. Initially, participants walked without frame and with goniometers for 60 s for system check and practice the walking on the treadmill. After the frame was attached to the participants, they walked without force application for 30 s to reach a steady state and calculate the planes of the angular space; then, the experimental measurement started. The participants walked for 30 s five times in each experimental condition: the first 15 s in non-force-application phase and the last 15 s in force-application phase. Total number of experimental conditions was four, and then 20 trials were performed for each participant. The trajectory and joint angles were compared between non-force-application and force-application phases. Gait data of 250 gait cycles were collected in total for non-force-application and force-application phases, respectively. To investigate only the effect of timings to apply the force, the force parameters were constant. The desired force value was 16 N and the motor activation duration was 0.18 s because we could observe if these parameters would affect human gait in the pre-experiment. The rising time of force application was approximately 0.10 s.

Table 2.9 Specifications of Raptor-E

CMOS sensor pixel	1.3 million
Number	8
Markers	Reflective marker
Analog input channel ch	64 (Force plate 48, others 16)
Sampling frequency Hz	120

Fig. 2.10 Raptor-E.

Fig. 2.11 Position of a marker.

2.3.2 Force application timings

The polar angle was calculated with the angles of hip, knee, and ankle joints. The polar angle varies periodically within the range of 0 to π rad. Figure 2.12 shows the time-series change of polar angles and relation of angles and toe clearance in one gait cycle when the subjects walked on the treadmill at 2.5 km/h in a preliminary experiment. The polar angle is a minimum (i.e., 0 rad) before toe-off and a maximum (i.e., π rad) before the time point of minimum toe clearance. The positive direction of the hip joint angle, knee joint angle, and ankle joint angle are the extension, bending, and the dorsiflexion directions, respectively. The hip joint angle was in flexion when the phase increased from about 0.2 rad to the maximum value (about 3.0 rad) and then decreased to about 2.4 rad.

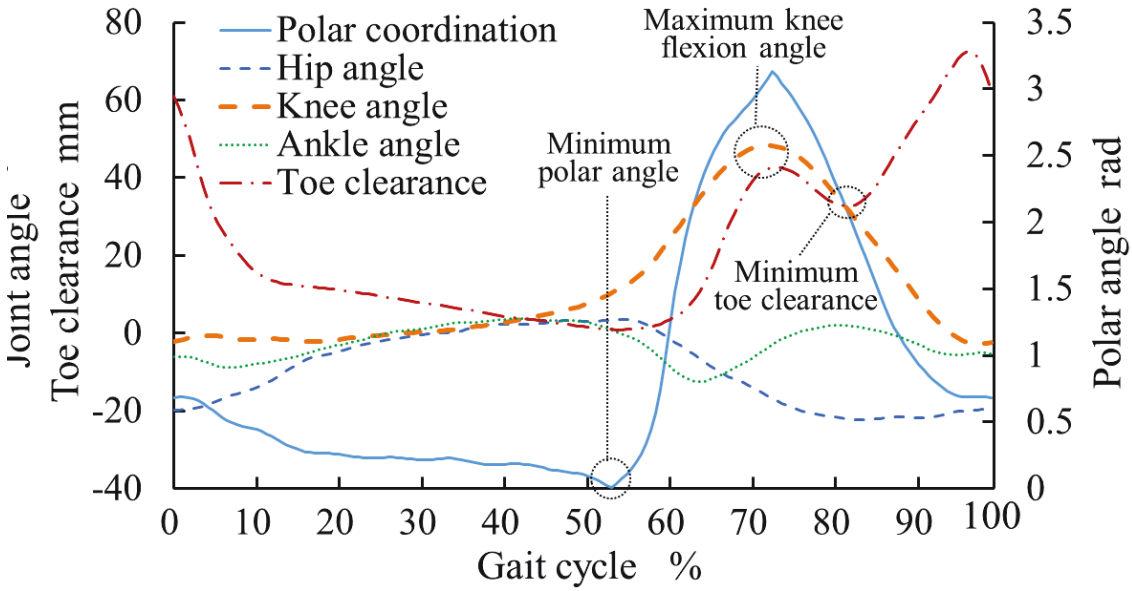

Fig. 2.12 Time series of the polar angle, toe clearance, and joint angles.

The knee joint was in flexion when the polar angle was from about 0.2 rad to about 3.0 rad.

The author investigated the effects of the force application timing on toe clearance. Four time points of force application were considered based on knee flexion motion, i.e., condition 1, time when the knee joint started flexing in pre-swing phase; condition 2, time when the toe was lifted by knee flexion motion; condition 3: time when the knee joint was flexing after toe-off; and condition 4: time when knee joint was about to finish flexing. It was decided that the polar angles for stating force application were 0, 0.8, 1.6, and 2.4 rad with increasing polar angle as experimental conditions considering that the rise time of the force application was approximately 0.1 s. The system obtained lower-limb joints angular data and derived the planes using principal component analysis in the phase when participants walked without robotic assistance.

2.3.3 Evaluation method

At first, the author evaluated the control result of the motor system to apply the force and determine if the force application conditions were satisfied for the experiment. The

ratio of the hip flexion angle at the time when the force applied to the maximum flexion angle was calculated to evaluate the difference in the force application timings. Moreover, the ratio of knee flexion angle at the time when the force applied to the maximum flexion angle was calculated to evaluate the difference in the force application timings. The significance of the force strength and the timing of force application was investigated. In this experiment, the significance level was set to 5%.

It was analyzed how the attachment of the robot affects the human motion, using 40 gait data for each participant. The range of knee joint angle with the frame was compared to the range of the knee joint without the frame because the participants wore the frame with their knee joint. The t-test to determine the significance of the range of knee angle with and without frame was conducted.

Moreover, the change in toe trajectory during the swing phase in each experimental condition was analyzed using approximately 50 gait data. Averages of the toe clearance in gait phases were calculated for evaluation of toe trajectory change. The percentage of gait cycle was derived based on the minimum value of the toe clearance in the stance phase just before toe-off. The effect of the force application on the toe trajectory was analyzed by deriving the difference between maximum and minimum toe clearance without and with force application. The toe clearance when the gait phase was between 72% and 92% showed a change of toe trajectory in the swing phase after the toe was in the highest position.

The change in the lower limb joint (hip, knee, and ankle joints) angles was derived because these parameters generated the toe motion. The hip and knee joint flexion angles and ankle joint dorsiflexion angle were normalized to analyze the relationship between the joints. The hip maximum flexion and knee minimum flexion angles and the ankle minimum dorsiflexion angles were subscribed from these angles, and divided by the maximum value in the phase before the force application. A total of 50 data were used for deriving the average of the normalized angle in each gait phase. Particularly, the change of the knee flexion angle was analyzed because the knee joint flexion affects the toe height. The knee maximum flexion angle that is related to the highest toe position in the swing

phase was compared between the non-force-application and force-application phases. Furthermore, the change in the knee flexion angle when the gait phase was 90% was evaluated to consider the joint change related to MTC. The t-test was conducted to determine significant differences between the knee flexion angles with and without the force application when the knee angle was the maximum and the gait phase was 90%.

2.4 Experimental results in young people

2.4.1 Force application

Fig. 2.13 indicates the relationship between force application timing and the knee flexion angle in each experimental condition. Table 2.10 indicates the average and variance of parameters related to the force application in each condition. The maximum force strength was not significantly different between the experimental conditions. The normalized angle of the hip, knee and ankle joints when the polar angle was 0 rad were shown in Fig. 2.14. The joint angles were normalized because the normalization of

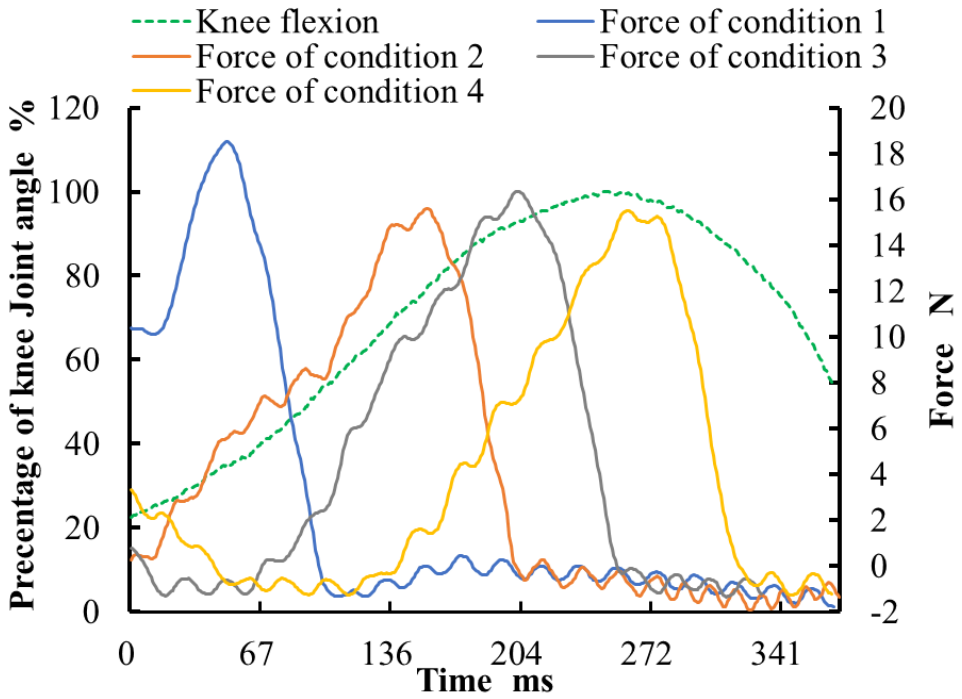

Fig. 2.13 Force application timing in each condition.

Table 2.10 Force application strength and timing for each experimental condition.

	Condition 1	Condition 2	Condition 3	Condition 4
Average of the maximum force [N]	16.8	16.0	15.9	16.2
Standard deviation of the maximum force [N]	2.60	2.36	1.83	2.05
Normalized hip flexion angle to maximum flexion angle [%]	90.6	61.5	41.7	35.5
Standard deviation of normalized hip flexion angle [%]	11.8	9.42	12.8	16.1
Normalized knee flexion angle to maximum flexion angle [%]	21.8	73.6	87.0	90.2
Standard deviation of normalized knee flexion angle [%]	9.26	17.0	18.4	12.0

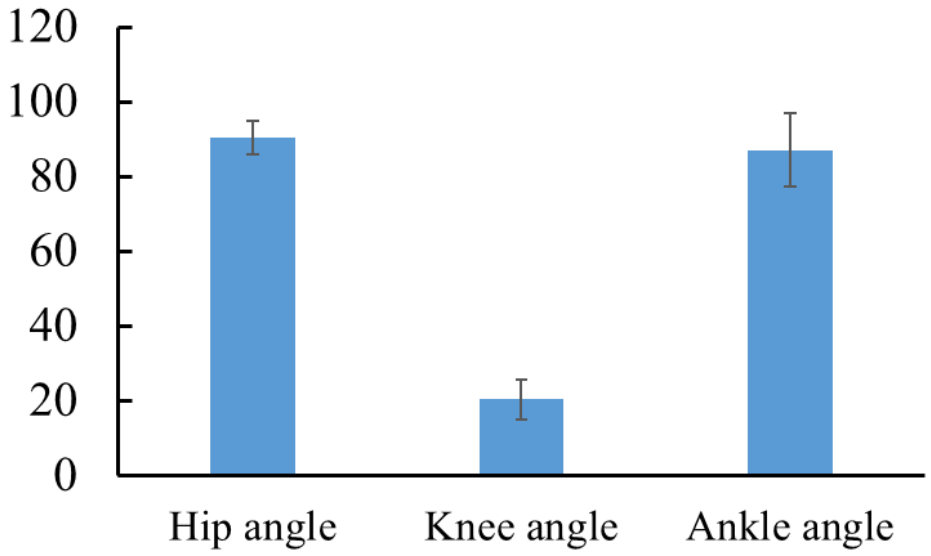

Fig. 2.14 Normalized angles of leg joints when the polar angle was 0 rad.

angles could decrease individual differences about the range of the joint angles and indicate the phase of joints movements. The definition of normalization was as follows: the maximum hip joint extension, knee joint flexion, and ankle joint dorsiflexion angles were 100 % and the maximum hip joint flexion, knee joint extension, and ankle joint plantar flexion angles were 0 %. The difference of the force application timing (normalized knee joint angle when the force was applied) among experimental conditions 1, 2, and 3 was significant ($p<0.05$). In contrast, the timing was not significantly different between the conditions 3 and 4.

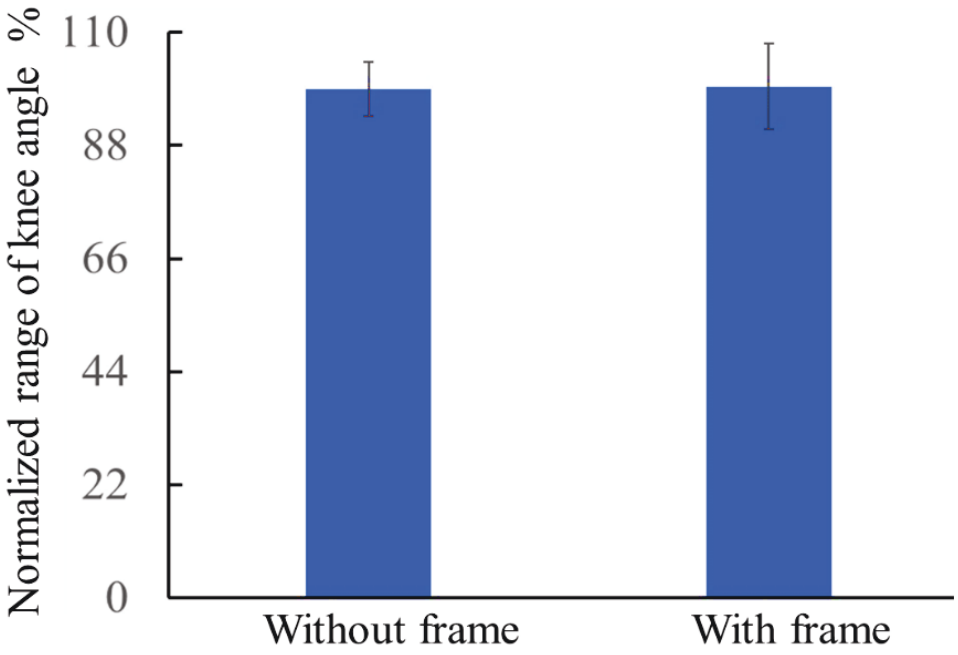

Fig. 2.15 Comparison of angular range of knee flexion without and with frame.

2.4.2 Comparison of the range of knee angles without and with frame

An effect of the frame on the range of knee joint angle was investigated. Fig. 2.15 compares the range of normalized knee angle during walking in case where participants wore the frame and in case where they did not wear. The error bar shows the standard deviation in all subjects. To normalize the angular range, it was defined that the average of the angular range in the condition where the participants walked without the frame is 100 %. The result shows that the range of the knee joint angle with frame was not significantly lower than the range without frame. Consequently, wearing the frame (using the cable-driven robot) did not disturb the knee joint motion in this experiment.

2.4.3 Change in the toe trajectory

An example of the toe trajectory changes between the conditions with and without force application is indicated in Fig. 2.16. The blue spots are data of the toe trajectory when the force was not applied, and the orange spots are data when the force was applied. The error bar indicates the standard deviation of the toe clearance in each the percentage

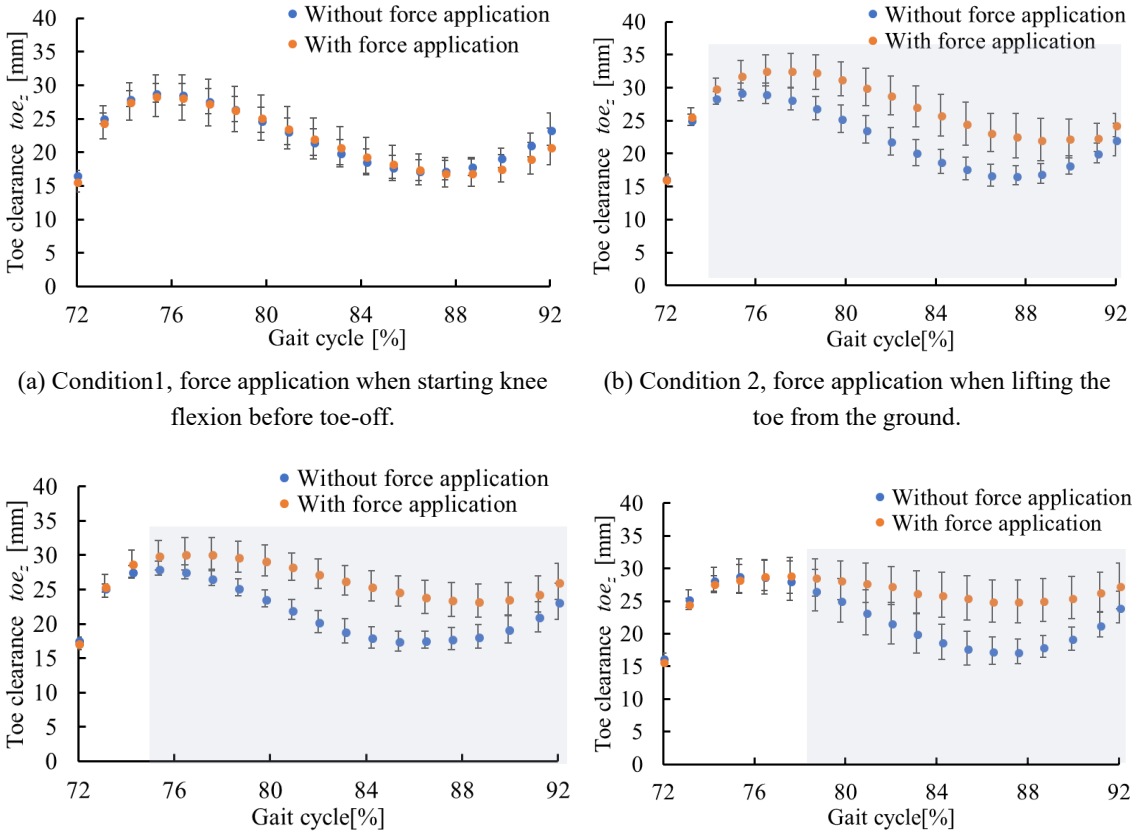

(a) Condition1, force application when starting knee flexion before toe-off.

(b) Condition 2, force application when lifting the toe from the ground.

(c) Condition 3, force application when maintaining knee flexion after toe-off.

(d) Condition 4, force application when finishing knee flexion after toe-off.

Fig. 2.16 Change of toe trajectory in each condition.

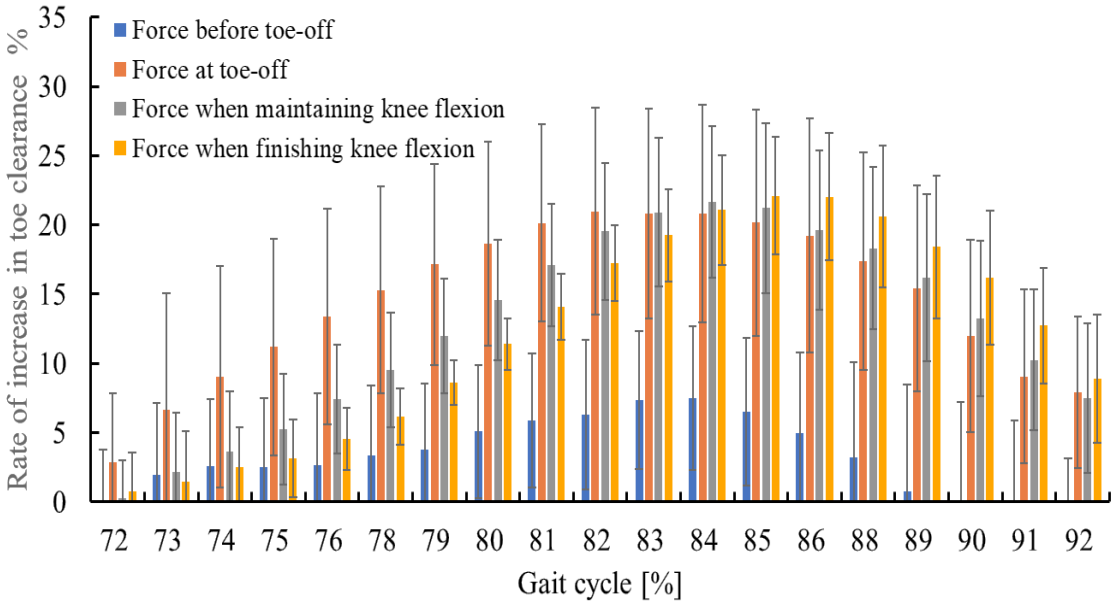

Fig. 2.17 Rate of increase in toe clearance in each stride cycle.

of the gait cycle. No significant change in toe clearance was confirmed for condition 1. For conditions 2 and 3, the toe clearance from the maximum to the minimum value significantly increased. The minimum toe clearance also was higher in condition 4 when the gait phase was approximately 88 %.

Fig. 2.17 indicates the average change in the mean toe clearance in each percentage of the gait cycle that was derived from all data. Blue, orange, green, and yellow bars respectively show the increases in toe clearance caused by the force application in each condition; condition 1, time when the knee joint started flexing in pre-swing phase; condition 2, time when the toe was lifted by knee flexion motion; condition 3: time when the knee joint was flexing after toe-off; and condition 4: time when knee joint was about to finish flexing. The error bar shows the standard deviation of the toe clearance in each the percentage of the gait cycle. The increase of toe clearance was highest before 76% of the gait cycle when the force application timing was around toe-off. The increase of toe clearance was highest at approximately 85% of the gait cycle when the force application timing was after toe-off.

2.4.4 Change in the leg joint angles

Fig. 2.18 indicates mean angles in each the percentage of the gait cycle that were derived by data of all participant with and without force application. The positive direction of the hip joint, the knee joint, and the ankle joint angles is the extension, the bending, and the dorsiflexion directions, respectively. The mean knee joint flexion angles in more than 80% of the gait phase (after the knee joint flexion angle was maximum) when the force was applied increased from when the force was not applied for conditions 2, 3, and 4. For all conditions, the maximum values of the knee joint flexion angle when the force was applied significantly rose ($p<0.05$) from when the force was not applied, as shown in Fig. 2.19. For conditions 2, 3, and 4, the knee joint flexion angle when the force was applied significantly rose ($p<0.05$) when the force was not applied in later swing phase (the percentage of the gait phase was approximately 90 %), as shown in Fig. 2.20.

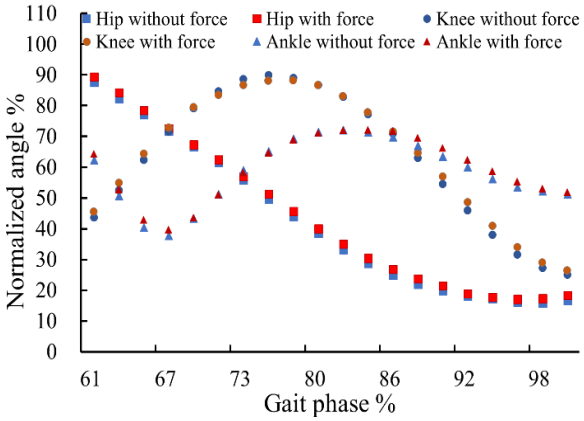

(a) Condition1, force application when starting knee flexion before toe-off.

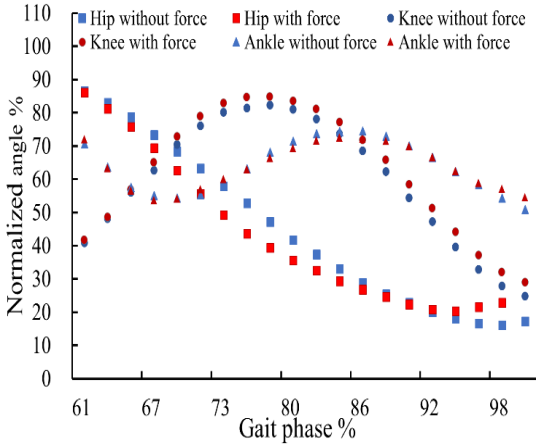

(b) Condition 2, force application when lifting the toe from the ground.

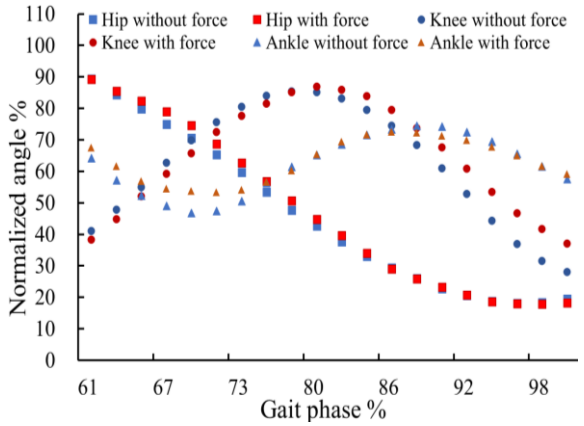

(c) Condition 3, force application when maintaining knee flexion after toe-off.

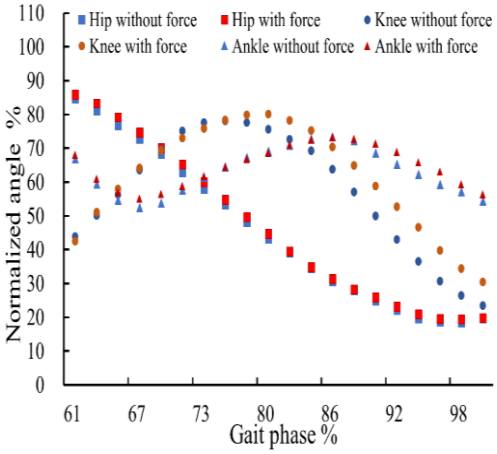

(d) Condition 4, force application when finishing knee flexion after toe-off.

Fig. 2.18 The average of angles of leg joints in the swing phase for all participants.

2.5. Experiment in older people

2.5.1 Protocol

The participants were three healthy older people (two male and one female; age 65 ± 2 years, body weight 62 ± 2 kg, height 1.64 ± 0.07 cm) having no neurological injuries or gait disorders. This experiment follows the principles of the institutional review board of Waseda University. The author gave the participants detailed the experimental objectives and explained that they were able to withdraw from the experiment whenever they desired. The experiment was conducted after the obtainment of their consents.

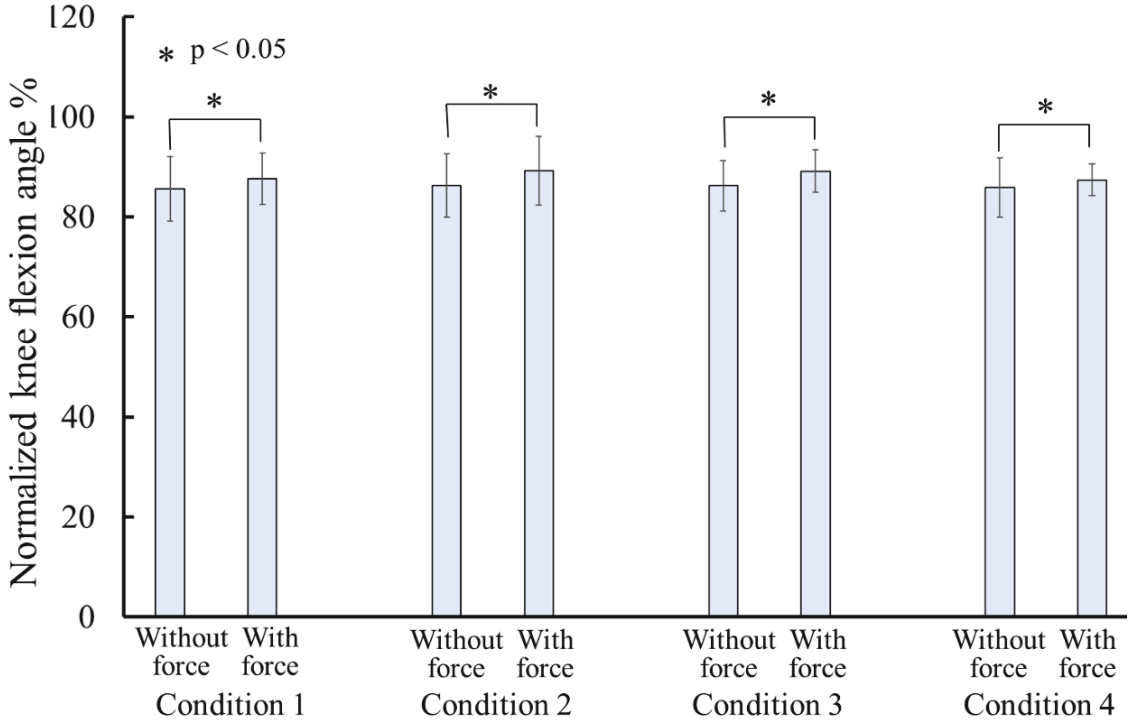

Fig. 2.19 The maximum knee flexion angle before and while force application. The error bars indicate the standard deviation.

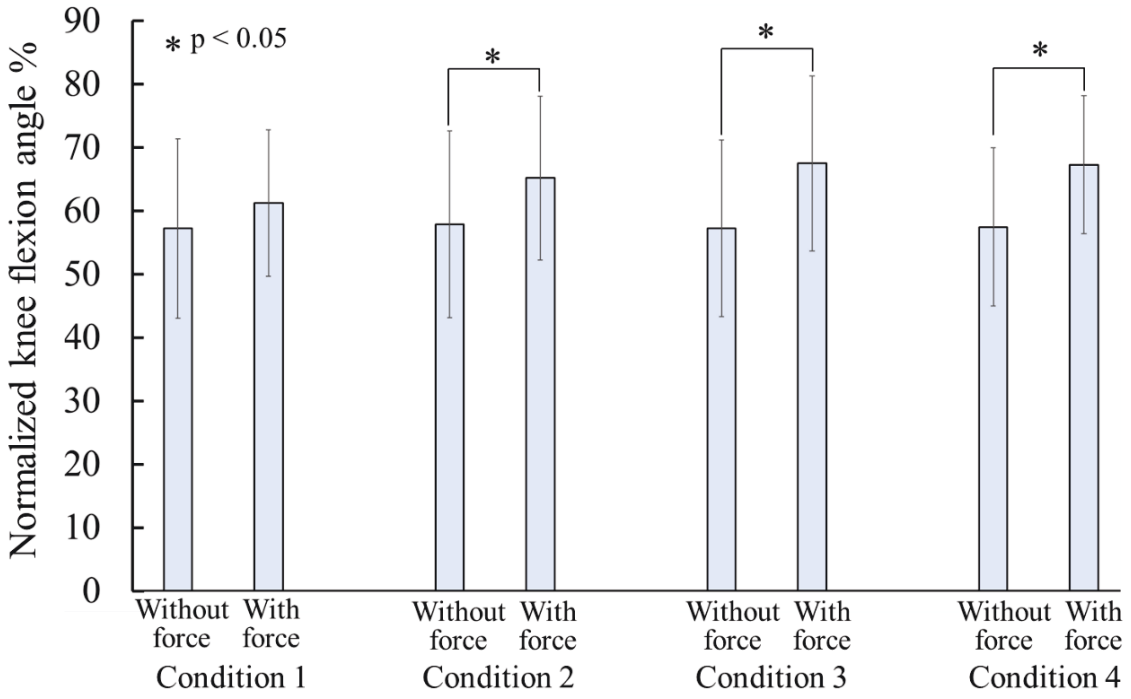

Fig. 2.20 The knee flexion angle when the gait phase was 90 % before and while force application. The error bars indicate the standard deviation.

After the explanation, each subject wore the harness and robot. The goniometers were attached to the subjects using elastic therapeutic tape. In the experiment, the subjects walked on a treadmill at 2.5 km/h. Before we started obtaining measurements, the subjects walked on the treadmill for 10 s to reach a steady state. The walking data of 50 gait cycles with and without force application for each subject were compared. For the investigation in the experiment, the desired value of the force was 16 N, because in a preliminary experiment at this value the author was able to sense a change in the knee flexion angle. The subjects continued to walk throughout two periods. In the first period, during which the subjects walked without the robot's intervention, the robot recorded the angle data of the lower limb joints and, at the end of the period, calculated the planes of the swing and stance phases using principal component analysis.

The minimum toe clearance change in the swing phase to investigate the effect of the force application on the toe clearance was evaluated. The number of samples in each period was approximately 50 for each subject.

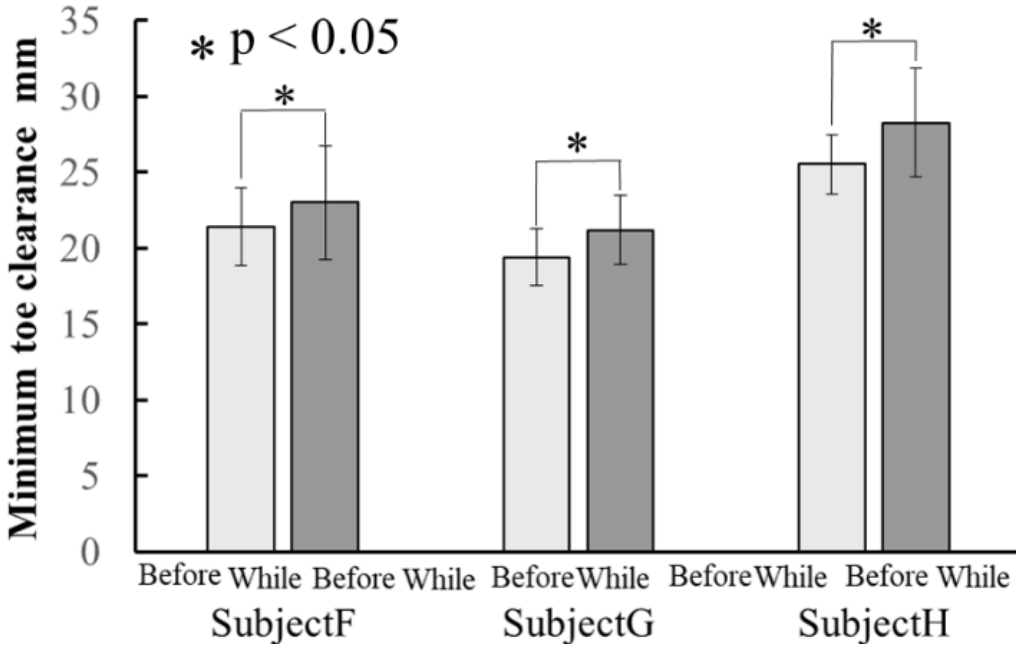

Fig. 2.21 Change in minimum toe clearance. The p value indicates the probability that two data groups are the same. The error bars indicate the standard deviation.

2.5.2 Result in older people

Fig. 2.21 shows the change in the minimum toe clearance. In all subjects, the minimum toe clearance significantly increased during the force application.

2.7 Discussion

The more the knee joint flexes in the early swing phase, the higher the toe position is in that phase. As shown in Figs. 2.16 and 2.18, the maximum knee flexion angle and maximum toe clearance increased by the assistance when the gait phase was approximately 78 % in conditions where the force was applied around and after toe-off when people kept flexing the knee joint. The author confirmed that the increase in the maximum knee flexion angle caused the increase of the maximum toe clearance in the swing phase. Because the knee flexion torque could be generated by the applied force, the knee flexion could be increased. The increase in the maximum knee flexion angle when the force was applied after toe-off (people kept the knee joint flexion) was smaller than when the force was applied around toe-off. Considering that the acceleration is maximized at the beginning of the movement, it is better to apply the force is at the beginning of the swing phase for the assistance of lifting the toe in the earlier phase. The duration of the gait phase when the toe clearance increased significantly was largest when the force was applied around toe-off. In contrast, the force application does not affect the maximum knee flexion angle if the knee is extending after knee flexion finishes.

Changes in the ratio of the hip angle to the knee angle after maximum toe clearance can be considered as the cause of increased minimum toe clearance. As the toe clearance value becomes minimum during the knee joint extension, the effect of the assistance that applies the flexion torque to the knee on the minimum toe clearance is small. The ankle joint tends to be kept in a neutral position when the toe clearance value becomes minimum. As shown in Fig. 2.16, the force application at or after toe-off increased the toe clearance in the later swing phase. If the hip flexion angle was higher during knee extension and the knee joint angle was the same, the knee joint position and toe position were higher. In

addition, as hip joint movement is generated by the action of the rectus femoris, the increase in potential energy due to the extension of the rectus femoris can contribute to an increase in the bending angular velocity of the hip joint. This indicates that changes in the knee flexion angle at an early stage might affect changes in the toe trajectory at a later stage.

The increasing degree in toe clearance in the swing phase varied between trials. The author assumed that the variance of the timing of applying the force was one of the causes of this difference. The author observed that several data show that the robot applied the force in the stance phase and did not increase the toe clearance. When the force application timing was earlier in conditions 3 and 4, that is, the force was applied nearer at toe-off, the degree of the increase in the toe clearance was higher. In contrast, the degree of increase in the toe clearance tended to be similar in some data in conditions 3 and 4. Because the significant difference of the force application timing was not observed between conditions 3 and 4, might increase the variance of the results related to the toe clearance change might be increased although the system satisfied the experimental conditions in most trials. The described method of gait phase detection still had a large error for use online because the detection of the start point of the swing phase was difficult in this method. Therefore, a more accurate algorithm is important to detect toe-off for achieving the final goal. The improved algorithm is described in Chapter 3.

The author observed that the force application generating knee flexion torque in the later swing phase did not inhibit the knee extension in the experiment for younger participants. This means that the robot could knee flexion motion without inhibition of foot contact. The author assumed that this is because the force strength was not sufficient to inhibit the knee extension for younger people. However, the force application in the later swing phase might inhibit older people from extending the knee and contacting the ground. The minimum toe clearance could be increased by the force application around toe-off even in older people. Consequently, the force application around toe-off was effective as an assistance to increase the minimum toe clearance.

The force application to the shank around toe-off generated knee flexion torque and

increased the toe trajectory throughout the swing phase. Although the figures show averages derived by all participants' data and ignore the individual difference, the tendency of these results was general for all participants. The shape of the toe trajectory did not change when the force was applied around toe-off, which could be regarded as a natural change. In addition, the increase in the minimum toe clearance was approximately 3 mm, while its variance was approximately 5 mm [2.6]. Therefore, the robotic assistance around toe-off is sufficient to ensure toe clearance of the ground and does not excessively increase it. Misalignment problem might occur every time when people wear the frame. It affects the generated assistance torque and degree of change of motion. Because this system can monitor the angle, the real-time evaluation of the joint angles can address this issue by adjusting the force strength based on evaluation results.

2.8 Summary

Cable-driven hardware was developed as an assistance robot to increase the toe clearance with intermittent force application. To establish the system to assist human toe motion as needed, it was needed to analyze the changes of the toe trajectory and the lower limb joint angles for determining the force application timing. The force is applied to assist the shank movement and generate mainly knee flexion torque. First, the effect of force application timings on the joints and the toe was investigated in younger people. Four time points of force application were considered based on knee flexion motion, i.e., condition 1, time when the knee joint started flexing in pre-swing phase; condition 2, time when the toe was lifted by knee flexion motion; condition 3: time when the knee joint was flexing after toe-off; and condition 4: time when knee joint was about to finish flexing. The increase in the maximum knee flexion angle caused the increase of the maximum toe clearance in the swing phase. Changes in the ratio of the hip angle to the knee angle after maximum toe clearance can be considered as the cause of increased minimum toe clearance. The force application in the later swing phase might inhibit older people from extending the knee and contacting the ground. Next, the effect of force application at toe-off was investigated in older people. MTC could be increased by the force application

around toe-off even in older people. Consequently, the author concludes that the force application around toe-off was effective as an assistance to increase MTC.

Chapter 3 Gait event detection algorithm

3.1 Related Research about Gait Event Detection

Identification of the human gait phase is necessary for decision and control of the motion of the robot assisting a human gait motion because walking is a periodic movement [3.1]. The gait phase detection method has been researched not only for robotic assistance but also for human gait analysis and rehabilitation training, such as functional electrical stimulation [3.2]. Because the gait phase mainly consists of swing and stance phases [3.1, 3.3], heel-contact and toe-off need be identified for the gait phase detection. Methods with a floor force or a camera are the gold standards for the detection of the heel-contact and toe-off [3.4, 3.5]. However, they cannot detect the gait events outside. Detection of the gait phase using wearable sensors is required for use outdoors.

A footswitch is the most common wearable sensor to identify whether the foot contacts the ground or not. The footswitch is a thin force sensor that can be attached to the sole of the foot. Particularly, a force-sensing resistor (FSR) that is a thin film of a conductive polymer is used. A voltage is outputted depending on the force value applied to the FSR. Therefore, foot contact information can be monitored if a threshold of FSRs voltage is set appropriately [3.2, 3.6–3.8]. The reliability can be adversely affected by different locations of attachment and long-term use (durability issue) [3.8, 3.9]. In particular, the durability issue affects the robotic control system seriously, that is, makes the control results incorrect or stops the robotic function. Additionally, the method relying only on the FSR cannot obtain the kinematic trajectory information of the leg joints. A more robust method of gait phase detection, which adapts automatically to differences in attachment placement using the sensor that can obtain the kinematic information of leg joints, is required.

In previous researches, the computational technology has been developed for

identifying foot-contact state with wearable sensors (i.e., accelerometers [3.10, 3.11], gyroscopes [3.12, 3.13], and inertial measurement units [3.14]). To extract patterns of features of gait parameters, many detection methods based on machine learning techniques have been proposed using support vector machines [3.15], linear discriminant analysis [3.16], Gaussian mixture model [3.17], and hidden Markov model (HMM) [3.18, 3.19]. In particular, classifiers based on hierarchical weighted decisions combined with the HMM resulted in accurate classification because this model can recognize a temporal pattern through estimation of a hidden state that cannot be observed directly by considering a transition probability of phases using gait parameters that can be directly obtained [3.19]. Nonetheless, the detection rate is not perfect; i.e., it is less than 100%. Moreover, these methods using supervised learning required true values for the training phase. In addition, the detection accuracy of toe-off remains unclear. The classifier algorithm of gait event detection extracting a feature of human gait kinematics might be used fast and more accurately than the algorithm using machine learning because the kinematics feature is a characteristic of gait motion in each gait phase.

Angular information is essential for control and evaluation of the gait training robot. When the gait phase can be detected using only angular information, it is not necessary to install different types of sensors to the gait training robot. There were found few studies that have proposed the gait events detection algorithm using only angular information. The adaptive oscillator, which is a real-time algorithm that learns the frequency and amplitude of a periodic signal, has been applied with angular sensors [3.20]. Although it can estimate a periodic joint movement in real time, it is difficult to detect the gait events. In another method, a multilayer perceptron neural network was used with hip and knee joints angles, which does not perfectly identify phases [3.21]. There remains a need for establishing a novel detection algorithm that uses the features of joint angles associated with heel contact and toe-off.

In this chapter, the objective is to establish the algorithm to detect toe-off using only angular information of the leg for control and prediction of the gait training robot. The heel contact was also detected for investigation of the usability of the proposed algorithm as a gait phase detection algorithm because the heel-contact is the basic gait event. The

requirements of the algorithm were real-time use, detection of gait events in every gait cycle, and immediate and automatic learning of the parameters in each person. The objective error was set as 50 ms or less considering the delay of the force application of the cable-driven robot (about 50 ms), duration of force application (about 130 ms in this thesis), and duration of the gait phases (duration of the knee flexion in the swing phase was about 230 ms). There is a coordination pattern between joint angles of the lower limb which might be different between gait phases [3.1]. The hypothesis was that the heel-contact and toe-off could be detected in real-time by detecting the change of the coordination patterns once they were classified.

3.2 Algorithm

The algorithm was based on a lower-dimensional structure of the leg joints during walking, which is a characteristic of inter-joint coordination [3.22, 3.23]. The periodic trajectory in the space that consists of the hip, knee, and ankle joint angles (i.e., three variables) during walking is embedded on planes, which means that three-dimensional angular parameters can be expressed with two variables. The gait motion of the lower limb consists of the swing of the leg for lifting and moving the foot forward (swing up), the swing of the leg for preparing foot-ground contact (swing down), the loading response for absorbing the shock of foot contact (loading response), and support for the body (support). The author assumed that there were four coordination patterns (corresponding to the swing up, swing down, loading response, and support) during one gait cycle, and the angular trajectory could be embedded on four planes. The hypothesis was that the heel-contact and toe-off can be detected by identifying switching points from the plane of the swing down to the plane of the loading response and from the plane of the support to the plane of the swing up, respectively. Thus, the proposed algorithm calculates the parameter of the four planes and finds their switching points (Fig. 3.1). The sensed angular data were classified, and the plane to which the data belongs was identified. The parameters of four planes were calculated from the recorded angular data of one gait cycle.

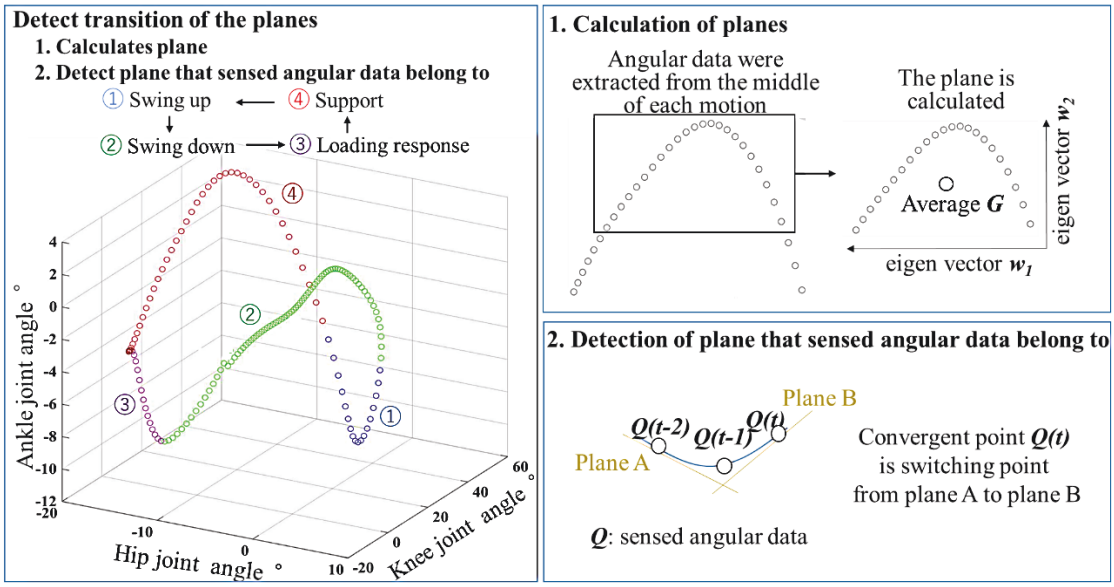

Figure 3.1. Overview of the algorithm for the detection of gait events.

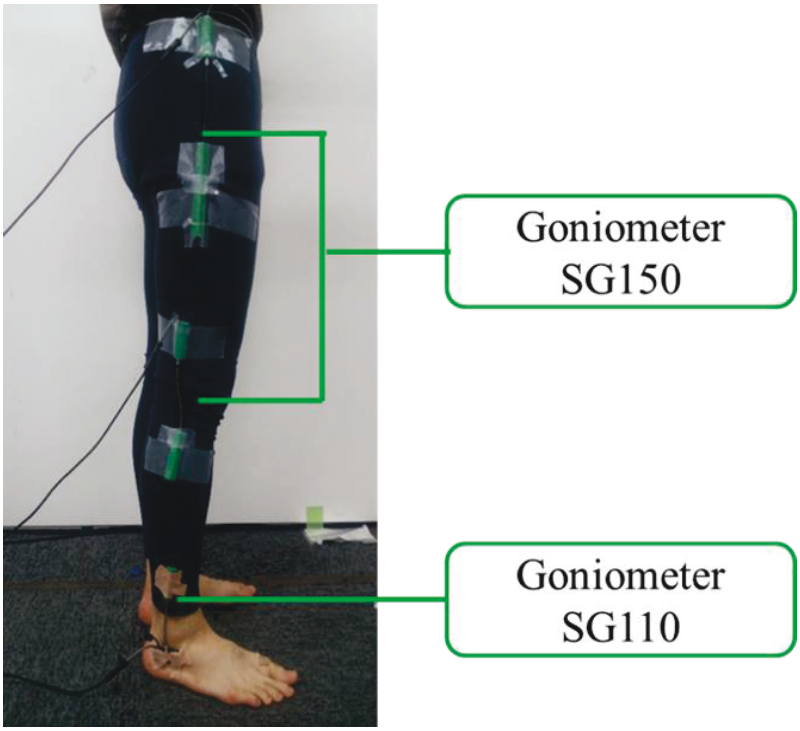

Figure 3.2. Attachment and placement of the goniometers.

Angles of hip, knee, and ankle joints in the sagittal plane were measured by the

electrical goniometers (SG110・SG150, Biometrics Ltd., Newport, UK) (Fig. 3.2). The goniometers were attached across the joints with medical adhesive tape, which did not inhibit the participant movement. The goniometers consisted of a cable inside a protective spring and strain gauges that sense the joint angles in the sagittal plane by detecting a change in strain along the length of the cable. Electronic voltages were outputted, and signals were transferred to a robotic controller. The calibration was performed so that the ankle joint angle was zero when the shank and foot were orthogonal, the knee joint angle was zero when the thigh and shank were in line, and the hip joint angle was zero when the torso and thigh were in line. The positive directions of the hip joint angle, the knee joint angle, and ankle joint angle were the extension, the flexion, and the dorsiflexion directions, respectively.

Parameters of four planes in the angular space are calculated by classifying angular data. The equation of the plane can be derived if the basis vectors of the plane and any selected point on the plane are derived. The coordinates $\boldsymbol{P}$ on the plane are expressed by

$$\boldsymbol{P} = \alpha 1\boldsymbol{w1} + \alpha 2\boldsymbol{w2} + \boldsymbol{R}, \tag{3.1}$$

where $\boldsymbol{w1}$ and $\boldsymbol{w2}$ indicate basis vectors, $\alpha 1$ and $\alpha 2$ are coefficients of the basis vectors, and $\boldsymbol{R}$ indicates the coordinates of the mean angle data in the swing phase.

Angular data are extracted from the middle of each motion for derivation of the basis vectors and one point of the four planes because it is difficult to detect the border of the planes. The maximum hip flexion angle was defined as 100º and the minimum hip flexion angle was defined as 0º. Angular data categorized as belonging to the motion of the swing up are extracted when the hip motion is in flexion and hip flexion angle is more than 10º and the knee joint is in flexion. Next, angular data categorized as the swing down motion are extracted when the knee joint is extending, and the hip flexion angle is less than 30º after the swing motion. Additionally, angular data categorized as the loading response (i.e., dual-support phase) are extracted when the hip joint is extending, the knee joint is flexing, and dorsiflexion angle of the ankle joint is less than 10% of the range of ankle joint angle from the second minimum value. Finally, parts of angular data categorized as the motion of supporting the body are extracted when the hip joint is extending and the

ankle joint is dorsiflexing. The coordinates $\boldsymbol{R}$ of the planes are derived by calculating the average of the extracted angular data for each motion. The extraction range does not change the basis vectors of the plane if the extracted data is on the same plane.

After extracting angular data, the basis vectors of each plane are calculated from the eigenvectors of the first and second components in principal component analysis (PCA) [3.24]. The first principal component is the vector that maximizes the data variance when all data are projected onto the axis of this vector. The second principal component is calculated to maximize the variance under the constraint condition that it is orthogonal to the first principal component. The principal components can be derived by solving the eigenvalue problem on the covariance matrix of the extracted angular data. There is an eigenvector corresponding to each derived eigenvalue; the eigenvector of the largest eigenvalue is the first principal component while the eigenvector of the second-largest eigenvalue is the second principal component.

Next, the algorithm detects in which plane the current measured angular data are by projecting the measured angular data onto the planes and comparing projection distance. The switching time point of the gait phase can be detected by monitoring the change of the planes to which the angular data belong based on the distance from a point before the projection to points projected onto each plane. The vectors from the coordinates before projection to the coordinates after projection and the two eigenvectors, $\boldsymbol{w1}$ and $\boldsymbol{w2}$, are perpendicular to each other; i.e.,

$$(\boldsymbol{P} - \boldsymbol{Q}) \cdot \boldsymbol{w1} = 0, \tag{3.2}$$

$$(\boldsymbol{P} - \boldsymbol{Q}) \cdot \boldsymbol{w2} = 0, \tag{3.3}$$

where $\boldsymbol{Q}$ indicates the coordinates of the lower-limb articular angular space before projection.

The norm of vectors $\boldsymbol{w1}$ and $\boldsymbol{w2}$ is one, and the inner product of $\boldsymbol{w1}$ and $\boldsymbol{w2}$ is zero. Therefore, $\alpha 1$ and $\alpha 2$ of each plane are calculated to derive the projected points, as follows:

$$\alpha 1 = \boldsymbol{Q} \cdot \boldsymbol{w1} - \boldsymbol{R} \cdot \boldsymbol{w1}, \tag{3.4}$$

$$\alpha 2 = \boldsymbol{Q} \cdot \boldsymbol{w2} - \boldsymbol{R} \cdot \boldsymbol{w2}, \tag{3.5}$$

The algorithm compares distances from a sensed angular point to a point projected onto each plane (Fig. 3.3). Moreover, the algorithm derives the inner product between the unit vector from previous to current sensed angular coordinates and the unit vector from previous to current projected coordinates for evaluating whether the data transition in the angular space is parallel with the plane or not. The switching time points (i.e., the time points of heel contact and toe-off) are obtained by detecting the state transition of the plane. The tangent line of the time function and projection distance from the measured angular point to the next motion's plane of the current plane, to which angular data belong, is calculated when the inner product is more than 0.9 and the projection distance to the next motion's plane is closer to the measured angular point than the current plane. The time of the switching point is detected by calculating the time when the tangent line reaches zero.

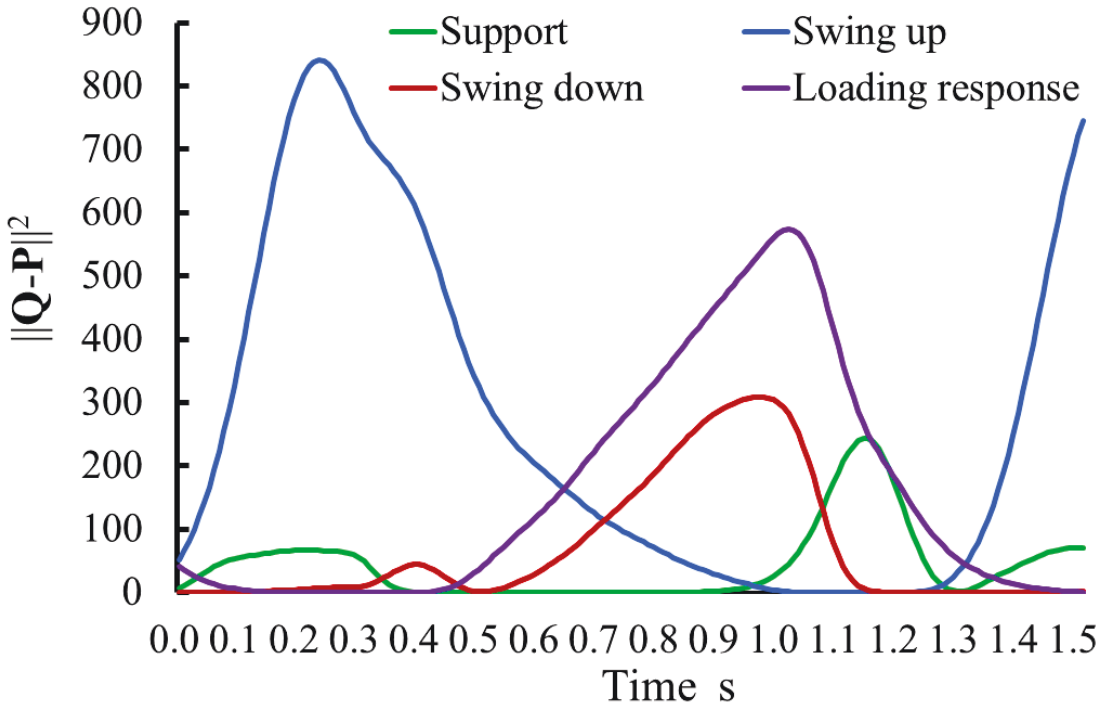

Figure 3.3. Distance from a sensed angular point ***Q*** to a projected point ***P***.

The author assumed that the switching point from the plane related to the swing down to the plane related to the loading response showed the timing of heel-contact and that the switching point from the plane related to the supporting to the plane related to the swing up showed the timing of toe-off.

3.3 Evaluation experiment protocol

Seven healthy adults (four men and three women; age: 27 ± 5 years, body weight: 57 ± 13 kg, height: 1.65 ± 0.14 m) with no neurological injuries or gait disorders were recruited. This experiment follows the principles of the institutional review board of Waseda University. The experimenter gave the participants detailed the experimental objectives and explained that they were able to withdraw from the experiment whenever they desired. The experiment was conducted after the obtainment of their consents.

Eight force plates (OR 6-7 2000, AMTI, Berkshire, UK) were used to detect the toe-off and heel-contact. Fig. 3.4 shows that two force plates in the lateral direction and four force plates were placed in the longitudinal direction. Table 3.1 shows the specification of the force plate. The data were measured when the participants walked at their preferred speed on the force plates. They started to walk approximately 60 cm before the force plates and stopped at a point approximately 60 cm after the plates. The experimenter instructed them to step on the left side of the force plates with their left foot and on the right side of the force plates with their right foot. Each participant walked 20 times.

20 gait cycles were extracted for analysis data of angles and floor force in each participant. The total number of gait cycles that were extracted was 138 (the data were not recorded in two parts) to evaluate the proposed algorithm. Measurements were performed only for the right lower limb because the gait phase and events can be obtained by measuring only one side. The sampling frequency of the measurement instruments was 125 Hz. Raw data were smoothed with a low-pass filter (cutoff frequency was 6 Hz) to remove high-frequency noise considering that the frequency of the cyclic joint movements during walking was less than 6 Hz in this experiment.

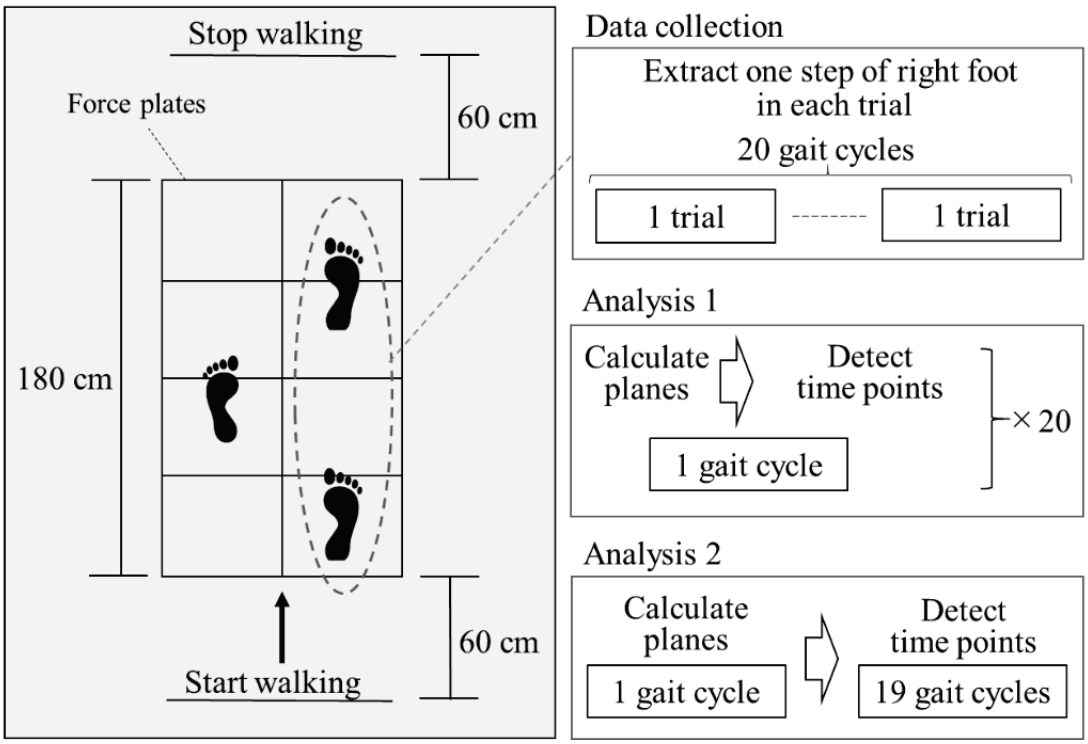

Figure 3.4. Experimental protocol.

Table 3.1 Specifications of the force plate.

Dimensions mm		464×508×83
Sensing elements		Strain gage bridge
Channels		Fx, Fy, Fz, Mx, My, Mz
Analog outputs		6 Channels
Temperature range	℃	-17.78 to 51.67
Fx, Fy, Fz hysteresis	%	±0.2 full scale output
Fx, Fy, Fz non-linearity	%	±0.2 full scale output

Initially, the parameters related to the plane for each gait cycle was calculated to investigate whether the proposed algorithm could classify the planes and detect time points of toe-off and heel-contact based on the switching points of the planes. To evaluate whether the points in the three-dimensional angular space was embedded on the planes or not, the contribution rates of the first and second components were derived by calculating the eigenvalue of each eigenvector divided by the sum of the eigenvalues. The mean value of the error and root-mean-square error (RMSE) between the calculation

results of the time points with the proposed algorithm and the force-plate-based method were derived. The toe-off and heel-contact were detected based on the values of the force plates by setting a threshold. The maximum force value of the unloaded plates was derived for deciding on-off threshold of the force plates. As shown in Fig. 3.5, the foot was recognized to be on the force plate if the reading of the force plate was higher than the maximum value of approximately the first 500 data that were collected when people were not on the floor force.

In sequence, the parameters of the planes were calculated using only the data of the first gait cycle. The time points of toe-off and heel-contact were derived using the other data of the 19 gait cycles to investigate whether toe-off and heel-contact could be detected in real time when the plane parameters are previously calculated with data of one gait cycle. The data were processed offline for time synchronization of joint angular data and floor force data. However, the detection of the plane to which the measured angular data belong was performed in time series. The mean value of the error and the RMSE between the calculation results of time points with the proposed algorithm and the force-plate-based method were derived.

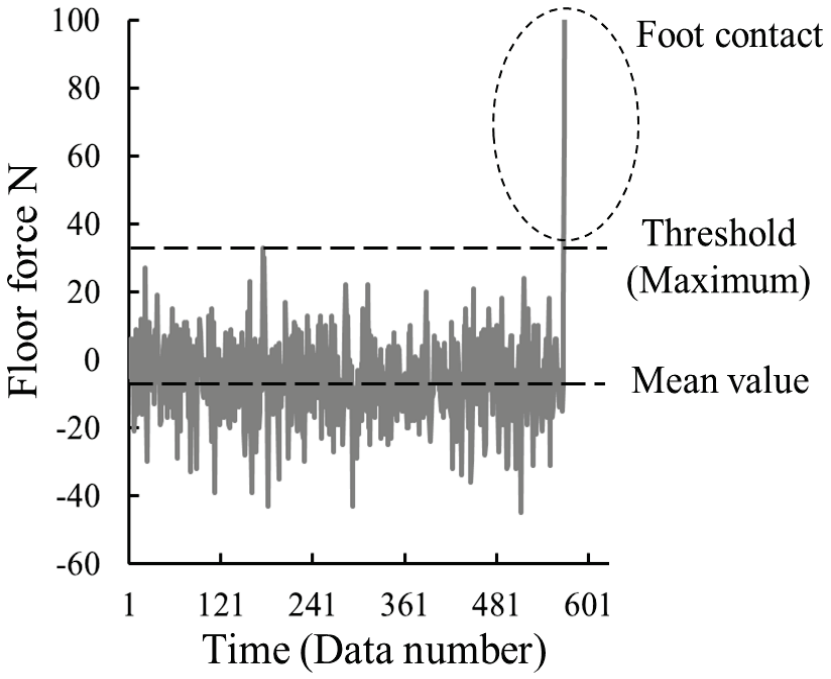

Figure 3.5. Force-plate method for detection of foot contact.

3.4 Result

Table 3.2 shows the contribution rates of the eigenvalues calculated with all participants data. The contribution rates of the first and second components were derived, and their sum exceeded 99%.

Table 3.2 Contribution rate of eigenvectors.

Type of motion	**Contribution rate**					
	First component		***Second component***		***First and Second components***	
	Mean %	***SD %***	***Mean %***	***SD %***	***Mean %***	***SD %***
Swing up	0.906	0.0783	0.0913	0.0761	0.998	0.0037
Swing down	0.964	0.0489	0.0331	0.0461	0.997	0.0054
Loading response	0.954	0.0665	0.0434	0.0632	0.9977	0.0050
Support	0.931	0.0931	0.0624	0.0766	0.994	0.0148

Table 3.3 Mean error between points.

	Mean error between time points derived by the proposed algorithm and the force-plate-based method	
	Time of heel contact (s)	***Time of toe-off (s)***
Analysis 1	0.00236	-0.00649
Analysis 2	-0.0151	0.0257

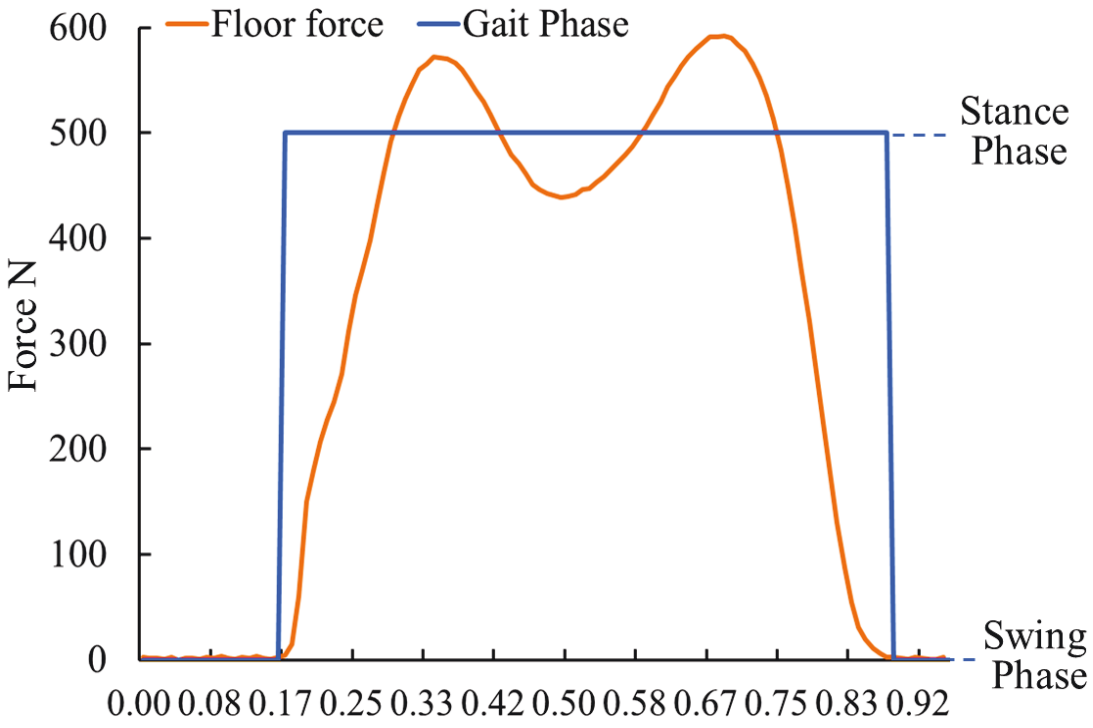

Figure. 3.6 Time-series floor force and gait phase detection of the proposed algorithm.

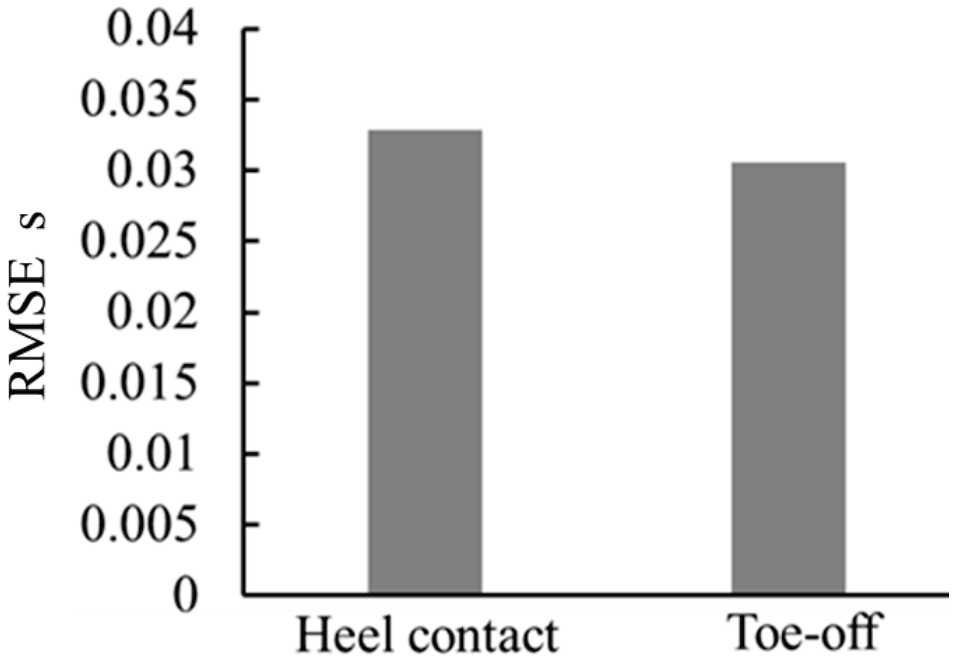

Figure. 3.7 RMSE using a plane calculated for each gait datum.

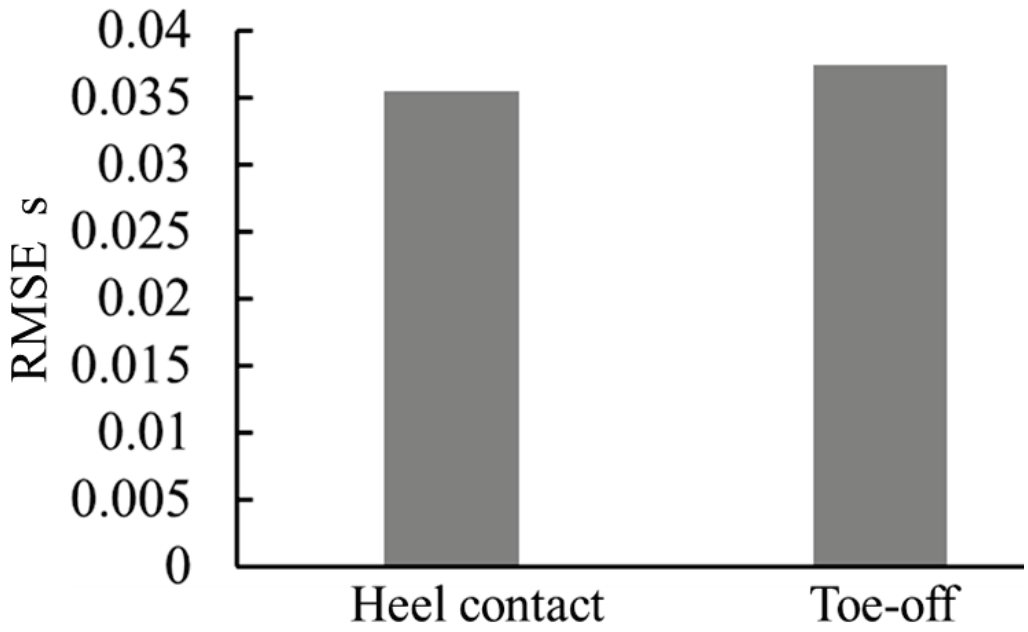

Figure. 3.8 RMSE using a plane calculated by one gait datum.

Table 3.3 indicates the mean error of time points of the heel-contact and toe-off. In Analysis 1, the force-plate-based method and the proposed algorithm were compared with each plane calculated for each gait datum. In Analysis 2, the force-plate-based method and the proposed algorithm were compared with the data of 19 gait cycles after deriving a plane with the one gait cycle data for each participant. Fig. 3.6 indicates one of the time-series results comparing the floor force data of the force plate and the gait phase derived with the proposed algorithm. Fig. 3.7 indicates the total RMSE of the heel contact and toe-off between the results of the force-plate-based method and the proposed algorithm with a plane derived for each gait datum. Fig. 3.8 indicates the total RMSE of the heel-contact and toe-off between the results of the force-plate-based method and the proposed algorithm based on a plane derived using data of one gait cycle. The heel-contact and toe-off were able to be detected in every gait cycle. The average duration of one gait cycle was 1.21± 0.0596 s.

3.5 Discussion

Table 3.2 indicates that the sum of the contribution rates of the first and second eigenvectors was approximately 99%, that is, little variance in each motion while the contribution rate of each component varied. Each combination of eigenvectors was calculated using angular data in the middle duration of each phase. This result shows that the three dimensions of angular variables of lower limb joints were reduced to two dimensions; i.e., a plane. Therefore, the planes in the angular space of lower limb joints could be extracted as a feature of inter-joint coordination during locomotion.

Both RMSEs of the heel-contact and toe-off detection were approximately 0.030 s between the results of the analysis based on force-plate and the proposed algorithm that derived a plane in every gait cycle, as shown in Fig. 3.7. The error was lower than 3% of the duration of one gait cycle. The result indicates that the transition of the plane is correlated with the phase transition of swing and stance phases. The joints motions in the stance phase are extension of the hip joint, small flexion and extension of the knee joint, and two repetitions of dorsiflexion and planar flexion of the ankle joints. The joints motions in the swing phase are flexion followed by extension of the knee joint during flexion of the hip joint, and dorsiflexion and planar flexion of the ankle joint. The number of parameters which are controlled for generating an endpoint motion is reduced as a strategy of the human central neural control system because the degree of freedom of the joints is abundant. The control objective of lower limb joints is different among gait phases: swing of the leg for lifting the foot and moving it forward, swing of the leg for preparing foot–ground contact, loading response for absorbing the shock of foot contact, and support for the body. The manner to reduce the degrees of freedom (i.e., the patterns of the inter-joint coordination) changes between gait phases. Therefore, there are some planes in the three-dimensional angular space corresponding to the gait phases. The point of switching from the plane of swing down to the plane of the loading response and the point of switching from the plane of support to the plane of swing up need to be detected for the identification of toe-off and heel-contact.

The RMSEs of the time points between results of the method based on the force plates

and the method using the proposed algorithm with a created plane were lower than 0.040 s as shown in Fig. 3.8, which accounts for 4 % of the gait cycle duration. The result implies that the plane in the angular space varies during walking because the accuracy was lower in the case where the plane was calculated using angular data of the first gait cycle than in case where the plane was calculated for every gait cycle. In contrast, the clustering results of the planes were not different except for data around the switching points. Although the analysis was performed offline, the algorithm could be used in real-time as soon as the angles were sensed once the planes were derived because the data were processed in a time-series order. Therefore, the planes could be classified and detected as a gait phase detection in real time. As the start of the stance and swing phases are identified, more detail gait events, such as a heel rise, can be identified by calculating the percentage of the gait cycle duration or the polar angle of the trajectory in angular space. Furthermore, the system can obtain the motion information of the lower limb joints in each phase. Therefore, the proposed algorithm can be used for the synchronization of a robot and a human during steady locomotion with only angular information. Although the sampling frequency of the measurement equipment (125 Hz) might increase the error of the detection of the timepoints, it did not affect the identification of the gait phase because the increase was smaller than 0.7% of the duration of one gait cycle. The result of the toe-off detection required the objective value in this study.

The wearable sensors were applied for the proposed gait phase detection algorithm because they can be easily attached to the body in daily life. Wearable angular sensors are more suitable for real-time gait training robotic control than force plates and cameras because the data of the goniometer are easily processed without location limitation. Moreover, because the goniometers are more durable than FSRs, the system can reduce the possibility of damaging the sensor and having the system behaving incorrectly during gait training comparing to the FSRs method. Furthermore, the estimation does not depend on the initial attachment placement of wearable sensors because the algorithm can be calibrated immediately and automatically, and features can be extracted using the PCA immediately.

Partitioning the data space of sensed variables is needed for classification. It is

difficult to find the margin of the cyclic trajectory of the angular data using the unsupervised machine learning algorithm because there is no gap between each part of the trajectory corresponding to gait phases. The adaptive oscillator can derive the frequency of the cyclic signal of the angles but cannot detect timings of heel contact and toe-off from the angular information. In previous methods, the margins of the angular cyclic trajectory were detected using the supervised methods, which requires the calibration with accurate training dataset by taking a time to collect the accurate dataset and train the algorithm. In contrast, the proposed algorithm allows the classifier to automatically find the margins corresponding to the heel-contact and toe-off. The proposed algorithm has advantages in terms of a lower computational load and quick adaptation to an individual relative to the supervised method because the proposed method does not require the accurate dataset for the training of the algorithm. Moreover, the proposed algorithm could detect the heel-contact and toe-off every gait cycle, i.e., the rate of the detection is higher than the rate of the conventional detection algorithms with the machine learning.

The algorithm had two main limitations in this work. First, noise influences the detection results because it is difficult to extract patterns of coordination between joint angles if the noise fluctuates the angular values. In particular, the author assumed that the degree of noise that depends on the electrical environment caused the individual differences in the proportions of two basis vectors to all variables and the detection accuracy. When the threshold of the low-pass filter was higher, the algorithm had a difficulty in detecting heel-contact and toe-off. Second, the algorithm was evaluated only for the forward gait. The coordination patterns of joints change depending on the types of gait, such as turns to the left or right. The classification of the planes related to more types of gait in multiple environments will be needed for future studies on the gait phase detection. The author assumes that the plane of the stance phase might not change and it can be detected even though the motion in the swing phase changes because the movement and coordination patterns of lower-limb joints in the stance phase do not change during stable walking in several locomotion tasks, such as stepping over an obstacle. This investigation focused on inter-joint coordination of one leg, but considering

inter-limb coordination will be beneficial for further accurate detection because both legs coordinate mutually.

3.6 Summary

In this chapter, the novel detection algorithm of the heel contact and toe-off was proposed. The algorithm derives the four planes in angular space of hip, knee, and ankle joints, and finds the switching points of the planes. The results of the experiment involving seven people shows that the change in the planes reflected the change in gait phases. Moreover, although the analysis was performed offline, the algorithm could be used in real-time as soon as the angles were sensed once the planes were derived because the data were processed in a time-series order. The RMSEs of the time points between results of the method based on the force plates and the method using the proposed algorithm with a created plane were lower than 0.040 s, which accounts for 4 % of the gait cycle duration. The result of the toe-off detection required the objective value in this study.

Chapter 4 Prediction algorithm of MTC

4.1 Background

The dispersion of the minimum toe clearance (MTC) needs to be controlled to ensure toe clearance and avoid tripping. The tripping possibility increases if the toe height becomes lower at an arbitrary timing. The prediction of toe clearance is necessary for robotic guidance to inhibit the toe clearance from reducing.

Methodologies of calculation using wearable sensors to estimate toe clearance have been studied mainly for monitoring the toe motion in daily life [4.1-4.5]. The integration of the inertial parameters of inertial measurement unit (IMU), which consists of tri-axial accelerometers and gyroscopes, was performed to estimate the toe parameters [4.1-4.3]. The de-drifted integration of two cableless IMUs attached to the feet can estimate the foot clearance with an error of approximately 20 mm [4.3]. Because this integration method has a large estimation error, it is difficult to calculate the position. The calculation method with a machine learning has been studied for estimation or prediction of the toe parameters after training the algorithm in each person [4.4-4.6]. Using machine learning with Gaussian functions and a hill-climbing feature-selection method, the root mean square error (RMSE) of 6.6 mm was estimated for young individuals [4.5]. The prediction of the toe parameters was also performed using the regression model with Gaussian function [4.6]. The author believes that gaussian functions that were applied using acceleration features through the double differentiation of the toe position captured with a motion capture system could predict the MTC most accurately (an RMSE of 3.7 mm) for one gait cycle ahead.

The conventional prediction method cannot increase the toe clearance only when it reduces for intermittent assistance of the gait training robot. This is because the proposal did not use the sensors that could be embedded with the robotic online control system. If

the wearable inertial sensor is used for obtaining toe acceleration information as an alternative to the camera system, the calculation accuracy is reduced. Furthermore, the conventional method did not have a sufficient accuracy to detect the lower values of MTC considering the MTC variability. The interquartile range of MTC is approximately 4.3 mm for young individuals and approximately 5.3 mm for older individuals [4.7]. Therefore, detection of lower values of MTC might be lower than 50 % and difficult for the proposal gait training assistance. A more accurate prediction method that uses wearable sensors to obtain the input data is required.

The hypothesis is that the information related to lower limb joints motion at toe-off is related to the future toe clearance because the swing joints motion generate the toe motion. The leg motion is controlled based on inter-joint coordination that maintains low variability of the position of the end point [4.9]. The author assumed that the difference between the angular information in a certain phase is related to the difference of toe clearance amongst the gait cycles. Moreover, the author believes the information of the angular velocity and acceleration of the lower limb joint would be helpful for prediction because these parameters contain information regarding the movement over time.

In this chapter, an algorithm to predict MTC using the angles, angular velocities, and angular accelerations of the lower limb joints is proposed. Machine learning based regression with Gaussian functions to probabilistically predict the toe clearance with consideration to the noise of the input data was applied. Moreover, maximum toe clearance during the swing phase was also predicted by the proposed algorithm because the information of both maximum and minimum toe clearance is helpful to monitor the toe trajectory and can be used for future research of robotic gait training system. Additionally, the author investigated the relationship between the number of training data and the prediction accuracy, and evaluated the prediction algorithm to investigate whether the method could predict more accurately the toe clearance and detect the lower value of toe clearance. The objective value of the MTC prediction error was lower than 2.5 mm considering MTC variability.

4.2 Methods

The proposed algorithm extracts input data based on gait event algorithm proposed in Chap. 3, and partitioned the data with a regression for prediction of characteristic parameters of the toe clearance. The radial basis function network (RBFN) was applied to partition the input data. The input values could be extracted automatically at toe-off, and toe parameters could be outputted after learning the RBFN. Fig. 4.1 shows overviews of the proposed algorithm.

As explained in Chap. 3, the gait event detection was based on the synergy between the leg joints. The four planes were derived by calculating the basis vectors constituting the planes when people started to walk. To extract the input data, only the switching time point from the stance phase to the swing phase was detected. The switching points were derived in each gait phase. The section plane of the angular trajectory was derived using the switching points.

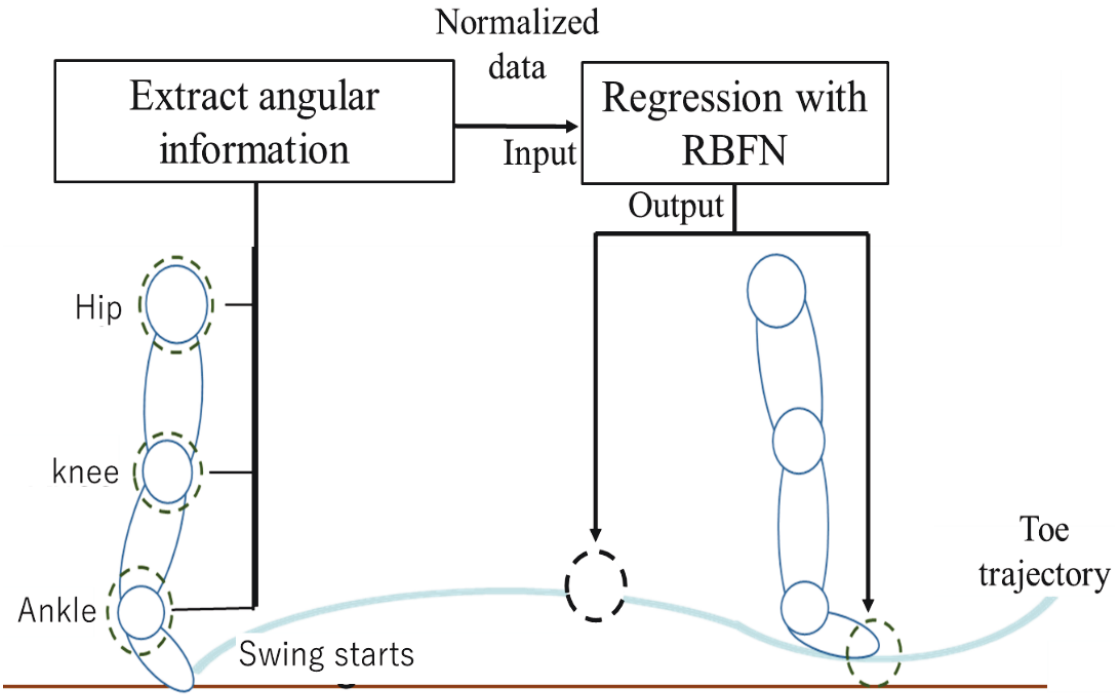

Figure 4.1: Overview of dataflow of proposed algorithm.

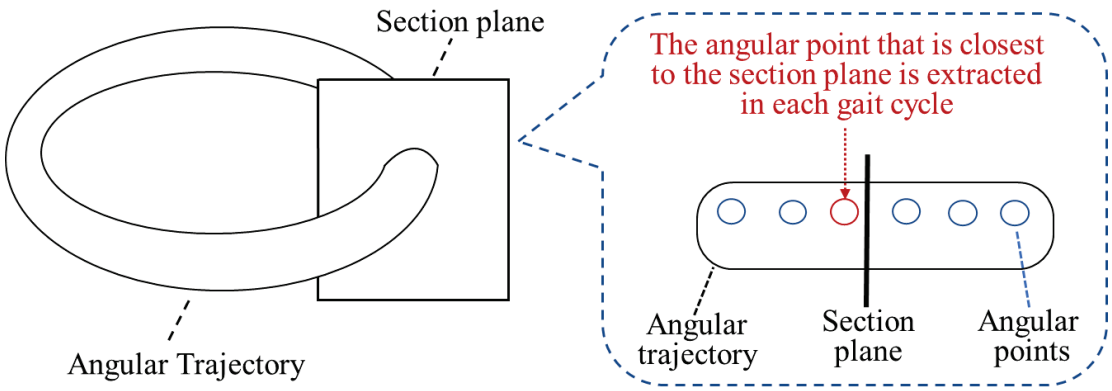

Figure 4.2 Extraction method of input values.

To derive the basis vectors of the planes, parts of the angular data were classified by reading the angles of the joints. After calculating the basis vectors with the PCA in each plane, the distance from the pre-projection coordinates to the post-projection coordinates onto each plane was calculated. Moreover, the algorithm evaluated whether the sensed angular trajectory was parallel to each plane or not. The unit vectors from a previous to the current sensed angular point and from a previous to the current projected point were derived. The sensed angular data were regarded as a point on a plane which was closer to the data than other planes, when the projection distance was the local minimum and the inner product was higher than 0.9.

The projection distance might vary because the planes shift during walking. The shifting of the plane makes the detection difficult in real-time. The author derived the section plane to detect the phase transition in real-time. Toe-off was detected by observing whether the angular trajectory passes through the section plane that was previously calculated using the plane structure, as shown in Fig. 4.2. To derive the section plane, 20 switching points were extracted, and mean value of switching points and basis vectors of the section plane were calculated. The basis vectors were derived by calculating the normal vector of the section plane that was the mean vector from the detected switching points to the next measured angular point. The orthogonal vector $\boldsymbol{O}$ of the normal vector was derived as follows:

$$\boldsymbol{O} = [2bc, -ac, -ab], \tag{4.1}$$

where *a*, *b*, and *c* indicate angles of the hip, knee, and ankle joint that are parameters of the normal vector, respectively. The other orthogonal vector was derived by calculating the cross product between the normal vector and the first orthogonal vector. The Angular values at toe-off were extracted by detecting the point where the distance from the measured angular point to the projected point onto the section plane was minimum, as shown in Fig. 4.3.

The toe clearance parameters were predicted with the RBFN consisting of Gaussian functions (Fig. 4.4). The RBFN is a three-layer artificial neural network whose hidden layer consists of radial basis functions. Because the RBFN is the linear sum of the radial basis functions, the parameters of the RBFN could be derived with linear square method. Therefore, nonlinear regression can be performed rapidly with the RBFN. The RBFN calculates output values based on the Euclidean distance between the vector of the input data and the centroids of each Gaussian. The centroids were derived with the K-means clustering algorithm which partitions the dataset into a predetermined number of groups based on the Euclidean distance. The RBFN structure is expressed as follows:

$$\boldsymbol{y} = \sum_{k=1}^{N} \boldsymbol{W_k} \exp\left(-\frac{\|\boldsymbol{x} - \mathbf{c_k}\|^2}{\sigma}\right) + \gamma \tag{4.2}$$

where $\boldsymbol{y}$ indicates the output vector, $\boldsymbol{W_k}$ indicates the weight vector, $\boldsymbol{x}$ indicates the input vector, $\boldsymbol{c_k}$ indicates the centroid vector, N means the number of RBF units, γ means a variable coefficient, and σ means a variable of the standard deviation of the Gaussian function. σ was derived as follows [31]:

$$\sigma = \frac{d_{max}}{\sqrt[m]{Nm}} \tag{4.3}$$

where $\boldsymbol{d_{max}}$ indicates the maximum distance amongst the data and, m indicates the data dimension.

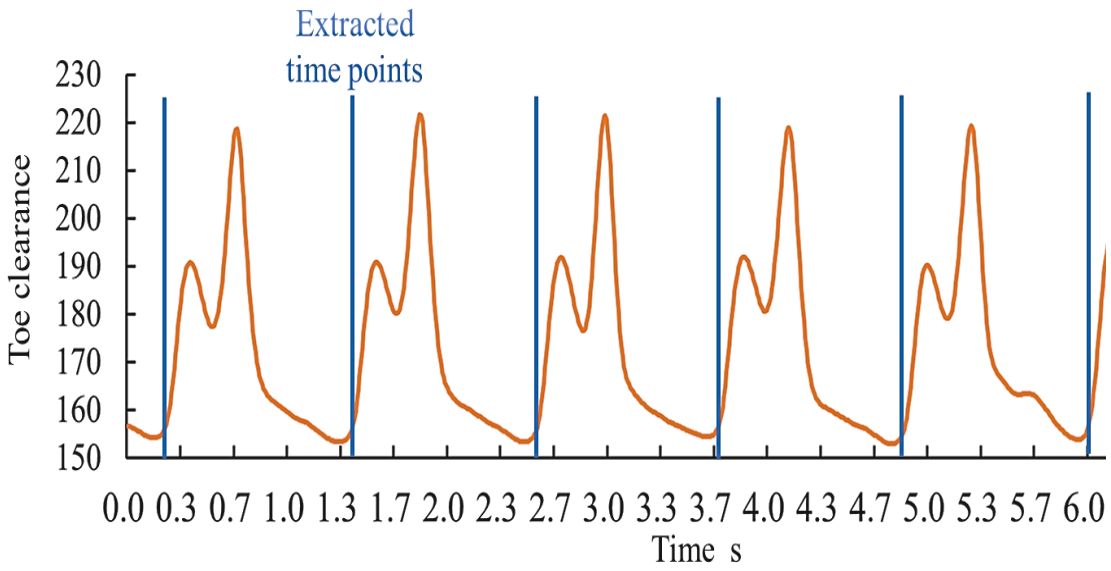

Fig. 4.3 Gait phase detection result of extracting time points.

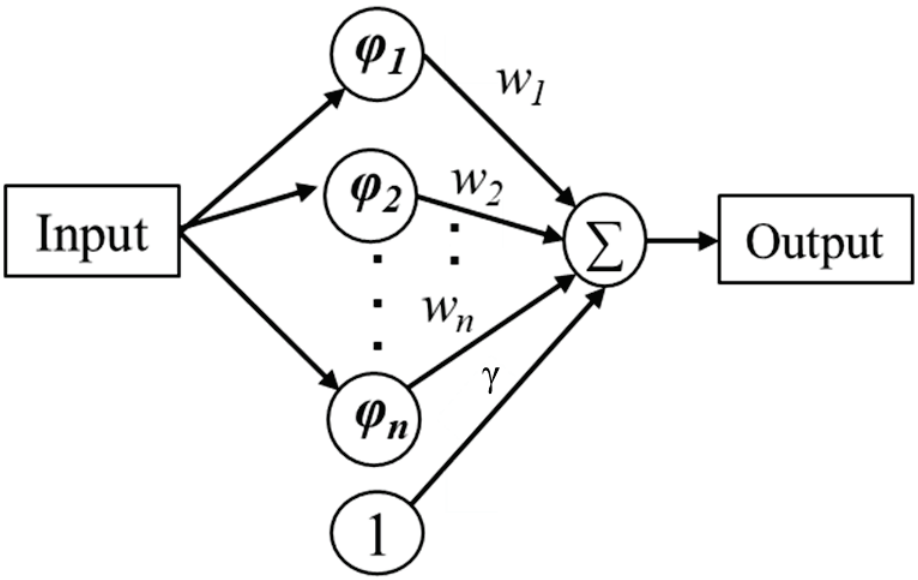

Fig. 4.4 Structure of radial basis function network (RBFN).

The hip, knee, and ankle joints angles in the sagittal plane were measured using the goniometers. The angular velocity and angular acceleration of these joints were calculated by differentiating the angles using a pseudo differential. The angles were smoothed using a low pass filter (cutoff frequency was 6 Hz). The transfer function of the pseudo differential was:

$$\frac{x_{out}}{x_{in}} = \frac{s}{1+T_d s}, \tag{4.4}$$

where T_d indicates the time constant. In this work, T_d was 167 ms to differentiate data whose frequency was lower than 6 Hz. An s-plane to z-plane transform based on the backward difference were conducted as:

$$s = \frac{1 - z^{-1}}{\Delta T}, \tag{4.5}$$

where ΔT indicates the sampling time, which was 8.33 ms in this chapter's experiment. The equation of the pseudo differential was substituted into (4.4) as

$$\boldsymbol{x_{out\_n}} = \frac{\boldsymbol{x_{in\_n}} - \boldsymbol{x_{in\_n-1}} + T_d \boldsymbol{x_{out\_n-1}}}{\Delta T}, \tag{4.6}$$

where $\boldsymbol{x}_{out\_n}$ and $\boldsymbol{x}_{in\_n}$ indicate the nth differential value and the nth input value, respectively.

All input values were normalized for reducing the effect of the attachment position deviation of the wearable angle sensors. The minimum values in the previous gait cycle were subtracted from the input values. Additionally, all values of input data were divided by their range of values in the first gait cycle in the phase of learning RBFN parameters in order to decrease the effect of difference in the range of values.

4. 3 Evaluation experiment

Four healthy young adults (four male and one female; aged 27 ± 5 years, body weight 57 ± 13 kg, height 1.64 ± 0.13 cm) and two healthy old adults (two male; aged 65 ± 2 years, body weight 62 ± 1 kg, height 1.68 ± 0.03 cm) took part in the first experiment. Five healthy young adults (four male and one female; aged 25 ± 3 years, body weight 58 ± 9 kg, height 1.63 ± 0.7 cm) took part in the second experiment. All of them did not present neurological injuries or gait disorders. The subjects walked on a treadmill, as shown in Fig. 4.5. This experiment follows the principles of the institutional review board of Waseda University. The author gave the participants detailed the experimental

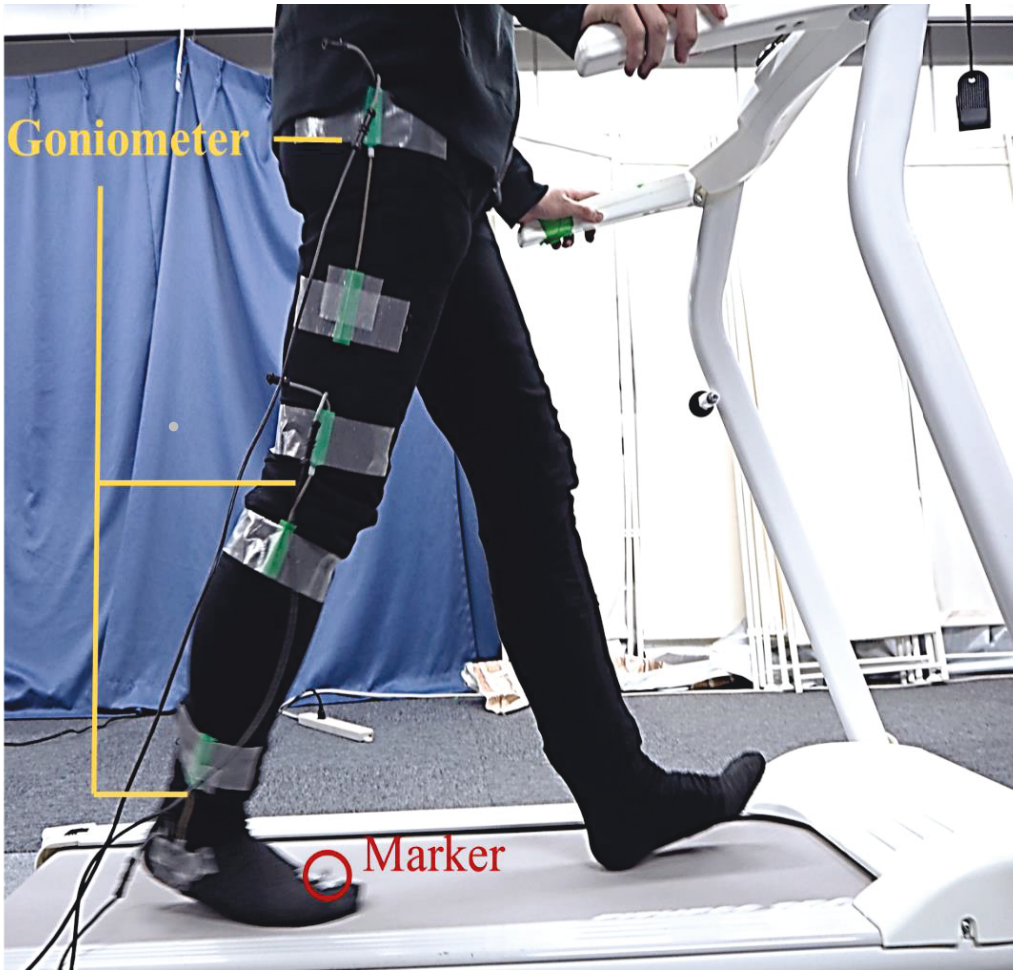

Figure 4.5 Experimental image of subjects walking on treadmill.

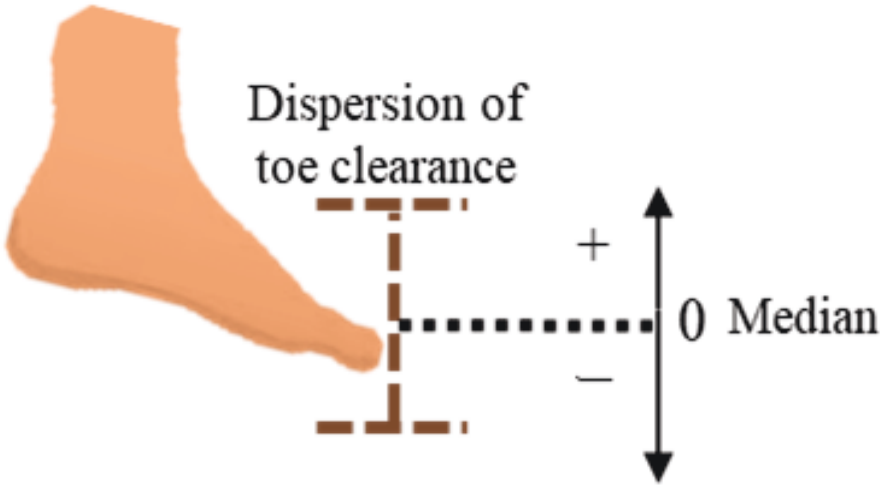

Figure 4.6 Normalization of toe clearance data.

objectives and explained that they were able to withdraw from the experiment whenever they desired. The experiment was conducted after the obtainment of their consents.

As the maximum and minimum values are an indicator of how high a person lifted the toe and how high a person can keep the toe from the ground, respectively, the maximum toe clearance that was detected in the earlier swing phase and MTC that was detected in the later swing phase were extracted as characteristic toe clearance parameters. The goniometers (SG110 and SG150, Biometrics Ltd., Newport, UK) were used to sense the leg joints angles. The toe height information of the right foot was obtained using the motion capture system (Raptor-E; Motion Analysis, Santa Rosa, CA, USA). The author attached the marker that was captured by the motion capture system to the first metatarsophalangeal joint of the right foot.

In the first experiment, the 6 subjects participated in the experiment and walked on the treadmill for 360 s at a preferred constant speed (2.1 to 3.0 km/h). The needed number of training data points for learning the RBFN parameters which improved the accuracy of the prediction was investigated. 20 to 200 gait cycle data points for training of the RBFN and 100 gait cycle data points for RBFN test were used. The number of RBF units was set from two to twenty.

In the second experiment, the 5 subjects were instructed to walk on the treadmill for 600 s at 2.0 km/h, 2.5 km/h, and 3.0km/h. The duration of walking at 2.5 km/h was 360 s, and the durations of walking at 2.0 km/h and 3.0 km/h were 120 s, respectively. Investigation for the prediction ability of the RBFN was performed when the gait speed changed. The approximately 160 cycle data were collected as the training data when people walked at 2.5 km/h in the first experiment, and the 100 gait cycle data points were collected as the test data when people walked at 2.0 km/h and 3.0 km/h. The number of RBF units was set from two to twenty. Additionally, the goniometers that measured the angles of the left leg were also used in this experiment.

The time from the point where the input data were extracted to the points where the toe clearance reached the maximum and minimum values were derived. The average time of all training data and the standard deviation were calculated to evaluate whether both

the maximum and minimum clearances could be previously predicted.

The maximum and minimum toe clearance values were normalized. As shown in Fig. 4.6, the mean value of the training data was defined as zero. The values of maximum or minimum toe clearance that were higher than the mean value were positive (plus sign), and the values that were lower than the mean value were negative (minus sign). The RMSE between the grand truth data and the predicted data of the maximum and minimum toe clearances was calculated, as follows:

$$\mathrm{RMSE}=\sqrt{\frac{\sum_{k=1}^{n}(y_k-\tilde{y}_k)^2}{n}} \tag{10}$$

where y_k indicates the true value, $\widetilde{y_k}$ indicates the predicted value, and n means the number of data points.

Moreover, the accuracy percentage of the predicted data was calculated based on the accuracy of the plus or minus signs, i.e., the ratio of the number of predicted values that were the same sign as the measured value to the total number of data points.

4.4 Results and Discussion

Fig. 4.7 indicates the time from the points where input data were extracted to the points where the toe clearance reached the maximum or minimum value. The input data could be extracted 0.1 s before the toe clearance was the maximum in the earlier swing phase.

Fig. 4.8 shows an example of the calculation result of MTC using the training dataset. The horizontal axis shows the real MTC that was measured by the motion capture system, and the vertical axis shows the calculated MTC as a result of learning parameters of the algorithm. Zero value of each axis means the median in a subject. Although it has a large variance, the tendency of the correlation can be observed. In contrast, the range of the calculated values was smaller than the real value. Moreover, the larger or smaller MTC is, the higher number of outliers could be observed. The author assumed that the number

of values near the maximum or minimum MTC was fewer and it was difficult to extract the pattern of these values. However, the plus or minus could be detected.

Fig. 4.9 shows an example of RMSE between the predicted MTC and the true MTC for each number of RBFN units in a subject. Although the number of RBFN units that minimized the RMSE differed in each subject, the RMSE tended to increase when the unit number was over 17. The author assumed that overtraining occurred and the accuracy decreased when the unit number was over 17. The number of RBF units that minimized the RMSE was applied in each participant.

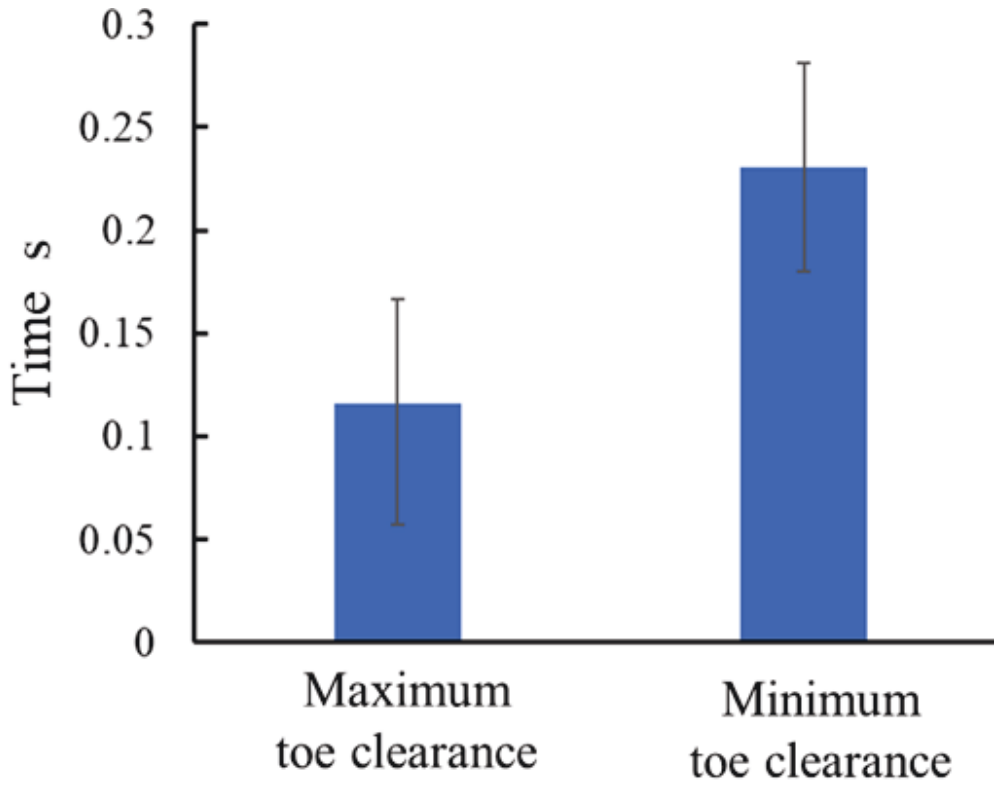

Fig. 4.7 Duration from extraction time to the time of parameters of toe clearances. The error bars indicate the standard deviation.

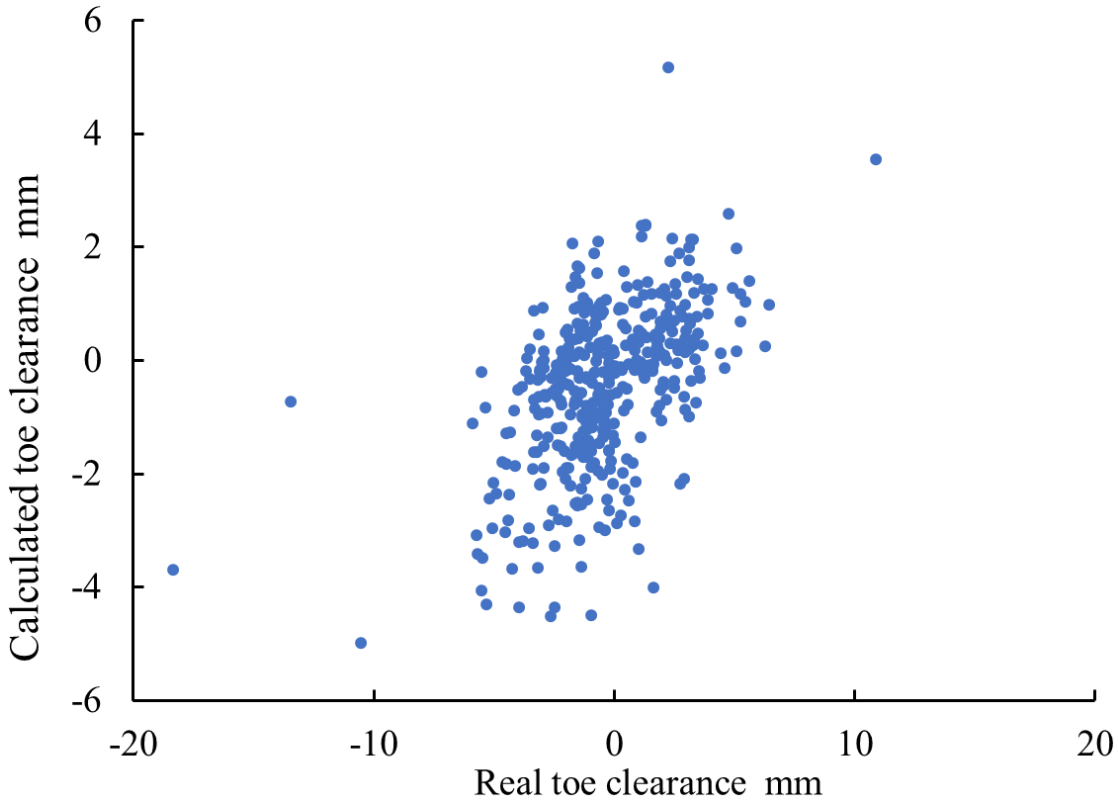

Fig. 4.8 Example of calculated versus real MTC in training data.

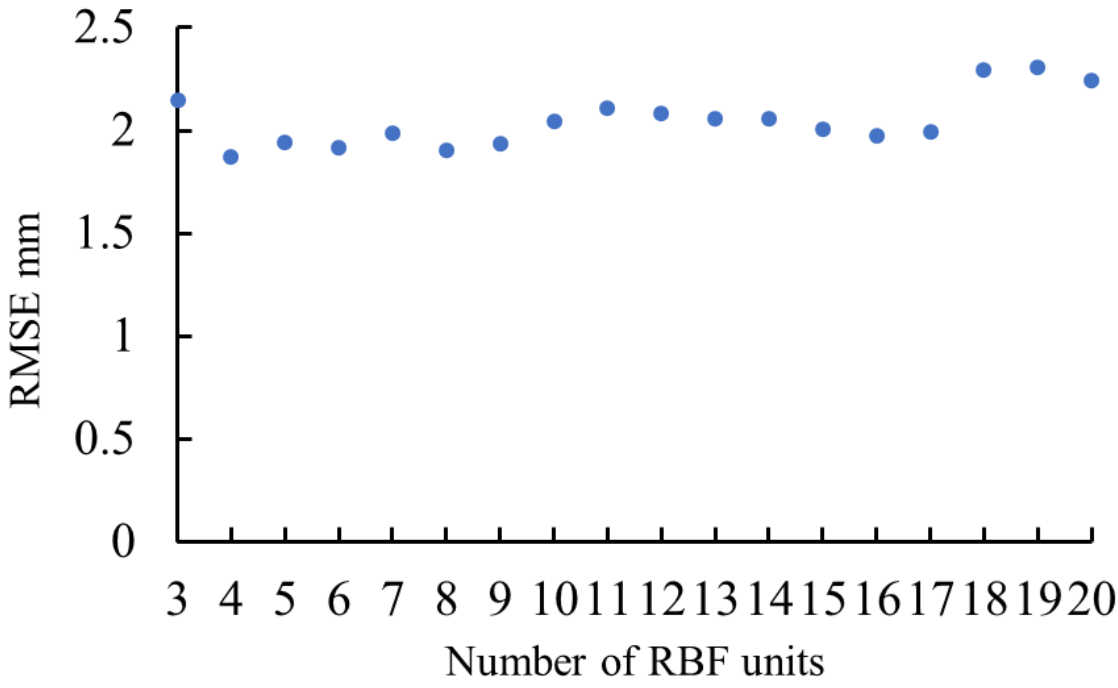

Fig. 4.9 Example RMSE between the predicted MTC and the true MTC for each number of RBFN units.

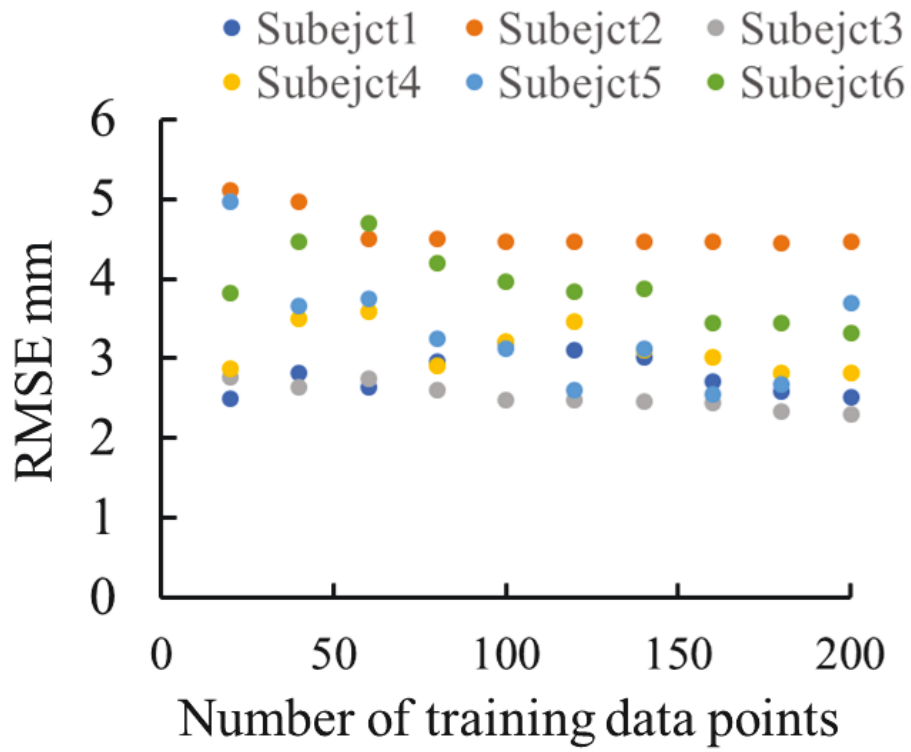

Fig. 4.10 Prediction result for maximum toe clearance using 100 test gait data (RMSE).

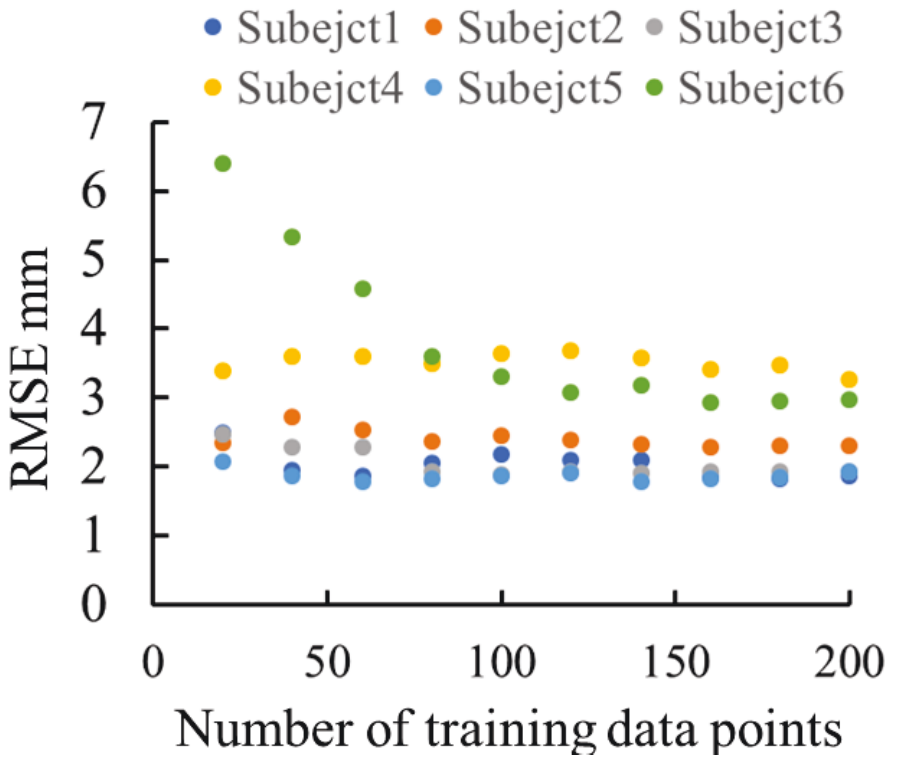

Fig. 4.11 Prediction result for minimum toe clearance using 100 test gait data

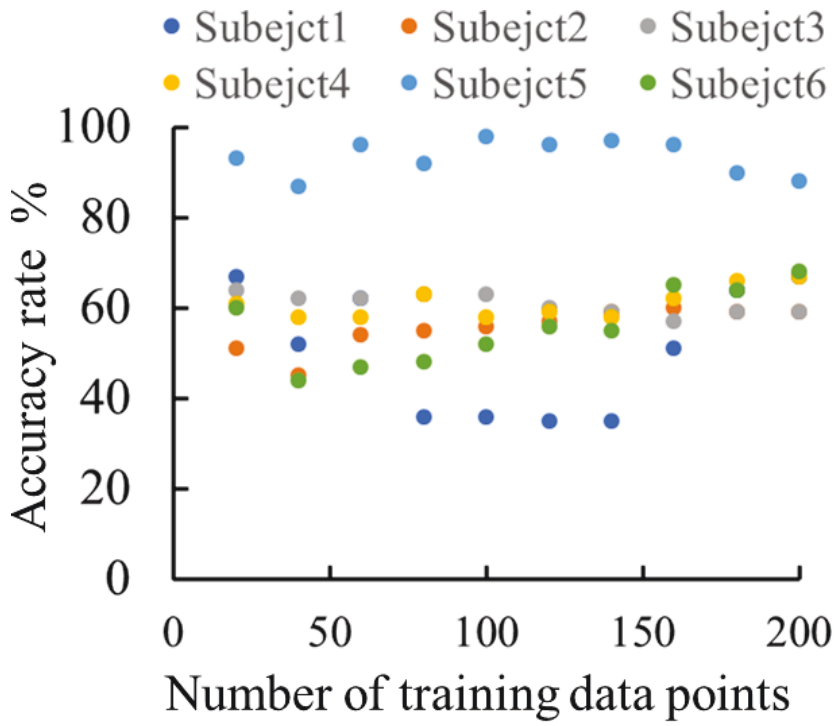

Fig. 4.12 Prediction result for maximum toe clearance (accuracy rate).

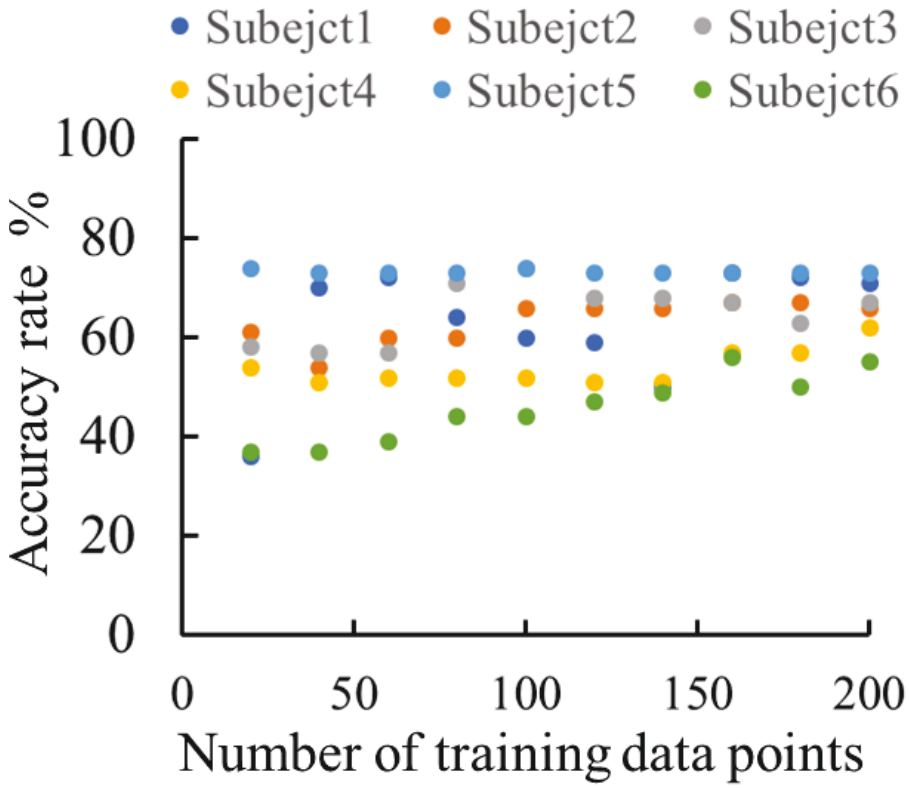

Fig. 4.13 Prediction result for minimum toe clearance (accuracy rate).

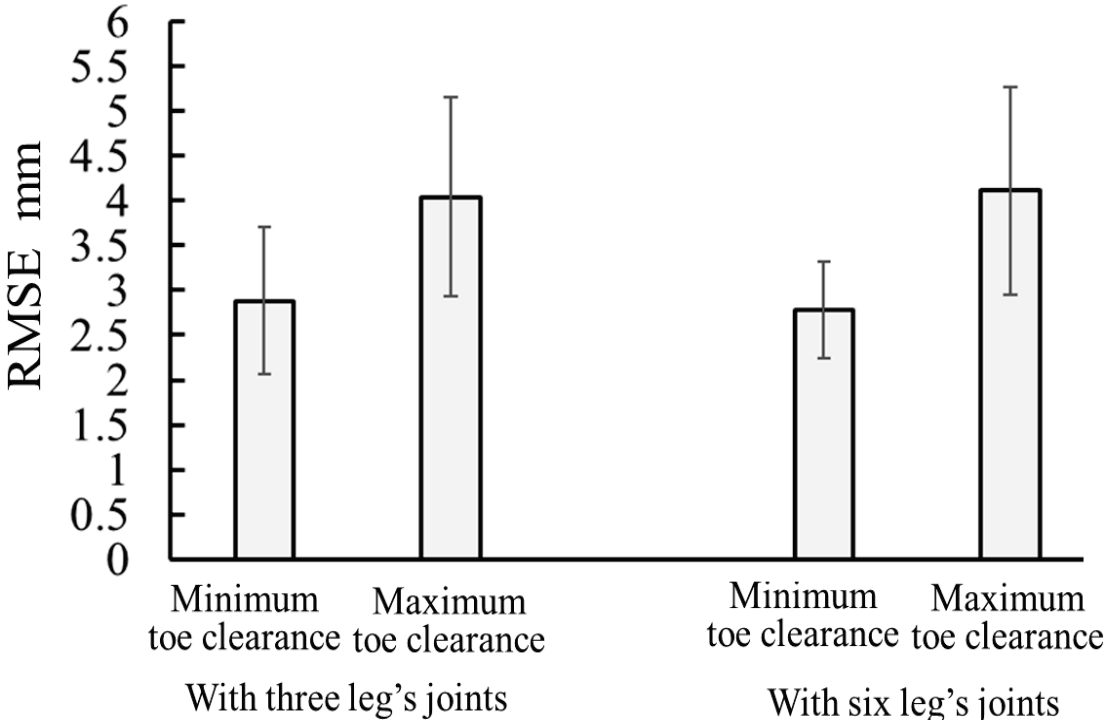

Fig. 4.14 The prediction result when the walking velocity changes (RMSE). The error bars indicate the standard deviation.

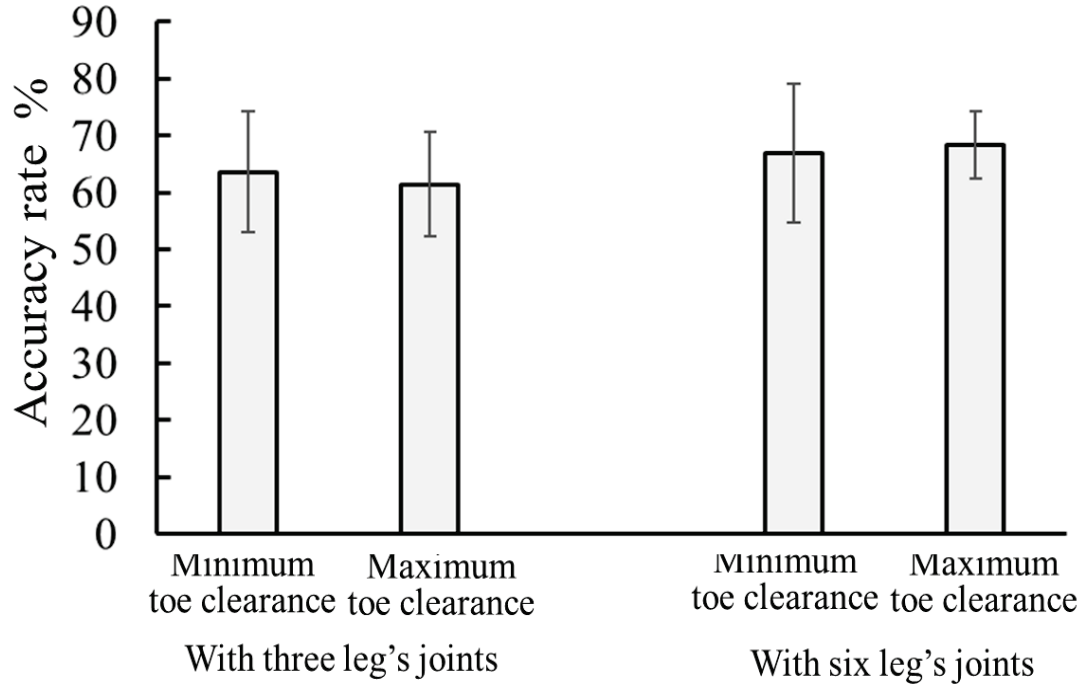

Fig. 4.15 The prediction result when the walking velocity changes (Accuracy rate). The error bars indicate the standard deviation.

Figs. 4.10 and 4.11 show the RMSE between the true and predicted data for the maximum and minimum toe clearances corresponding to the number of training data points. The RMSE tended to reduce if the higher number of training dataset was used. In particular, the use of 200 dataset made the RMSE minimum for subjects 1, 3, and 6. The RMSE was minimum for other subjects if the number of training dataset was between 80 and 180. The average minimum RMSE of maximum toe clearance was 2.99 mm, and the lowest RMSE was 2.31 mm. The average minimum RMSE of the MTC was 2.34 mm, and the lowest RMSE was 1.79 mm. The accuracy rate of the predicted data of both the maximum and minimum toe clearances in each the number of training dataset is shown in Figs. 4.12 and 4.13, respectively. The average accuracy rate was 71% and 68% for the maximum and minimum toe clearances, respectively.

Fig. 4.7 shows the average time from the time points where the system extracted the input data to the time points where the maximum or minimum toe clearances were positive. This indicates that the algorithm could calculate and derive the parameters of the toe clearance previously using input parameters in the early swing phase.

Figs. 4.10 and 4.11 show that the RMSE between the ground truth toe clearance measured by the motion capture system and the predicted toe clearance was the lowest if the number of training dataset was between 80 and 200. Furthermore, the increase in the number of training datasets tended to improve the prediction accuracy rate. Therefore, it is better for the algorithm to include a higher number of training dataset because it easies the extraction of the characteristics of the dataset. The RBFN algorithm classifies the input data space and derives the medians of each cluster during the training of the network. The output value is calculated based on the deference of the input data value from the medians. As the number of training data points is reduced, the effect of input data noise increases, which hinders the accurate determination of RBFN parameters. Classification of training dataset and determination of medians required about 100-200 training dataset to reduce the variance and impact of noise that is always included in the data in the experiment.

As shown in Figs. 4.10 and 4.11, the RMSE was 2.99 mm for the maximum toe

clearance and 2.34 mm for the MTC, which is a more accurate prediction compared with previous methods. The RMSE of the maximum toe clearance was higher than the RMSE of the MTC because the deviation in maximum toe clearance was higher than the deviation in MTC. Individual differences in RMSE tended to increase when the variability of toe clearance between gait cycles was higher. The probability of detection of values that were lower than the median was over 68%. In other words, the probability was higher than the probability of random detection.

Figs. 4.14 and 4.15 show the RMSE and the accuracy rate as the predicted results for the maximum toe clearance and MTC using approximately 160 training datasets in cases where the walking velocity changed. The MTC prediction error was lower than the results of the previous studies even if the gait speed was different from the constant gait speed when the RBFN was trained. Moreover, the RBFN algorithm could find the values that were lower than the median toe clearance with the higher rate than the random detection rate even in case where the gait velocity changed. The author assumed that the RBFN parameters represented difference of foot movement related to the change of the gait velocity because the input variables corresponded to the kinematics generating the foot movement. However, the change of the gait velocity increased the RMSE of both maximum and minimum toe clearances. Therefore, it might be better for RBFN to be trained using the input dataset in multiple gait speed conditions for generalization of the regression. Furthermore, the standard deviation of the RMSE in all subjects reduced if the angle, angular velocity, angular acceleration of the left leg joints were used as input variables. The author assumed that it indicated that the prediction accuracy can be improved if more numbers of input variables related to kinematics generating foot movement are used. As a future study, both feet and increase in input parameters of joints of both lower limbs will be considered.

The proposed algorithm has the advantage of predicting preliminary toe clearance in real time, while the conventional calculation methods were created to estimate toe clearance [4.10-4.14]. Furthermore, the proposed algorithm was more accurate comparing the previous prediction methods [4.15]. The output value of the RBFN was the normalized toe clearance value to evaluate if the algorithm could detect the lower

values than median toe clearance. However, the real toe clearance value can be derived by adding the subtracted value. One of limitations of the proposal algorithm is that the training of the RBFN is needed in each person, which is the same as previous MTC estimation methods using wearable sensors. The system requires a training phase using a camera system before using the prediction algorithm.

The accuracy became lower if subjects had a tendency of changing the planes of the angular space during walking. As shown in Fig. 4.7, the duration varied between gait cycles. The variance of the phase timing to extract input data might reduce the prediction accuracy. The angular information always changes with time within one gait cycle. One point on the periodic trajectory in angular space was extracted in each gait cycle. If phase detection errors occur, it is difficult to compare the articular angle, angular velocity, and angular acceleration differences among the gait cycles. The plane structure of the angular space of the lower limb joints was used for detection of the phase transition. The basis vectors of the planes might change between the gait cycles because the trajectory shape was different between the cycles. Therefore, the proposed algorithm calculated the section plane of the angular trajectory when the phase changed to the swing phase (swing up) from the stance phase (support) to consider the change of planes. Although this study demonstrated that the toe clearance parameters can be predicted using only angular information in the sagittal plane, the algorithm can still be improved and more robust. The accuracy of gait phase detection and the prediction of toe clearance may improve by increasing the input parameters, such as the angles in coronal plane or the foot contact information.

4. 5 Summary

In this chapter, a novel prediction of toe clearance parameters algorithm with an RBFN using the angles, angular velocities, and angular accelerations of the hip, knee, and ankle joints in the sagittal plane was proposed. The proposed algorithm aimed at predicting MTC in the later swing phase. In addition, the algorithm could predict the

maximum toe clearance in the earlier swing phase. The RMSE was 2.99 mm for the maximum toe clearance and 2.34 mm for the MTC. Additionally, the RMSE between true and predicted values was 4.04 mm for the maximum toe clearance, and 2.88 mm for the MTC in the condition where the gait velocity changed. The RMSEs of the MTC are smaller than previous studies. Values of the MTC that were lower than the median could be detected with higher probability than 68%; that is, the detection accuracy of the proposed algorithm was better than the random detection. The proposal met the objective value in this study. Therefore, a robot using this algorithm may be able to influence the distribution of the MTC. In future studies, the gait phase detection method will be improved. Moreover, experiments to investigate the effect of robotic assistance with the proposed toe clearance prediction algorithm on older people will be performed

Chapter 5 Evaluation of prediction-based assistance

5.1 System flow

The proposal robotic system performed the intermittent force application to increase lower values of the MTC based on prediction results of the MTC. The overview of the system flow is shown in Fig. 5.1. The robotic system was controlled using the lower limb joints angles based on the hardware system that was proposed in Chap. 2, the detection algorithm of toe-off that was proposed in Chap. 3, and the prediction algorithm that was proposed in Chap. 4. The proposal system is the prediction-based assistance of MTC to achieve the assistance as needed in terms of toe control for prevention training to avoid tripping.

The input data were eighteen variables related to the motion of foot: angles, angular velocity, angular acceleration of hip, knee, and ankle joints in the sagittal and coronal planes. The angles were measured using the same wearable two-axis angular sensors as the ones explained in Chap. 4. The angular velocity and angular acceleration of these joints were derived by differentiating the angles with a pseudo differential. The input parameters were smoothed with a low pass filter (cutoff frequency was 6 Hz) because noise frequency was over 6 Hz.

The timing of toe-off was detected by the plane-based detection algorithm that was proposed in Chap. 3 using an angular space consisting of the lower limb joints' angles in sagittal plane. The system calculated vectors constituting four planes corresponding to four motions (lifting of the foot, foot–ground contact, loading response, and support for the body), and extracted the switching points to the plane related to lifting of the foot from the plane related to support of the body by considering the distance of the sensed angular

point from the section plane. The section plane was calculated by deriving previously switching points from the plane related to supporting the body to the plane related to lifting foot with the data of the 20 gait cycles.

The RBFN was applied after extracting the input data as explained in Chap. 4. The RBFN parameters were the centroids of the gaussian functions and weight vectors of each gaussian function. The centroids were derived using the K-means method clustering the input parameters into a predetermined number of groups (2 to 20 units). The weight vectors were calculated with the least squares problem of example input-output pairs. The training of the RBFN can be performed rapidly (less than 1 s in this work) after collecting the training dataset.

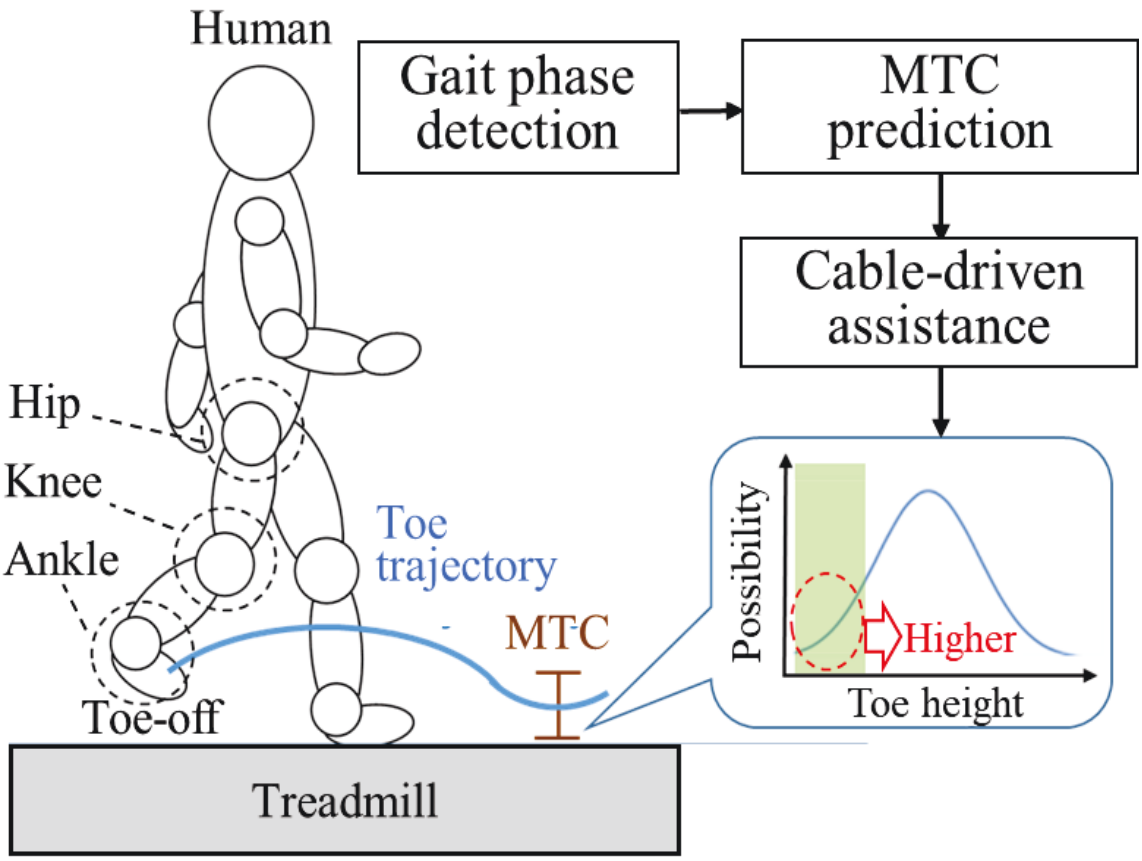

Figure 5.1. Overview of the proposed system.

The input variables were normalized to eliminate the difference of the range of values because the output of RBFN relied on the difference of the input values from the centroids. First, the standard deviation of each variable in the training dataset was derived. Next, each measured input value was divided by each standard deviation, that is, the measured input vector was divided by the vector of the standard deviation.

A cable-driven system that could switch between modes in which force is applied and not applied was used. Force was applied to a part of the shank and generated the knee flexion torque, which lifted the toe because knee flexion has the largest contribution to toe clearance. The start timing of the force application was at toe-off after prediction because generating assistive knee flexion torque around toe-off can increase MTC, which was shown in Chap. 2. The motor was not activated when the prediction MTC was higher than the mean value or the gait phase was not the early swing phase, and the movable pulley compensated for the cable length. After detecting that the predicted MTC was lower than the mean value, the motor was activated to pull the cable for force application while the knee joint was flexing. The pulled cable tension was controlled by the rotational position control of the motor. The motor rotational position returned to original position after short-term force application.

5.2 Evaluation experiment

5.2.1. Investigation of the effect of intermittent force application

Effect of the intermittent force application without prediction on after-effect was analyzed in the first experiment. Five healthy adults (four men and one woman; aged 27 ± 5 years, body weight 57 ± 13 kg, height 1.64 ± 0.13 cm) with no neurological injuries or gait disorders participated in the experiment. This experiment follows the principles of the institutional review board of Waseda University. The author gave the participants detailed the experimental objectives and explained that they were able to withdraw from the experiment whenever they desired. The experiment was conducted after the obtainment of their consents.

Initially, the harness and robot were attached to the participants. In the experiment, the participants were instructed to walk on a treadmill at 2.5 km/h. A measurement always started after participants walked on the treadmill for 10 s and their gait reached a steady state. The gait was analyzed for 20 s before and after the intermittent force application phase because working memory remains for 20 s [5.1]. The first phase duration was 20 s with normal walking without the intermittent force application. The next phase duration was 40 s with the intermittent application of tensile force to the knee. The final phase also lasted with 20 s of normal walking without the intermittent force application. The participants continued to walk throughout all phases.

The frequency of the force application of the gait-training robot was changed to either once in one gait cycle, once in two gait cycles, or once in three gait cycles. The force was applied at approximately 28 times when the force application frequency was once in one gait cycle. The force was applied for a short time from toe-off, which was detected based on the parameters of the planes that the system calculated in the first phase before the robot started assistance. Three sets of trials for each subject were conducted. The mean frequency of the gait cycle was approximately 0.70 Hz.

The change of maximum knee joint flexion angle between before and after the force application phase was analyzed. In addition, the mean value of the increase rate for each force application frequency of each subject was calculated to investigate the effect of the force application frequency on the change of the gait. Moreover, the increase rate of maximum knee joint flexion angle between before and during the force application phase was analyzed in a condition where the increase in the knee joint angle after the duration of the force application was maximum in each subject for investigating whether the change in gait was caused by the robotic assistance or not. Furthermore, the increase rate of the MTC which was sensed with the motion capture system (Raptor-E; Motion Analysis, Santa Rosa, CA, USA) was also analyzed in the same condition. The analysis of variance on the data was performed in each subject for investigating whether the angles significantly increased or not. There were approximately 13 samples in each trial for each participant.

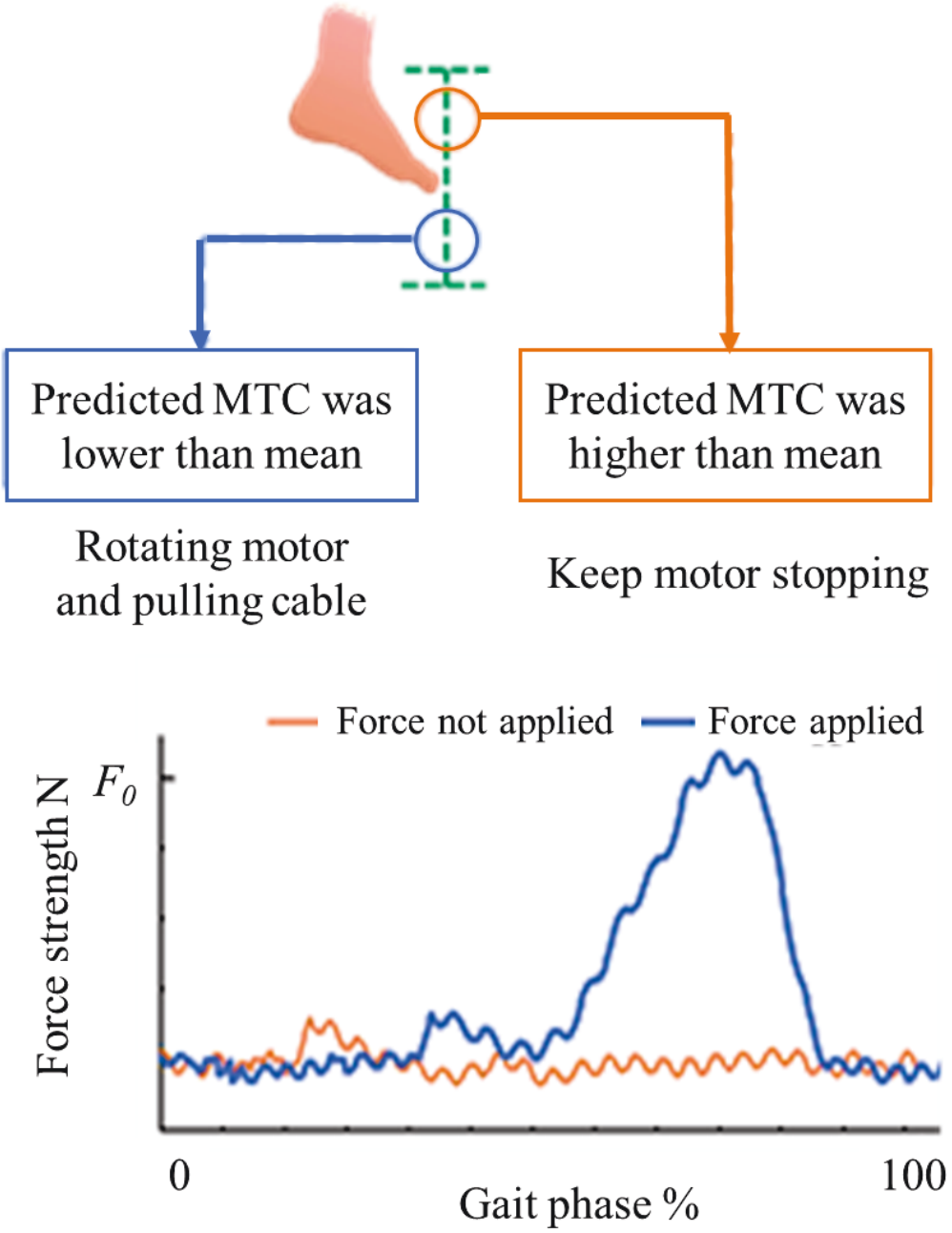

Figure 5.2 Intermittent force application method.

5.2.2. Evaluation of the effect of prediction-based training

Eight younger adults (four men and four women; mean age 25 ± 5 years, mean weight 56 ± 16 kg, mean height 1.63 ± 0.09 m) with no neurological injuries or gait disorders participated in the study. Before the experiment, the subjects were provided with details

of the study goal (the objectives of this experiment were not explained). The author explained that they were able to withdraw from the experiment whenever they desired. The experiment was conducted after the obtainment of their consents. This experiment follows the principles of the institutional review board of Waseda University.

The toe coordinates of the right foot were measured using a motion capture system (Raptor-E; Motion Analysis, Santa Rosa, CA, USA) that could measure marker coordinates with an error of 0.1 mm or less. The marker for the measurement was attached to the first metatarsophalangeal joint of the foot. The angles of the right hip, knee, and ankle joints were measured through goniometers (SG110 and SG150, Biometrics Ltd., Newport, UK), which are wearable angle sensors. The participants wore the cable-driven system and the sensors on their right leg.

The experiment task consisted of the measurement of gait data for training the RBFN and testing the robotic assistance by using the prediction algorithm. At first, the experimental participants were guided to continue walking for 5 min, in which they decided their preferred walking speed (2.5 ± 0.27 km/h). Next, they walked on a treadmill for 400 s; this was considered the measurement phase (approximately 200 datasets were used for training and 100 datasets were used to check the results). The measured toe height data obtained from the motion capture system and the measured angular data at toe-off obtained from the robotic system were used for the machine learning of the RBFN. After training of the parameters of the RBFN using 2-20 Gaussian functions, the participants were asked to walk on the treadmill for 270 s. After 30 s, the robot intermittently applied the force when the algorithm predicted that the MTC would be lower than the mean for 120 s. The duration of application of the tensile force was approximately 0.18 s, and the desired force value was 16 N based on a previous research. The robot stopped the intermittent assistance for the last 120 s of walking.

The author analyzed how the MTC changed according to the intermittent force application and whether the change of MTC remained after the assistance phase by using a t-test. Approximately 90 gait data during steady locomotion in each phase (before, during, and after intermittent assistance) were analyzed for each participant. The first

quartile, mean, third quartile, and maximum values of the MTC were derived to analyze the change of the MTC distribution. The minimum value and first quartile of MTC were analyzed to evaluate whether the lower MTC values could be increased through robotic assistance. The first and third quartiles showed the values of the lowest and highest 25% of the data, respectively. Furthermore, the RMSE was calculated using 100 data in measurement phase for test of RBFN training results.

5.3 Results and discussion

5.3.1. Investigation of the effect of intermittent force application

Fig. 5.3 shows the mean value of change in maximum knee flexion angle between before and after the force application phase for each frequency of force application for each subject. The maximum knee flexion angle was higher after the force application phase finished than before. The frequency of the force application of the case of once in two gait cycles significantly increased the maximum knee flexion angle after the force application phase for subjects A, C, D, and E. The angle increased significantly when the force application frequency was once in three gait cycles for subjects A and B. The knee flexion angle significantly increased when the force was applied in every gait cycle for subject D. Intermittent force application that does not assist knee flexion motion every gait cycle could increase the range of the knee joint flexion angle significantly when people walked after force application was stopped. In contrast, the force application that assists knee flexion motion every gait cycle could not increase the range of the knee joint flexion angle after force application was stopped in all subjects. The non-application of assistive force in every gait cycle, compared to the case in which it was applied, was more beneficial in encouraging subjects to learn the induced gait.

Fig. 5.4 shows the change in maximum knee flexion angle between before and while the force was applied in condition where the increase of the angle after the force application phase was a maximum for each subject. Fig. 5.5 indicates the change in MTC between before and after the force application phase in case where the increase of the

angle after the force application phase was maximum for each subject. The frequency of the force application was once in two gait cycles in subjects A, C, D, and E, and once in three gait cycles in subject B.

The increase of the maximum knee flexion angle was significant in subjects A, B, and D in a condition where the degree of increase was the most among all conditions in each subject. There are two types of gait cycles; when the motor was activated (force was applied) and not activated (force was not applied) during intermittent force application. The author observed the tendency that the greater knee flexion angle was in the gait cycles where the motor stopped during force application, the more the increase of the knee flexion angle was. Therefore, the increase of the knee flexion motion remains after force application phase if the subjects keeps the larger knee flexion motion without force application between times of exposure to the force application. The author interpreted that reduction of force application frequency was beneficial to encourage people to walk with greater maximum knee flexion angle. In the case of subject C, the angle decreased and then increased again after the duration of the intermittent force application. The author assumed that subject C tried to return to the gait when assisted.

The maximum knee flexion angle when the force was applied was not higher before the force was applied in subjects A or E. The author observed that the maximum knee flexion angle increased when the force was not applied during the intermittent force application phase although the angle did not increase when the force was applied in subject A. The author assumed that the reason why no increase in the knee flexion angle was caused when the force was applied was that subject A tended to rely on the robotic assistance and decrease his activation to flex the knee joint. In this experiment, the subjects could easily predict the timing of the application of assistance by the gait-training robot because the force application frequency was constant in each trial. There was a possibility that subject A kept his activation to flex his knee joint only when the force was not applied during the force application phase. Conversely, the author assumed an error in the force application.

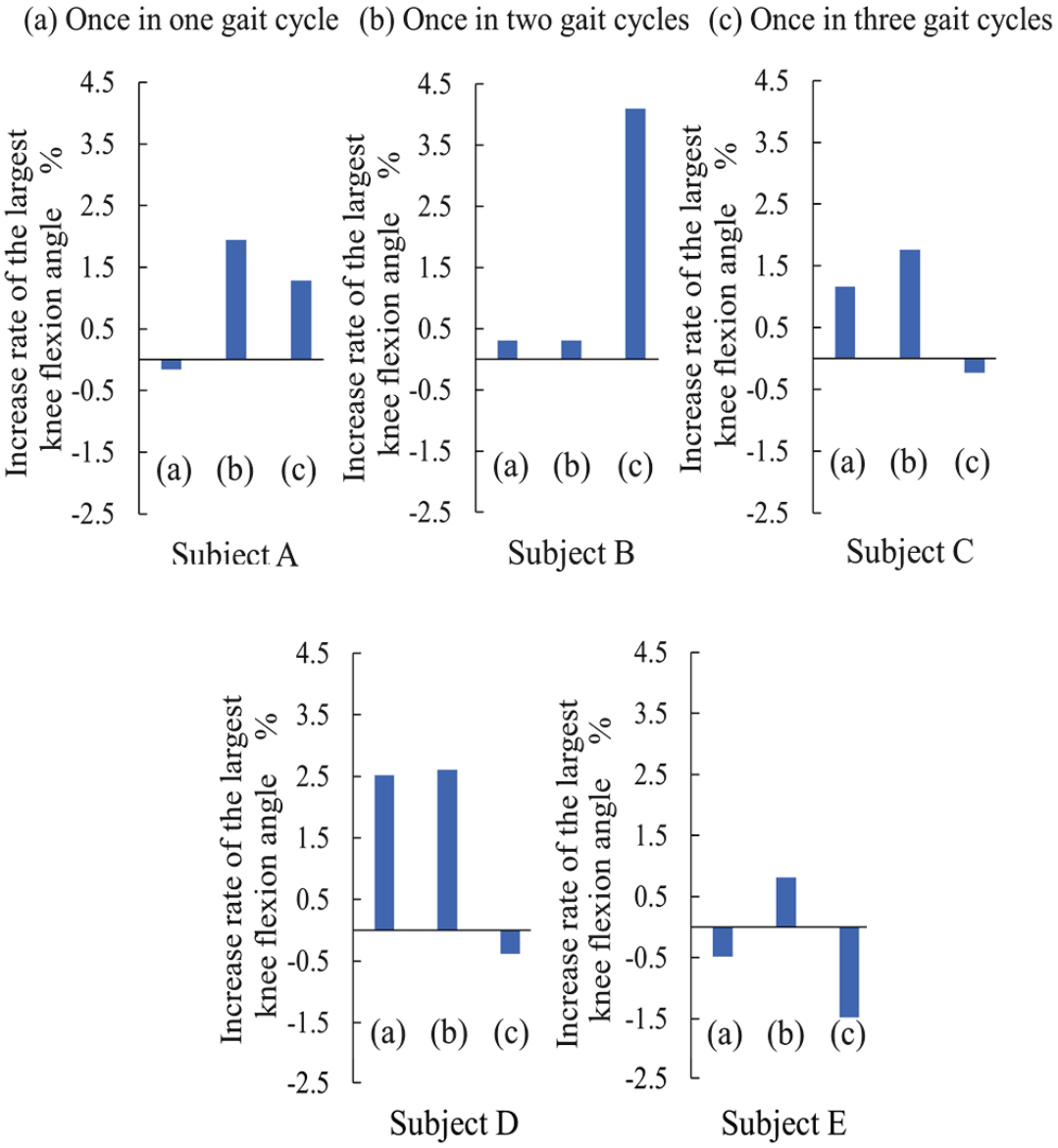

Figure. 5.3 The result of increase in the largest knee flexion angle between before and after the duration of the force application. (a), (b), (c) indicate the conditions that the frequency of the force application was once in one gait cycle, once in two gait cycle, once in three gait cycles, respectively.

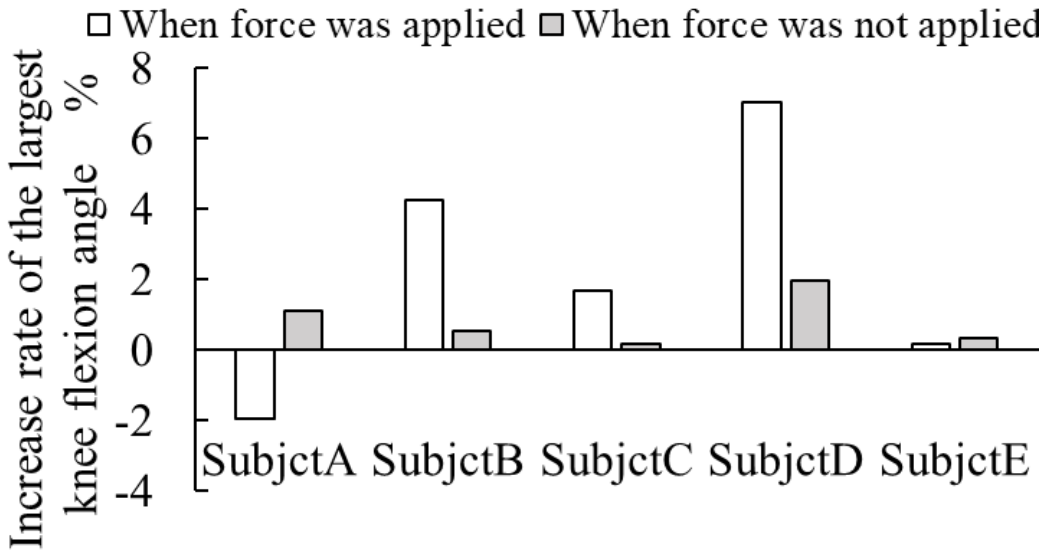

Figure 5.4. Increase in maximum knee flexion angle between before and during intermittent force application phase, where the increase of the angle after the duration of the force application was maximum in each subject.

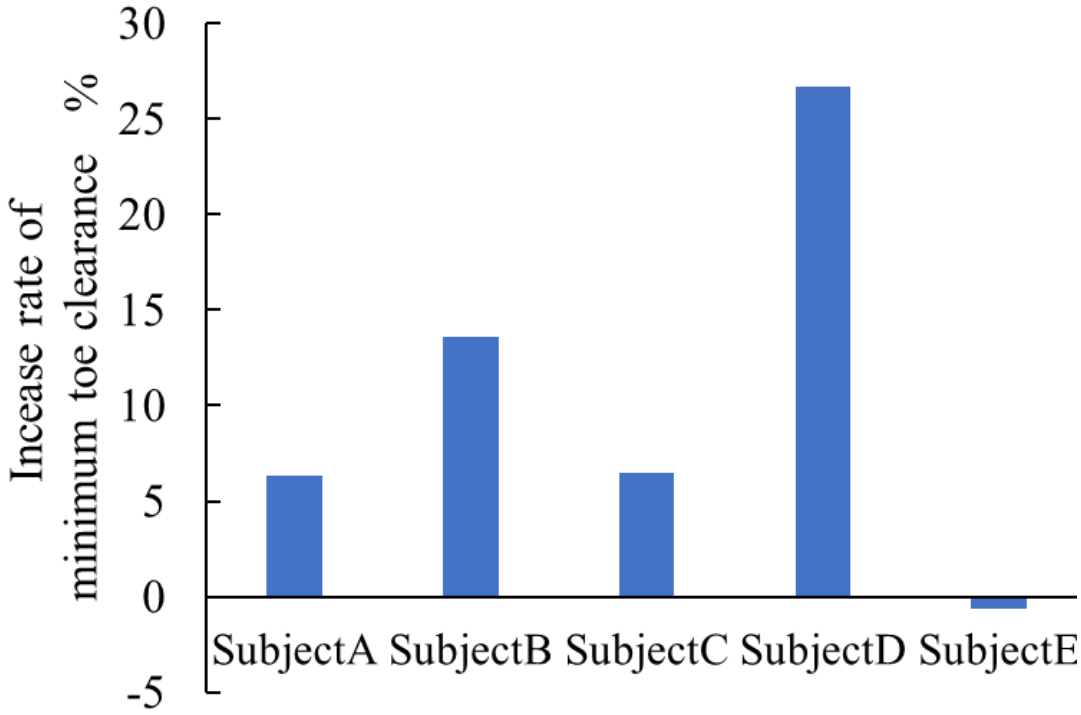

Figure 5.5. Increase in minimum toe clearance angle between before and during intermittent force application, where the increase of the angle after the duration of the force application was maximum in each subject.

5.3.2. Evaluation of the effect of prediction-based training

The applied force of the cable-driven robot used in this experiment increased the knee flexion angle that was shown in Chap.2. The system could switch the force application mode based on the prediction result because the maximum force strength was 15.9 and -0.4 N when the predicted MTC was higher and lower than the mean MTC (before force application). The cable-driven robot was controlled based on the prediction results.

Fig. 5.6 indicates the minimum value before, during, and after intermittent-force application. Figs. 5.7, 5.8, 5.9, and 5.10 show the first quartile, mean, third quartile, and maximum value of the MTC in each phase, respectively.

The minimum and first-quartile values of the MTC increased significantly with the prediction-based intermittent-force application, as indicated in Figs. 5.6 and 5.7. The minimum value of the MTC during the application of intermittent force was lower than the mean MTC before the force was applied intermittently. In contrast, the first quartile of MTC during the intermittent force application did not significantly differ from the mean MTC before the application of the intermittent force. The original difference between the minimum and mean MTC values before the intermittent force application was approximately 5.1 mm. The difference between minimum MTC during the application of intermittent force and mean MTC before the application was approximately 3.5 mm. This implies that the system could inhibit the participants from producing the toe motion around the minimum value of the original MTC distribution. In the experiment, the proposed algorithm was able to predict MTC within an error of approximately 2.4 mm. As a result, approximately 84% of the MTC values during the force application were higher than the mean MTC before the intermittent force application.

The minimum and first quartile values of MTC increased even after the intermittent force application as shown in Figs. 5.6 and 5.7. As shown in the first experiment in this chapter, the reduction of the force application frequency contributed to increase the probability that the training effect remained. In addition, the prediction-based force application could modify the distribution of MTC. Because the training robot did not enhance the muscle strength, the gait change might result from the central nervous system

change. The after-effect generally appears as a result of the predictive adjustment which is the feedforward adaptation altering motion pattern memorized in the cerebellum [5.2]. When the motion is altered by external factors, people firstly try to adapt to the new motion based on the reactive adjustment with lower level of central nervous system. The proprioceptive sense related to toe motion is feedbacked to the cerebellum. The human reaction was switched from the reactive adjustment to the predictive adjustment through trial and error repetition [5.3]. People do not learn the new motion pattern if they are fully moved by the robot. The robotic assistance that intermittently applied the force, increasing MTC when it lowered, provides proprioceptive sense to avoid the MTC reduction. Although the participants did not know the objective of this experiment (increasing the lower values of MTC distribution), they automatically modified their motion to increase the lower values of MTC distribution. The author assumed that the proposed intermittent force application based on MTC prediction involved the modification of MTC control by encouraging participants to try to avoid reducing MTC unconsciously thorough proprioceptive stimulation by the robot to avoid the reduction of MTC.

The minimum, first quartile, mean, and third quartile values of MTC were not significantly different between, during, and after intermittent force application while the maximum values were significantly different. The increased MTC at the gait cycle when the force was applied was higher than the original MTC. It was observed that the more the third-quartile or maximum values of MTC increased during intermittent force application, the lesser was the increase in lower values of MTC after intermittent-force application as the after-effect. Fig. 5.11 indicates two examples of change in distribution of MTC. Variance of MTC increased, and the lower values of MTC was not different between after and before force application in one female case. In contrast, variance of MTC reduced, and the lower values of MTC was higher after force application finished than before force application in one male case. Considering that the interquartile change rate was approximately -47% (decrease) in male participants and 200% (increase) in female participants, the degree of the MTC change during intermittent force application had an effect on the after-effect. The individual physical differences influence the degree

of changes in joint angles and MTC. The force strength was constant in this experiment because the effect of the difference in force strength was not the focus of this study. As a future study, it would be beneficial to investigate the effect of the force strength on the after-effect and establish the method of the adaptive adjustment of force strength corresponding to the user's physique.

This experiment showed that the participants modified their MTC control using the proposed robotic assistance for short-term. Further investigation about long-term after-effects (MTC modification, change in spatiotemporal parameters of both legs, etc.) would be beneficial. The system is easily affected by the shift of the angular sensors. The gait phase detection and MTC prediction algorithms rely on the angular information. It was assumed that the angular sensors might shift thorough the long-term use of the system. Therefore, ensuring the calibration method of angular information during walking would be needed. Moreover, the focus was only on increasing the toe height to avoid tripping in this work. It was assumed that the proposed prediction-based assistance method will be used for other training systems to improve control ability.

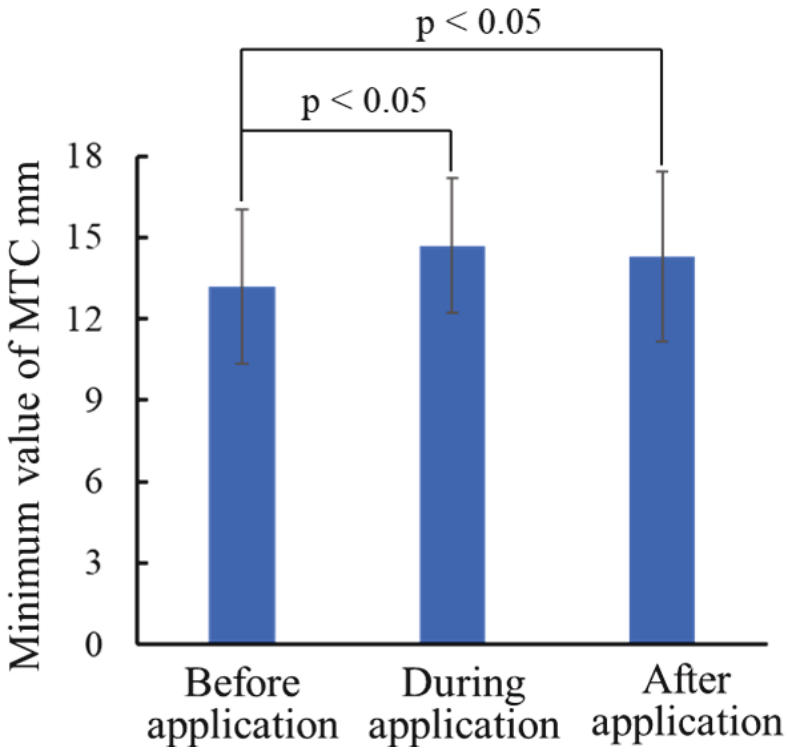

Figure 5.6 Minimum value of MTC. The error bars indicate the standard deviation.

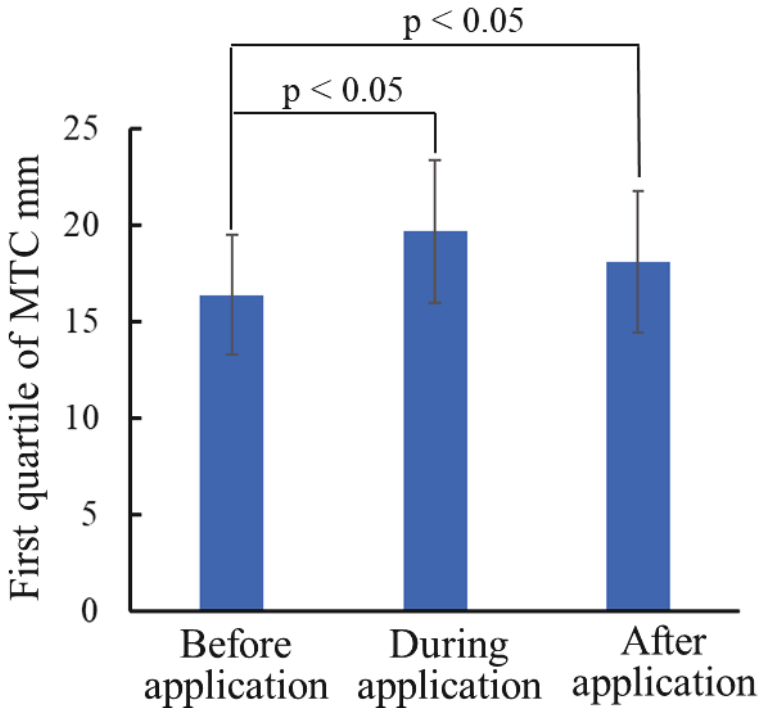

Figure 5.7 First quartile of MTC. The error bars indicate the standard deviation.

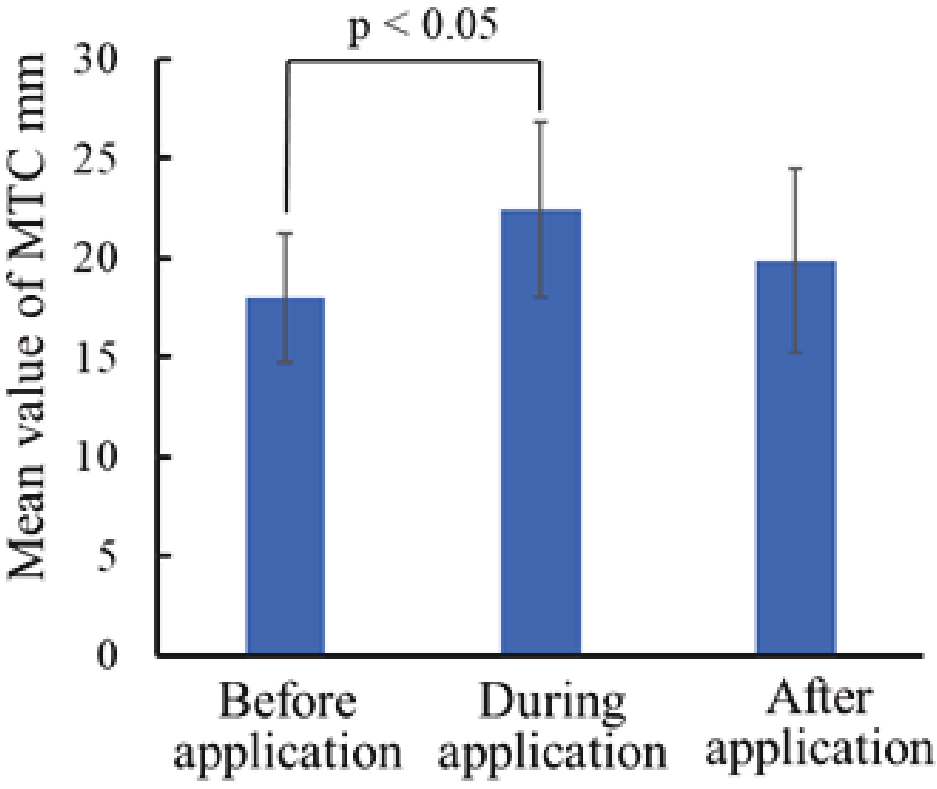

Figure 5.8 Mean value of MTC. The error bars indicate the standard deviation.

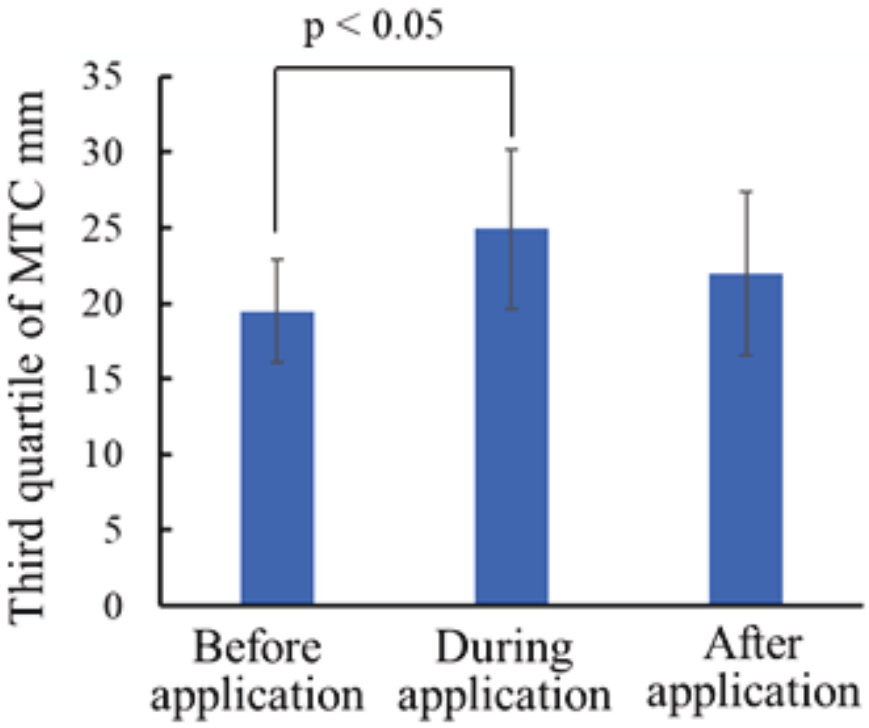

Figure 5.9 Third quartile of MTC. The error bars indicate the standard deviation.

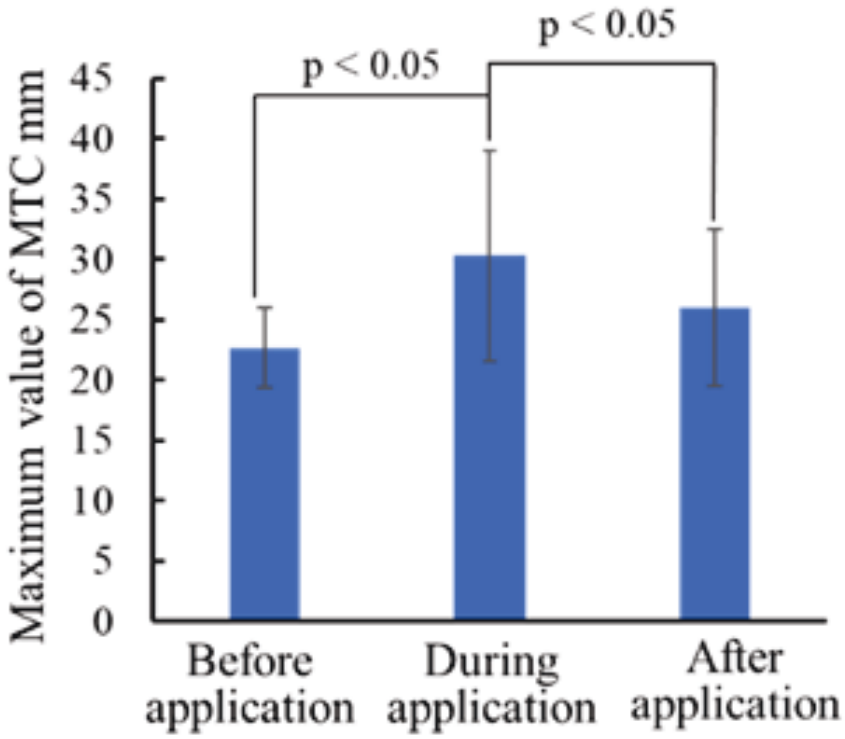

Figure 5.10 Maximum value of MTC. The error bars indicate the standard deviation.

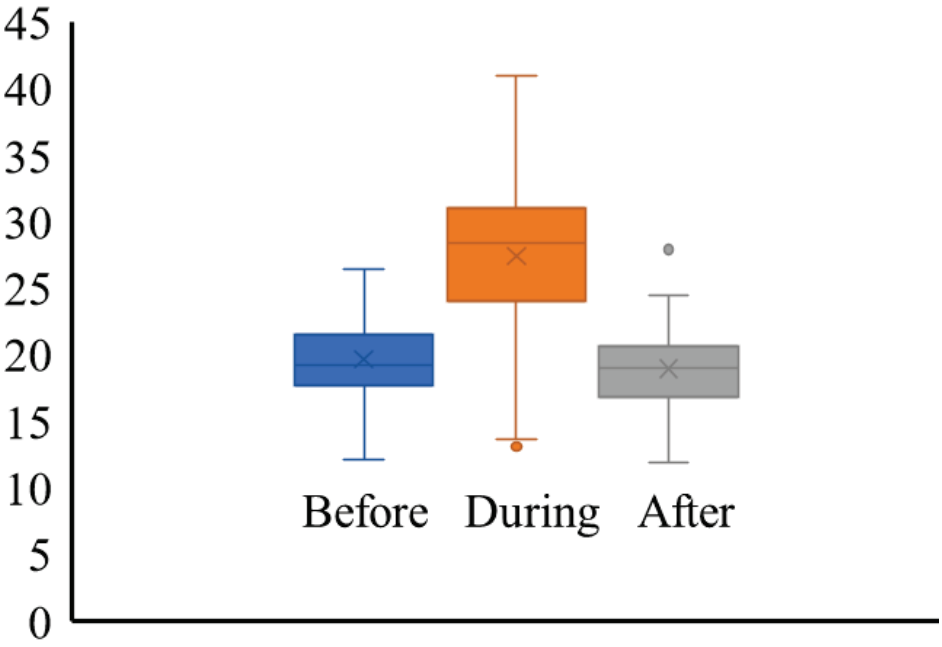

(a)

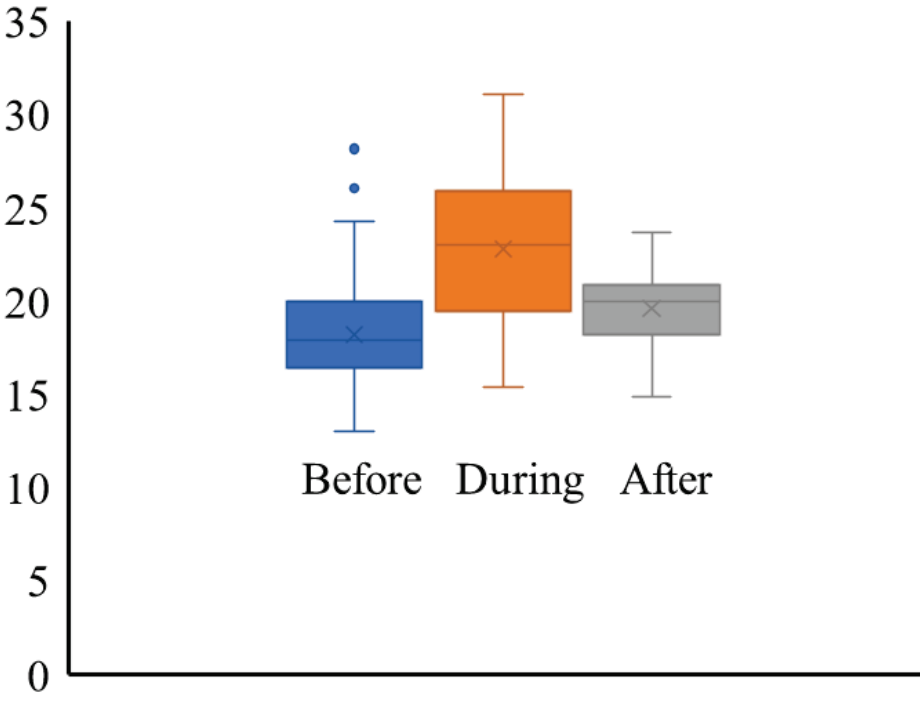

(b)

Figure 5.11 Change in distribution of MTC. (a) Example of one female participant; (b) Example of one male participant.

5. 4 Summary

Adaptive control of gait training robots has been determined to improve gait performance through motion assistance. Controlling MTC to avoid its decrease among gait cycles is important during walking to prevent tripping. No conventional gait training robots can adjust assistance timing based on MTC. In this chapter, the author proposes a system that intermittently applies force based on the MTC prediction algorithm to encourage people to walk by avoiding MTC reduction. This prediction algorithm is based on a radial basis function network, whose input data include the angles, angular velocities, and angular accelerations of the hip, knee, and ankle joints in the sagittal and coronal planes at toe-off. The cable-driven system that can switch between assistance and non-assistance modes applies a force when the predicted MTC is lower than the mean value. Eight participants were asked to walk on a treadmill, and the effect of the system was tested. The MTC data before, during, and after the assistance phase were analyzed for 120 s. The results showed that the minimum and first quartile values of MTC could be increased during and after the assistance phase.

Chapter 6 Conclusion

6. 1 Summary

The objective of this thesis was presenting a control system of gait training robot with intermittent force application based on the prediction of MTC to improve human toe control ability during walking. To encourage people to walk by avoiding MTC reduction, the MTC needs to be predicted previously and modified only when the value is lower. It is necessary to apply the force to the human for modifying the MTC in case of reduction. Therefore, the system needed to be designed to switch assistance-mode and non-assistance-mode. Moreover, the author assumed that the kinematic information of lower limb joints in the same phase between gait cycles was related to future toe clearance. Therefore, techniques of detection of phase and pattern classification were proposed and combined as the prediction algorithm. Moreover, gait phase detection technique is needed for robotic control. Prediction should be performed sufficiently early to assist the swing motion.

Chapter 1 introduces the background of the thesis in terms of aged-society and importance of walking for establishing the society health and longevity. Moreover, the author describes the purpose and originality of this study after summarizing the state-of-the-art of robotic technologies encouraging people to walk and neurophysiological mechanism of human locomotion.

In this work, a hardware system of the robot with cable-driven system that increases toe height was introduced. To establish the system to assist human toe motion as needed, it was needed to analyze the effect of force application timings on the changes of the toe trajectory and the lower limb joint angles. The author designed the system to apply the force to a part of the shank and the force direction was longitudinal along the shank toward the knee. The robot controls the motor rotation and transmits the cable tensile force to the

lower leg. This actuator system was designed to ensure safety: the motor does not pull the cable when it is not activated and almost all the pulleys are located far away from the body so that the cable tensile force is transmitted only to a frame which people wore. The cable tensile force was measured by the loadcell attached between the frame and the cable-spring component. First, the effect of force application timings on the joints and the toe was investigated in younger people. Four time points of force application were considered based on knee flexion motion, i.e., condition 1, time when the knee joint started flexing in pre-swing phase; condition 2, time when the toe was lifted by knee flexion motion; condition 3: time when the knee joint was flexing after toe-off; and condition 4: time when knee joint was about to finish flexing. The increase in the maximum knee flexion angle caused the increase of the maximum toe clearance in the swing phase. Changes in the ratio of the hip angle to the knee angle after maximum toe clearance can be considered as the cause of increased minimum toe clearance. The force application in the later swing phase might inhibit older people from extending the knee and contacting the ground. Next, the effect of force application at toe-off was investigated in older people. MTC could be increased by the force application around toe-off even in older people. Consequently, the author concludes that the force application around toe-off was effective as an assistance to increase MTC.

It was also proposed a novel gait event detection algorithm. For precise timing control of force application and prediction of MTC, the more precise algorithm of gait event detection than the method previously introduced was needed. The author proposed the algorithm using the plantar structure between lower limb joint angles that are different among phases. In chapter 2, the timing of force application to increase the MTC was toe-off or later. Therefore, the author aimed at ensuring the algorithm to detect the toe-off phase. First, the algorithm derives the four planes, which are related to swing motion, motion for preparing foot–ground contact, the loading response motion, and support motion for the body, in angular space of hip, knee, and ankle joints without supervised learning. Next, the switching points of the planes related to toe-off were detected by calculating the measured angular coordinates and the planes. The results of the experiment involving seven subjects joined show that the change in the planes reflected

the change in gait phases. The error was less than 0.035 s when the gait events were detected after calculating planes using the first gait datum. Moreover, although t analysis was performed, the results show that the heel contact and toe-off could be detected as soon as the angles were sensed once the planes were derived.

A novel toe clearance prediction algorithm with a radial basis function network using the angles, angular velocities, and angular accelerations of the hip, knee, and ankle joints in the sagittal plane was also proposed. The calculation timing of the proposed algorithm was the start of the swing phase, and the MTC was predicted that was appeared later in the same swing phase. The input data could be extracted with the algorithm based on the method established in Chapter 3. The author performed the experiments where six subjects walked on a treadmill for 360 s. In each subject, gait data with 20-200 gait cycles were used for training the radial basis function and 100 gait cycle data were used for evaluation in each person. The RMSE between the measured and the predicted MTC was 2.34 mm. Moreover, the RMSE was 2.88 mm in the condition where the gait velocity changed. The RMSEs of the MTC are smaller than previous studies. Values of the MTC that were lower than the median could be detected with higher probability than 68%; that is, the detection accuracy of the proposed algorithm was better than the random detection. Although the accuracy can still be improved, the author concludes that this algorithm is able to influence the distribution of MTC because the error was smaller than the original standard deviation of MTC.

An evaluation of the system that intermittently applies force based on the MTC prediction algorithm to encourage people to walk by avoiding MTC reduction was performed. The algorithms of Chapters 3 and 4 were implemented on the hardware system of Chapter 2. Eight participants were asked to walk on a treadmill, and we tested the effect of the system. First, the radial basis function network was trained with approximately 200 gait cycle data in each person. Next, the data of MTC before, during, and after the assistance phase were analyzed for 120 s. The force-application mode and non-force-application mode were switched based on the prediction result. The results showed that the minimum and first quartile values of MTC could be increased during and after the assistance phase. When people are fully moved by the robot, the after-effect does not

reflect the guided motion. Therefore, the author assumes that the proposed intermittent force application based on prediction-involved modification by encouraging the participants to try to avoid reducing MTC unconsciously thorough proprioceptive stimulation to avoid the reduction of MTC.

The novelty of this study is to establish the intermittent force application method of gait training robot based on prediction of minimum toe clearance and modify the distribution of minimum toe clearance. The proposed system that can allow people to move freely can be combined with the training system for reproducing environments such as obstacles. Moreover, the proposed prediction-based assistance method can be used for other training systems to modify the motion into the more precise motion and improve control ability in the future. Because the motor was located away from the body, the weight is smaller (approximately 100 g) than other gait training robots (several kilogram). The proposed system is a simple system (1 degree of freedom) compared to conventional exoskeleton gait training robots (approximately 6 degrees of freedom). To the best of my knowledge, no research related gait training robots has investigated the change in MTC distribution before.

6. 2 Future work

The contribution of this study is to establish the intermittent force application method of gait training robot based on prediction of MTC and modify the MTC distribution. The proposed prediction-based assistance method can be used for other training systems to modify the motion into the more precise motion and improve control ability in the future. It is beneficial to apply the prediction-based assistance method to other assistive devices for gait training, such as the ankle assistive devices.

Ensuring adaptive force strength method will be beneficial as a future study. The force strength was constant in this experiment because the effect of the difference in force strength was not the focus of this study. In addition, the physical differences affect the degree of movement changes. It was observed that the higher the third-quartile or

maximum values of MTC, the lesser was the increase in MTC after intermittent-force application (after-effect). Considering that the interquartile change rate decreased for male and increased for female subjects, the degree of the MTC change when the force was applied influenced the after-effect.

After ensuring the adaptive adjustment method, it was investigated the after-effect with diverse people including middle-age and old-age people. The training time to improve the toe control ability as a short-time after-effect and the effect of the training duration remains unclear. Investigations of long-term effects based on individual characteristics will be beneficial for making a future guideline to prompt the active aging.

One of the system limitations is that the training environment is constant. Considering human gait adaptation, experiencing multiple environments during training is important. In terms of toe height control to avoid tripping, the appropriate toe height during walking is different depending on obstacles or steps. The author assumes that augmented reality techniques could improve the gait training environment and enable the human to train and improve their ability of toe control to step over the obstacles. The proposed system allows people to freely move and can be combined with the training system for reproducing environments, such as obstacles. As a future study, the virtual obstacle system using the head-mounted display that could implement the augmented reality will be developed for gait training robotic system with multiple environments.

The scenario for the commercialization of the product is explained in this paragraph. The author estimates 3 years to establish the training robotic system with virtual obstacle adaptation to individual characteristics. Furthermore, the training system can be combined with other researches for commercialization of product. The actuation system of this study can be replaced by a soft actuator in the future. Although the applied force strength needs to be adjusted for each person, the required maximum force can be estimated to be just around 20 N or less, which is feasible for a soft actuation system. In addition, the training system could be combined with a personal life log system, which could provide information related to the human health state to the gait training system. Combination of services, such as insurance or fintech, can be achieved and cost for using

gait training robot might be reduced because sharing life log data is valuable for providing services. The author assumes that the gait training system for improving the toe control ability will be established as a commodity predictive training system for middle-aged people in ten years.

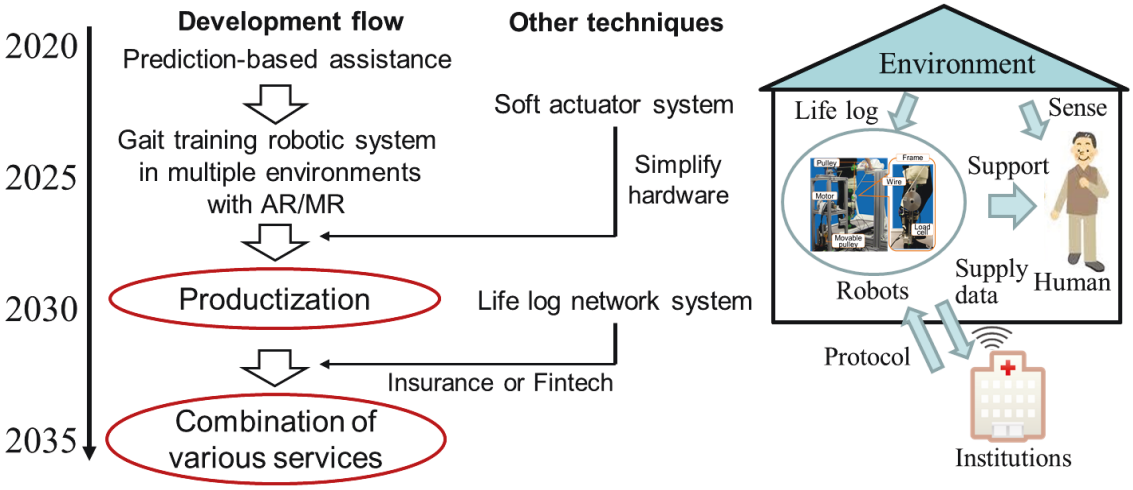

Fig. 6.1 Scenario of productization as a prevention training system.

References

Chapter 1

[1.1] 内閣府, “平成 30 年度　高齢化の状況及び高齢社会対策の実施状況 第 1 章 高齢化の状況,” [オンライン]. Available: https://www8.cao.go.jp/kourei/whitepaper/w-2019/zenbun/pdf/1s1s_01.pdf. [アクセス日: 2019 年 11 月 17 日].

[1.2] 内閣府, “平成 30 年度　高齢化の状況及び高齢社会対策の実施状況　高齢化の社会保障給付費に対する影響,” [オンライン]. Available: https://www8.cao.go.jp/kourei/whitepaper/w-2019/zenbun/pdf/1s1s_06.pdf. [アクセス日: 2019 年 11 月 17 日].

[1.3] ReportLinker, “Global Healthcare Sector Analysis: Latest Market Trends and Statistics,” [オンライン]. Available: https://www.reportlinker.com/ci02241/Healthcare.html. [アクセス日: 2019 年 11 月 17 日].

[1.4] Ministry of Economy. Trade, and Industry, “Announcement of 26 Enterprises Selected for the 2018 Health & Productivity Stock Selection,” [オンライン]. Available: https://www.meti.go.jp/english/press/2018/0220_002.html. [アクセス日: 2019 年 11 月 17 日].

[1.5] R. M. Henke, R. Z. Goetzel, J. McHugh , F. Isaac, “Recent Experience In Health Promotion At Johnson & Johnson: Lower Health Spending, Strong Return On Investment,” HEALTH AFFAIRS, vol. 30, pp. 460-469, 2011.

[1.6] 厚生労働省, “平成 29 年度 国民医療費の概況,” [オンライン]. Available: https://www.mhlw.go.jp/toukei/saikin/hw/k-iryohi/17/index.html. [アクセス日: 2019 年 11 月 17 日].

[1.7] 橋本修二, “厚生労働科学研究　健康寿命のページ　健康寿命の全国推移の

算定・評価に関する研究（都道府県と大都市の推移および、将来予測の試み）（平成 30 年度分担研究報告書）,” [オンライン]. Available: http://toukei.umin.jp/kenkoujyumyou/houkoku/H30.pdf. [アクセス日: 2019 年 11 月 17 日].

[1.8] W. H. Organization, “Active Ageing: A Policy Framework,” [オンライン]. Available: https://www.who.int/ageing/publications/active_ageing/en/. [アクセス日: 2019 年 11 月 17 日].

[1.9] S. Morrison, K. M. Newell, “Aging, Neuromuscular Decline, and the Change in Physiological and Behavioral Complexity of Upper-Limb Movement Dynamics,” Journal of Aging Research, Article ID 891218, 2012.

[1.10] Y. Okawa, S. Nakamura, M. Kudo, S. Ueda, “An evidence-based construction of the models of decline of functioning. Part 1: two major models of decline of functioning,” International Journal of Rehabilitation Research, vol. 32, pp. 189-192, 2009.

[1.11] 大川弥生, “ICF（国際生活機能分類）－「生きることの全体像」についての「共通言語」,” 第 1 回社会保障審議会統計分科会生活機能分類専門委員会参考資料, 2006.

[1.12] 草野修輔, “高齢者のリハビリテーション,” 理学療法科学, 2004.

[1.13] L. Ferrucci, R. Cooper, M. Shardell, E. M. Simonsick, J. A. Schrack , D. Kuh, “Age-Related Change in Mobility: Perspectives From Life Course Epidemiology and Geroscience,” J Gerontol. A Biol. Sci. Med. Sci., vol. 71, pp. 1184-1194, 2016.

[1.14] K. Nakamura, T. Ogata, “Locomotive Syndrome: Definition and Management,” Clin. Rev. Bone Miner Metab., vol. 14, pp. 56-57, 2016.

[1.15] 加. 雄. 太. 壽. 川上 治, “高齢者における転倒・骨折の疫学と予防,” 日本老年医学会雑誌, 2006.

[1.16] K. Delbaere, G. Crombez, G. Vanderstraeten, T. Willems , D. Cambier, “Fear-related avoidance of activities, falls and physical frailty. A prospective community-based cohort study,” Age and Ageing, vol. 33, pp. 368-373, 2004.

[1.17] A.J. Blake, K. Morgan, M.J. Bendall, H. Dallosso, S.B. Ebrahim, T.H. Arie, P.H. Fentem, E.J. Bassey, “FALLS BY ELDERLY PEOPLE AT HOME: PREVALENCE AND ASSOCIATED FACTORS,” Age Ageing, vol. 17, pp. 365-72 1988.

[1.18] L.R. Timsina, J.L. Willetts, M. J. Brennan, H. Marucci-Wellman, D. A. Lombardi, T. K. Courtney, S. K. Verm, “Circumstances of fall-related injuries by age and gender among community-dwelling adults in the United States,” PloS one, vol. 12, 2017.

[1.19] J. Perry, 歩行分析－正常歩行と異常歩行－, 医歯薬出版株式会社, pp. 51-62. 2007.

[1-20] 吉. 正. 牧川 方昭, 運動のバイオメカニクス, コロナ社, pp. 77, 151, 2008.

[1-21] 河島則天, 歩行運動における脊髄神経回路の役割, 国リハ研紀, 2010.

[1-22] S. Grillner , A. E. Manira, “Current Principles of Motor Control, with Special Reference to Vertebrate Locomotion,” Physiological Reviews, vol. 100, pp.271-320, 2020.

[1-23] K. Takakusaki, “Functional Neuroanatomy for Posture and Gait Control,” Journal of Movement Disorders, vol. 10, pp.1-17, 2017.

[1-24] P. A. Guertin, “Central Pattern Generator for Locomotion: Anatomical, Physiological, and Pathophysiological Considerations,” 183, Frontiers in Neurology, 2012.

[1-25] M. MacKay-Lyons, “Central Pattern Generation of Locomotion: A Review of the Evidence,” Physical Therapy, vol. 82, pp. 69-83, 2002.

[1-26] S. M. Morton , B. J. Amy , “Walking, Cerebellar Contributions to Locomotor Adaptations during Splitbelt Treadmill,” J Neurosci., vol.26, pp.9107-9116, 2006.

[1-27] G. Bosco , R. Poppele, “Proprioception from a spinocerebellar perspective,” Physiol Rev., vol. 81, pp. 539-568, 2001.

[1-28] J. Ashe, O. Lungu, A. Basford , X. Lu, “Cortical control of motor sequences,” Curr Opin Neurobiol, vol. 16, pp. 213-221, 2006.

[1-29] V. Puttemans, N. Wenderoth , S. Swinnen, “Changes in brain activation during the

acquision of a multifrequency bimanual coordination task: from the cognitive stage to advanced levels of automaticity," J Neurosci., vol. 25, pp. 4270-4278, 2005.

[1-30] L. Malone, A. Bastian, "Thinking about walking: effects of conscious correction versus distraction on locomotor adaptation," J. Neurophysiol., pp. 1954-1962, 2010.

[1.31] T. Higuchi, "Visuomotor control of human adaptive locomotion: understanding the anticipatory nature," Front. Psychol., 277, 2013.

[1.32] A. R. Wu, A. D. Kuo, "Determinants of preferred ground clearance during swing phase of human walking," J Exp Biol., vol. 219, pp. 3106-3113, 2016.

[1.33] T. Rosen, K. A. Mack , R. K. Noonan, "Slipping and tripping: fall injuries in adults associated with rugs and carpets," Journal of Injury and Violence Research, vol. 5, pp. 61-69, 2013.

[1.34] J. P. Scholz , G. Schöner, "The uncontrolled manifold concept: identifying control variables for a functional task.," Experimental Brain Research, vol. 126, pp. 289-306, 1999.

[1.35] M. L. Latash, "Motor Synergies and the Equilibrium-Point Hypothesis," Motor Control, vol. 14, pp. 294-322, 2010.

[1.36] R.S. Barrett, P.M. Mills, R.K. Begg, "A systematic review of the effect of ageing and falls history on minimum foot clearance characteristics during level walking," Gait & posture, vol. 32, pp. 429-35, 2010.

[1.37] R. Begg, R. Best, L. Dell'Oro, S. Taylor, "Minimum foot clearance during walking: Strategies for the minimisation of trip-related falls," Gait & posture, vol. 25, pp. 191-198, 2007.

[1.38] D. Winter, "Foot Trajectory in Human Gait - a Precise and Multifactorial Motor Control Task," Physical therapy, vol. 72, pp. 45-53, 1992.

[1.39] T. Killeen, C. S. Easthope, L. Demko, L. Filli, M. L. L. Lorincz, A. Curt, B. Zorner, M. Bolliger, "Minimum toe clearance: probing the neural control of locomotion," Sci. Rep., vol. 7, 2017.

[1.40] P. Mills, R. Barrett, S. Morrison, “Toe clearance variability during walking in young and elderly men,” Gait & posture, vol. 28, pp. 101-107, 2008.

[1.41] M. Moosabhoy , S. Gard, “Methodology for determining the sensitivity of swing leg toe clearance and leg length to swing leg joint angles during gait,” Gait & posture, vol. 24, pp. 493-501, 2006.

[1.42] B. W. Schulz, J. D. Lloyd, and W.E. 3rd Lee, “The effects of everyday concurrent tasks on overground minimum toe clearance and gait parameters,” Gait & posture, vol. 32, pp. 18-22, 2010.

[1.43] D. Martelli, V. Vashista, S. Micera, S. Agrawal, “Direction-Dependent Adaptation of Dynamic Gait Stability Following Waist-Pull Perturbations,” IEEE Transactions on Neural Systems and Rehabilitation Engineering, vol. 24, pp. 1304-1313, 2016.

[1.44] C. McCrum, M. Gerards, K. Karamanidis, W. Zijlstra , K. Meijer, “A systematic review of gait perturbation paradigms for improving reactive stepping responses and falls risk among healthy older adults,” Eur. Rev. Aging Phys. A., vol. 14, 3, 2017.

[1.45] F. Aprigliano, D. Martelli, J. Kang, S. Kuo, U. Kang, V. Monaco., S. Micera, S. Agrawal, “Effects of repeated waist-pull perturbations on gait stability in subjects with cerebellar ataxia,” Journal of NeuroEngineering and Rehabilitation, vol. 16, 50, 2019.

[1.46] J. Lurie, A. Zagaria, D. Pidgeon, J. Forman, K. Spratt, “Pilot comparative effectiveness study of surface perturbation treadmill training to prevent falls in older adults,” BMC geriatrics, vol. 13, 49, 2013.

[1.47] Y. Pai, T. Bhatt, F. Yang, E. Wang, “Perturbation Training Can Reduce Community-Dwelling Older Adults' Annual Fall Risk: A Randomized Controlled Trial,” J. Gerontol. a-Biol., vol. 69, pp. 1586-1594, 2014.

[1.48] H. Robotics, “Honda 歩行アシストとは,” [オンライン]. Available: https://www.honda.co.jp/walking-assist/. [アクセス日: 2019 年 11 月 18 日].

[1.49] 産業技術総合研究所, “介護ロボットポータルサイト,” [オンライン]. Available: http://robotcare.jp/jp/development/index.php. [アクセス日: 2019 年 11 月 18 日].

[1.50] HITACHI, “ロボティクス-日立のロボットの歴史-,” HITACHI, [オンライン]. Available: http://www.hitachi.co.jp/ rd/portal/highlight/robotics/history/2000.html.

[1.51] 野方誠, “高齢者歩行訓練支援ロボットにおける無拘束訓練動作判別,” 電気学会論文誌, 2011.

[1.52] H. Schmidt, C. Werner, R. Bernhardt, S. Hesse, J. Krüger, “Gait rehabilitation machines based on programmable footplates,” Journal of NeuroEngineering and Rehabilitation, vol. 4, 2, 2017.

[1.53] S. Xie , P. Jamwal, “An iterative fuzzy controller for pneumatic muscle driven rehabilitation robot,” Expert System with Applications, vol. 38, pp. 8128-8137, 2011.

[1.54] Q. Liu, B. Zhang, Y.-H. Liu, Y.-T. Hsiao, M.-D. Jeng , M. G. Fujie, “Integration of Visual Feedback System and Motor Current Based Gait Rehabilitation Robot for Motor Recovery,” 2016 IEEE International Conference on Systems, Man, and Cybernetics, 2016.

[1.55] Hokoma, “Lokomat®Pro - Features & Functions,” [オンライン]. Available: http://www.hocoma.com/pro ducts/lokomat/lokomatpro/features-functions/. [アクセス日: 2019 年 11 月 18 日].

[1.56] S. K. Banala, S. K. Agrawal, J. P. Scholz, “Active Leg Exoskeleton (ALEX) for Gait Rehabilitation of Motor-Impaired Patients,” IEEE 10th International Conference on Rehabilitation Robotics, 2007.

[1.57] J. Veneman, R. Kruidhof, E. Hekman, R. Ekkelenkamp, E. V. Asseldonk , H. v. d. Kooij, “Design and evaluation of the LOPES exoskeleton robot for interactive gait rehabilitation,” IEEE Transaction on Neural Systems and Rehabilitation Engineering, vol. 15, pp. 379 – 386, 2007.

[1.58] 蜂須賀研二, “リハビリテーション医療におけるロボット訓練,” [オンライン]. Available: http://www.seiai-riha.com/pdf/110125%20innaibenkyou02.pdf. [アクセス日: 2019 年 11 月 18 日].

[1.59] NEDO, “意思を読み取り自立動作をサポート福祉の現場で期待を集めるロボットスーツ HAL®,” [オンライン]. Available: http://www.nedo.go.jp/hyoukabu/articles/201012cyberdyne/index.html. [アクセス日:

2019 年 11 月 18 日].

[1.60] J. Meuleman, E. v. Asseldonk, G. v. Oort, H. Rietman , H. v. d. Kooij, “LOPES II—Design and Evaluation of an Admittance Controlled Gait Training Robot With Shadow-Leg Approach,” IEEE TRANSACTIONS ON NEURAL SYSTEMS AND REHABILITATION ENGINEERING, vol. 24, pp. 352-363, 2016.

[1.61] G. Zhao, M. A. Sharbafi, M. Vlutters, E. v. Asseldonk , A. Seyfarth, “Bio-inspired Balance Control Assistance Can Reduce Metabolic Energy Consumption In Human Walking,” IEEE Trans Neural Syst Rehabil Eng., vol. 27, pp. 1760-1769, 2019.

[1.62] “Toyota Refines Rehabilitation Assist Robot and Launches New Welwalk WW-2000,” TOYOTA, [オンライン]. Available: https://global.toyota/en/newsroom/corporate/30609584.html. [アクセス日: 2019 年 11 月 21 日].

[1.63] 株式会社オリジンメディカル事業部, “密着型歩行補助装置 RE-Gait®,” 2020. [オンライン]. Available: https://www.re-gait.com/. [アクセス日: 2019 年 11 月 21 日].

[1.64] J. Bae, C. Siviy, M. Rouleau, N. Menard, K. O’Donnell, I. Galiana, M. Athanassiu, D. Ryan, C. Bibeau, L. Sloot, P. Kudzia, T. Ellis, L. Awad , C. J. Walsh, “A lightweight and efficient portable soft exosuit for paretic ankle assistance in walking after stroke,” 2018 IEEE International Conference on Robotics and Automation , 2018.

[1.65] W. Meng, Q. Liu, Z. Zhou, Q. Ai, B. Sheng, S. S. Xie, “Recent development of mechanisms and control strategies for robot-assisted lower limb rehabilitation,” Mechatronics, vol. 31, pp. 132-145, 2015.

[1.66] J. Emken, S. Harkema, J. Beres-Jones, C. Ferreira, D. Reinkensmeyer, “Feasibility of manual teach-and-replay and continuous impedance shaping,” IEEE Trans. Biomed., vol. 55, pp. 322-334, 2008.

[1.67] J.L. Emken, S. J. Harkema, J. A. Beres-Jones, C. K. Ferreira, D. J. Reinkensmeyer, “Feasibility of manual teach-and-replay and continuous impedance shaping for robotic locomotor training following spinal cord injury,” IEEE TRANSACTIONS ON

BIOMEDICAL ENGINEERING, vol. 55, pp. 322-334, 2008.

[1.68] J. A. Saglia, N. G. Tsagarakis, J. S. Dai, D. G. Caldwell, “Control Strategies for Patient-Assisted Training Using the Ankle Rehabilitation Robot (ARBOT),” IEEE/ASME TRANSACTIONS ON MECHATRONICS, vol. 18, pp. 1799 – 1808, 2013.

[1.69] D. P. Ferris, K. E. Gordon, G. S. Sawicki, A. Peethambaran, “An improved powered ankle–foot orthosis using proportional myoelectric control,” Gait & Posture, vol. 23, pp. 425-428, 2006.

[1.70] H. Huang, F. Zhang, L. Hargrove, Z. Dou, D. Rogers, K. Englehart, “Continuous locomotion-mode identification for prosthetic legs based on neuromuscular-mechanical fusion,” IEEE Trans Biomed Eng., vol. 58, pp. 2867-2875, 2011.

[1.71] Y. Fan, Y. Yin, “Active and Progressive Exoskeleton Rehabilitation Using Multisource Information Fusion From EMG and Force-Position EPP,” IEEE TRANSACTIONS ON BIOMEDICAL ENGINEERING, vol. 60, pp. 3314-3321, 2013.

[1.72] H. Kawamoto, S. Lee, S. Kanbe , Y. Sankai, “Power assist method for HAL-3 using EMG-based feedback controlle,” Proc. International Conference on Systems, Man and Cybernetics, 2003.

[1.73] D. Ferris, C. Lewis, “Robotic lower limb exoskeletons using proportional myoelectric control,” Proceedings of the 31st annual international conference of the IEEE engineering in medicine and biology society, 2009.

[1.74] G. S. Sawicki, D. P. Ferris, “A pneumatically powered knee-ankle-foot orthosis (KAFO) with myoelectric activation and inhibition,” Journal of NeuroEngineering and Rehabilitation, vol. 6, 23, 2009.

[1.75] B. Koopman, E. H. v. Asseldonk , H. . v. d. Kooij, “Selective control of gait subtasks in robotic gait training: foot clearance support in stroke survivors with a powered exoskeleton,” vol. 10, 3, 2013.

[1.76] A. Roy, H. I. Krebs, D. J. Williams, C. T. Bever, L. W. Forrester, R. M. Macko , N. Hogan, “Robot-aided neurorehabilitation: A novel robot for ankle rehabilitation,” IEEE TRANSACTIONS ON ROBOTICS, vol. 25, pp. 569-582, 2009.

[1.77] S. K. Agrawal, S. K. Banala, A. Fattah, V. Sangwan, V. Krishnamoorthy, J. P. Scho , W.-L. Hsu, “Assessment of motion of a swing leg and gait rehabilitation with a gravity balancing exoskeleton,” IEEE TRANSACTIONS ON NEURAL SYSTEMS AND REHABILITATION ENGINEERING, vol. 15, pp. 410-420, 2007.

[1.78] J. Emken, D. Reinkensmeyer, “Robot-enhanced motor learning: accelerating internal model formation during locomotion by transient dynamic amplification,” IEEE Transaction on Neural Systems and Rehabilitation Engineering, vol. 13, pp. 33-39, 2005.

[1.79] A. Duschau-Wicke, J. v. Zitzewitz, A. Caprez, L. Luenenburger, R. Riener, “Path control: a method for patient-cooperative robot-aided gait rehabilitation,” IEEE Transaction on Neural Systems and Rehabilitation Engineering, vol. 18, pp. 38-48, 2010.

[1.80] R. Riener, L. Lėünenburger, G. Colombo, “Human-centered robotics applied to gait training and assessment,” J. Rehabil. Res. Dev., vol. 43, pp. 679-694, 2006.

[1.81] R. Riener, L. Lėünenburger, S. Jezernik, M. Anderschitz, G. Colombo, V. Dietz., “Patient-cooperative strategies for robot-aided treadmill training: first experimental results,” IEEE Trans. Neural Syst. Rehabil. Eng., vol. 13, pp. 380-394, 2005.

[1.82] S. Hussain, S. Q. Xie, P. K. Jamwal, “Robust Nonlinear Control of an Intrinsically Compliant Robotic Gait Training Orthosis,” IEEE Transactions on Systems, Man, and Cybernetics: Systems, vol. 43, pp. 655-665, 2013.

[1.83] J. A. Blaya, H. Herr, “Adaptive control of a variable-impedance ankle-foot orthosis,” IEEE Transactions on Neural Systems and Rehabilitation Engineering, vol. 12, pp. 24-31, 2004.

[1.84] S. Hussain, S. Q. Xie, P. K. Jamwal, “Adaptive impedance control of a robotic,” IEEE TRANSACTIONS ON CYBERNETICS, vol. 46, pp. 334-344, 2013.

[1.85] Q.-T. Dao, S.-i. Yamamoto, “Assist-as-Needed Control of a Robotic Orthosis Actuated by Pneumatic Artificial Muscle for Gait Rehabilitation,” Applied Sciences, vol. 8, 499, 2018.

[1.86] E. Wolbrecht, V. Chan, D. Reinkensmeyer , J. Bobrow, “Optimizing compliant, model-based robotic assistance to promote neurorehabilitation,” IEEE Trans.Neural Syst.

Rehabil. Eng., vol. 16, pp. 286-297, 2008.

[1.87] C. Krishnan, D. Kotsapouikis, Y. Y. Dhaher , W. Z. Rymer, “Reducing Robotic Guidance During Robot-Assisted Gait Training Improves Gait Function: A Case Report on a Stroke Survivor,” Arch. Phys. Med. Rehabil., vol. 94, 1202-1206, 2013.

[1.88] S. Lee, S. Crea, P. Malcolm, I. Galiana, A. Asbeck, and C. Walsh, “Controlling negative and positive power at the ankle with a soft exosuit,” IEEE Int. Conf. Robotics and Automation, 2016.

[1.89] J. Zhang, P. Fiers, K. A. Witte, R. W. Jackson, K. L. Poggensee, C. G. Atkeson , S. H. Collins, “Human-in-the-loop optimization of exoskeleton assistance during walking,” Science, vol. 356, pp. 1280-1284, 2017.

[1.90] O. Tirosh, A. Cambell, R. Begg, W. Sparrow, “Biofeedback training effects on minimum toe clearance variability during treadmill walking,” Annals of Biomedical Engineering, vol. 41, pp. 1661-1669, 2013.

Chapter 2

[2.1] Perry, J., Gait Analysis: Normal and Pathological Function (2007), pp.2–27 and pp.51–62, Ishiyaku Publishers.

[2.2] Anderson, F., C., Goldberg, S. R., Pandy, M. G. and Delp, S. L., Contributions of muscle forces and toe-off kinematics to peak knee flexion during the swing phase of normal gait: an induced position analysis, Journal of Biomechanics, Vol.37 (2004), pp.731–732.

[2.3] Ivanenko, Y. P., Cappellini, G., Dominici, N., Poppele, R. E. and Lacquaniti, F., Modular control of limb movements during human locomotion, Journal of Neuroscience, Vol.27 (2007), pp.11149–11161.

[2.4] Funato, T., Aoi, S., Oshima, H. and Tsuchiya, K., Variant and invariant patterns embedded in human locomotion through whole body kinematic coordination, Exp Brain Res, Vol.205 (2010), pp.497–511.

[2.5] Malone, L. A. and Bastian, J., Age-related forgetting in locomotor adaptation, Neurobiol Learn Mem., Vol.128 (2016), pp.1–6.

[2.6] P. M. Mills, R. S. Barrett, and S. Morrison, “Toe clearance variability during walking in young and elderly men,” Gait & Posture, vol. 28, pp. 101–107, 2008.

Chapter 3

[3.1] J. Perry, “GAIT ANALYSIS: Normal and Pathological Function,” Tokyo: Ishiyaku Publishers, pp. 2–27, pp. 30–75, Nov. 2007.

[3.2] M. Hanlon, R. Anderson, “Real-time gait event detection using wearable sensors,” Gait Posture, vol. 30, pp. 523–527, 2009.

[3.3] S. Khandelwal, N. Wickström, “Gait Event Detection in Real-World Environment for Long-Term Applications: Incorporating Domain Knowledge Into Time-Frequency Analysis,” vol. 24, IEEE Trans. Neural Syst. and Rehabil. Eng., Mar. 2016.

[3.4] C.M. O’Connor, S.K. Thorpe, M.J. O’Malley, C.L. Vaughan, “Automatic detection of gait events using kinematic data,” Gait Posture, vol. 25, pp. 469–474, 2007.

[3.5] J. Zeni Jr, J. Richards, J.S. Higginson, “Two simple methods for determining gait events during treadmill and overground walking using kinematic data,” Gait Posture, vol. 27, pp. 710–714, 2008.

[3.6] J.M. Hausdorff, Z. Ladin, and J.Y. Wei, “Footswitch system for measurement of the temporal parameters of gait,” J. Biomech., vol. 28, pp. 347–351, 1995.

[3.7] P.M. Mills, R.S. Barrett, and S. Morrison, “Agreement between footswitch and ground reaction force tech-niques for identifying gait events: inter-session repeatability and the effect of gait speed,” Gait Posture, vol. 26, pp. 32-36, 2007.

[3.8] B.T. Smith, D.J. Coiro, R. Finson, R.R. Betz, and J. McCarthy “Evaluation of force-sensing resistors for gait event detection to trigger electrical stimulation to improve walking in the child with cerebral palsy,” IEEE Trans Neural. Syst. Rehabil. Eng., vol. 10,

pp. 229, 2002.

[3.9] D. Gouwanda, A. A. Gopalai, “A robust real-time gait event detection using wireless gyroscope and its application on normal and altered gaits,” Med. Eng. Phys., vol. 37 pp. 219-225, 2015

[3.10] A. Mansfield and G.M. Lyons, “The use of accelerometry to detect heel contact events for use as a sensor in FES assisted walking,” Med. Eng. Phys., vol. 25, pp. 879-885, 2003.

[3.11] N. Mijailovi, M. Gavrilovi, S. Rafajlovi, and D.B. Popovi, “Gait Phases Recognition from Accelerations and Ground Reaction Forces,” Application of Neural Networks. Signal Process., vol.1, pp. 34-36, 2009.

[3.12] I.P.I. Pappas, M.R. Popovic, T. Keller, V. Dietz, and M. Morari, “A reliable gait phase detection system,” IEEE Trans. Neural Syst. Rehabil. Eng. vol. 9, pp. 113-125, 2001.

[3.13] A. Mannini and A.M. Sabatini, “Gait phase detection and discrimination between walking-jogging activities using hidden Markov models applied to foot motion data from a gyroscope,” Gait Posture, vol. 36, pp. 657-661, 2012.

[3.14] M. Gori, R. Kamnik, L. Ambroi, et al., “Online. Phase detection using wearable sensors for walking with a robotic prosthesis,” Sensors, vol. 14, pp. 2776-2794, 2014.

[3.15] W.C. Cheng, and D.M. Jhan, “Triaxial Accelerometer-Based Fall Detection Method Using a Self-Constructing,” IEEE J. Biomed. Heal. Inf., vol. 17, pp. 411–419, 2013.

[3.16] S. Li, J. Wang and X. Wang, “A novel gait recognition analysis system based on body sensor networks for patients with parkinson’s disease,” Proceedings of 2010 IEEE Globecom Workshops on Advanced Sensor Integration Technology, Miami, FL, USA; 6–10 Dec. 2010, pp. 256–260.

[3.17] J.U. Chu, K.I. Song, S. Han, et al., “Gait phase detection from sciatic nerve recordings in functional electrical stimulation systems for foot drop correction,” Physiol. Meas., vol. 34, pp. 541–565, 2013.

[3.18] A. Kolawole and A. Tavakkoli, “A novel gait recognition system based on Hidden Markov Models,” Adv. Vis. Comput. Lect. Notes Comput. Sci., vol. 7432, pp. 125–134, 2012.

[3.19] J. Taborri, S. Rossi, E. Palermo, F. Patanè, and Paolo Cappa, “A Novel HMM Distributed Classifier for the Detection of Gait Phases by Means of a Wearable Inertial Sensor Network,” Sensors, vol. 14, pp.16212-16234, 2014.

[3.20] R. Ronsse, T. Lenzi, N. Vitiello, et al., “Oscillator-based assistance of cyclical movements: model-based and model-free approaches,” Medical & Biological Engineering & Computing, vol. 49, pp. 1173, 2011.

[3.21] D.X. Liu, X. Wu, W. Du, C. Wang, and T. Xu. “Gait Phase Recognition for Lower-Limb Exoskeleton with Only Joint Angular Sensors,” Sensors, vol. 16, pp. 1579, 2016.

[3.22] Y.P. Ivanenko, G. Cappellini, N. Dominici, R.E., Poppele, and F. Lacquaniti, “Modular Control of Limb Movements during Human Locomotion,” Journal of Neuroscience, Vol. 27, pp. 11149 –11161, 2007.

[3.23] T. Funato, S. Aoi, H. Oshima, K. Tsuchiya, “Variant and invariant patterns embedded in human locomotion through whole body kinematic coordination,” Experimental Brain Research,” Vol. 205, no. 4, pp 497–511, Sep. 2010.

[3.24] S. Wold, K. Esbensen, P. Geladi, “Principal component analysis,” Chemometrics and Intelligent Laboratory Systems, vol. 2, pp. 37-52, 1987.

Chapter 4

[4.1] N. Kitagawa and N. Ogihara, “Estimation of foot trajectory during human walking by a wearable inertial measurement unit mounted to the foot,” Gait Posture, vol. 45, pp. 110–114, 2016.

[4.2] B. Mariani, C. Hoskovec, S. Rochat, C. Büla, J. Penders, K. Aminian, “3D gait assessment in young and elderly subjects using foot-worn inertial sensors,” J. Biomech., Vol. 43, pp. 2999-3006, 2010.

[4.3] B. Mariani, S. Rochat, C. J. Bu,x,la, K., Aminian, “Heel and toe clearance estimation for gait analysis using wireless inertial sensors,” IEEE Trans. Biomed. Eng. Vol. 59, pp. 3162–3168, 2012.

[4.4] D. McGrath, B. R. Greene, C. Walsh, and B. Caulfield, “Estimation of minimum ground clearance (MGC) using body worn inertial sensors,” J. Biomech., vol. 44, pp. 1083–1088, 2011.

[4.5] B. K. Santhiranayagam, D. T. Lai, W. A. Sparrow, and R. K. Begg, “A machine learning approach to estimate minimum toe clearance using inertial measurement units,” J. Biomech., vol. 48, pp. 4309–4316, 2015.

[4.6] D. T. Lai, S. B. Taylor, and R. K. Begg, “Prediction of foot clearance parameters as a precursor to forecasting the risk of tripping and falling,” Hum. Mov. Sci., vol. 31, pp. 271–283, 2012.

[4.7] P. M. Mills, R. S. Barrett, and S. Morrison, “Toe clearance variability during walking in young and elderly men,” Gait & Posture, vol. 28, pp. 101–107, 2008.

[4.8] Tamon Miyake, Masakatsu G Fujie, and Shigeki Sugano, “Prediction of Minimum Toe Clearance with a Radial Basis Function Network at the Start of the Swing Phase,” Proceedings of the 40th Annual International Conference of the IEEE Engineering in Medicine and Biology Society (EMBC), pp. 1664 - 1667, 2018.

[4.9] J. P. Scholz and G. Schöner, “The uncontrolled manifold concept: identifying control variables for a functional task,” Exp Brain Res., vol. 126, pp. 289–306, 1999.

[4.10] H. Nakayama, M. Arakawa, and R. Sasaki, “Simulation-based optimization using computational intelligence”, Optimization and Engineering, vol. 3, pp. 201–214, 2002.

Chapter 5

[5.1] J. P. Maxwell, R. S. Masters, F. F. Eves, “The role of working memory in motor learning and performance,” Conscious Cogn. vol. 3, pp. 376-402, Sep. 2013.

[5.2] S.M. Morton, A.J. Bastian, “Cerebellar contributions to locomotor adaptations during splitbelt treadmill walking,” J Neurosci.,vol. 26, pp. 9107–16, 2006.

[5.3] W.T. Thach, H.P. Goodkin, J.G. Keating, “The cerebellum and the adaptive coordination of movement,” Annu. Rev. Neurosci., vol. 15, pp. 403–442, 1992.

Acknowledgement

I would like to extend my most sincere gratitude to my Ph.D. supervisor, Prof. Dr. Shigeki Sugano of the Department of Modern Mechanical Engineering in the Graduate School of Creative Science and Engineering at Waseda University. I also express my thankfulness to my B.S. supervisor, Prof. emeritus Dr. Masakatsu G. Fujie at Future Robotics Organization at Waseda University, for their guidance and encouragement over the last 7 years, and above all, for providing me with this precious research opportunity.

I would like to thank my collaborative researcher, Dr. Yo Kobayashi, Dr. Akira Kato, and Dr. Naomi Okamura. I would also like to thank Dr. Daisuke Kaneishi, Dr. Satoshi Miura, Dr. Yang Cao, and Dr. Mariko Tsukune for their valuable comments on my research. I would also like to thank the researchers, and graduate and undergraduate students of Prof. Fujie's and Prof. Sugano's laboratories. I am also thankful to the other Fujie and Sugano Laboratory members and community members that I am a part of, such as Leading Graduate Program, Waseda University and young researchers in Global Robot Academia, Waseda University, for their comments and encouragement, and their interest in my research.

I would like to thank the secretaries at Fujie and Sugano Laboratory and all the staff at the Leading Graduate Program in Science and engineering, Waseda Univesity, Research Fellowships for Young Scientists, Japan Society for the Promotion of Science, for their continued research support.

I would especially also like to thank my friends and family for enriching my life. I was able to have a great time during my life as a student.

Tokyo, February 2020

Tamon Miyake

Publications list

Journals (Peer-reviewed)

○[1] Tamon Miyake, Masakatsu G Fujie, and Shigeki Sugano, "Prediction Algorithm of Parameters of Toe Clearance in the Swing Phase," Applied Bionics and Biomechanics, Volume 2019, Article ID 4502719, 2019.

○[2] Tamon Miyake, Yo Kobayashi, Masakatsu G Fujie, and Shigeki Sugano, “One-DOF Wire-driven Robot Assisting Both Hip and Knee Flexion Motion,” Journal of Robotics and Mechatronics, Vol.31, No.1, pp. 135-142, 2019.

○[3] Tamon Miyake, Yo Kobayashi, Masakatsu G Fujie, and Shigeki Sugano, “Effect of the Timing of Force Application on the Toe Trajectory in the Swing Phase for a Wire-driven Gait Assistance Robot,” Mechanical Engineering Journal, Vol. 5, No. 4, pp. 17-00660, 2018.

Proceedings of international conference (Peer-reviewed)

[4] Tamon Miyake, Zhengxue Cheng, Satoshi Hosono, Shintaro Yamamoto, Satoshi Funabashi, Cheng Zhang and Emi Tamaki, "Heel-Contact Gait Phase Detection Based on Specific Poses with Muscle Deformation," Proceedings of the 2019 IEEE International Conference on Robotics and Biomimetics (ROBIO), accepted in Nov. 2019.

[5] Namiko Saito, Peizhi Zhang, Tamon Miyake, Shigeki Sugano and Kinji Mori, "A Life-linkage Platform Service Supporting Diverse Lifestyles based on Individual Demands," Proceedings of the 2019 IEEE International Symposium on Autonomous Decentralized Systems (ISADS).

○ [6] Tamon Miyake, Yo Kobayashi, Masakatsu G Fujie, and Shigeki Sugano, "Intermittent Force Application of Wire-driven Gait Training Robot to Encourage User to Learn an Induced Gait," Proceedings of the 2018 IEEE International Conference on Robotics and Biomimetics (ROBIO), pp. 433 - 438, 2018.

[7] Takayuki Nakatsuka, Tamon Miyake, Kotaro Kikuchi, Ayano Kobayashi, Yoshihiko Hayashi, "Analyzing Human Avoidance Behavior in Narrow Passage," Proceedings of the 2018 IEEE International Conference on Systems, Man, and Cybernetics (SMC), pp. 3738 - 3743, 2018.

○[8] Tamon Miyake, Masakatsu G Fujie, and Shigeki Sugano, “Prediction of Minimum Toe Clearance with a Radial Basis Function Network at the Start of the Swing Phase,” Proceedings of the 40th Annual International Conference of the IEEE Engineering in Medicine and Biology Society (EMBC), pp. 1664 - 1667, 2018.

[9] Akira Kato, Haruno Nagumo, Tamon Miyake, Masakatsu G Fujie, and Shigeki Sugano, “Evaluation of Compensatory Movement by Shoulder Joint Torque During Gain Adjustment of a Powered Prosthetic Wrist Joint,” Proceedings of the 40th Annual International Conference of the IEEE Engineering in Medicine and Biology Society (EMBC), pp. 1891 - 1894, 2018.

○[10] Tamon Miyake, Yo Kobayashi, Masakatsu G Fujie, and Shigeki Sugano, “Timing of Intermittent Torque Control with Wire-driven Gait Training Robot Lifting Toe Trajectory for Trip Avoidance,” Proceedings of the 15th IEEE International Conference on Rehabilitation Robotics (ICORR), pp. 320 - 325, 2017.

[11] Satoshi Funabashi, Ryuya Sato, Tamon Miyake, Ryosuke Tsumura and Kinji Mori, "Inverse Innovation: Ripple Railway Model to Acquire Local Industries Based on User’s Viewpoint in Thailand," 2017 IEEE 13th International Symposium on Autonomous Decentralized System (ISADS), Bangkok, pp. 281-286, 2017.

[12] Tamon Miyake, Yo Kobayashi, Masakatsu G Fujie, and Shigeki Sugano, “Relation between Magnitude of Applied Torque during Pre-Swing Phase and Toe Clearance Change to Prevent Trip of Elderly People,” Proceedings of the 2016 IEEE International Conference on Systems, Man, and Cybernetics (SMC), pp. 2448–2453, 2016. (DOI: 10.1109/SMC.2016.7844606).

[13] Tamon Miyake, Mariko Tsukune, Yo Kobayashi, Shigeki Sugano, and Masakatsu G Fujie, “Relationship between Magnitude of Applied Torque in Pre-Swing Phase and Gait Change for Prevention of Trip in Older People,” Proceedings of the 38th Annual International Conference of the IEEE Engineering in Medicine and Biology Society (EMBC), pp. 6154 – 6157, 2016.（DOI: 10.1109/EMBC.2016.7592133).

Presentation in international conference (Peer-reviewed)

[14] Tamon Miyake, Yo Kobayashi, Masakatsu G Fujie, and Shigeki Sugano, “Wire-Driven Gait Training Robot Assisting Both Hip and Knee Motion with One-DOF Intermittent Force Control,” IROS 2017 workshop on Adaptive Control Methods in Assistive Technologies. (peer reviewed)

[15] Tamon Miyake, Mariko Tsukune, Yo Kobayashi, Shigeki sugano, and Masakatsu G. Fujie, “The Influence of Applying Torque in the Pre-swing Phase on the Minimum Toe Clearance for Prevention of Falls in Elderly People,” 2015 JSME International Conference on Advanced Mechatronics, 2A1-08, Nishiwaseda Campus of Waseda University, Tokyo, Japan, December 5-8, 2015.

Presentation in international conference (Non-peer-reviewed)

[16] Ryuya Sato, Tamon Miyake, Satoshi Funabashi, and Kinji Mori, “Innovation of Railway system,” The 3rd International Symposium on Railway System (ISRS) Workshop, Jun 6-11, 2016, Chulalongkorn University, Bangkok, Thailand, Sponsor: IEEE Thailand Section. (no peer review)

[17] Ryuya Sato, Tamon Miyake, Satoshi Funabashi, and Kinji Mori, “Innovation of Railway system,” The 2nd International Symposium on Railway System (ISRS) Workshop, Nov 19-20, 2015, Chulalongkorn University, Bangkok, Thailand, Sponsor: IEEE Thailand Section. (no peer review)

Presentation in domestic conference

[18] 三宅 太文，鈴木 智幸，船橋 賢，亀崎 允啓，荘田 隆博，石居 真， 菅野 重樹，“リチウムイオン電池の等価回路モデル解析による劣化箇所を特定するベイズ推定手法に関する研究”，第 20 回計測自動制御学会システムインテグレーション部門講演会，香川，2019 年 12 月 12－14 日，2019 年

[19] 三宅 太文，小林 洋，藤江 正克，菅野 重樹，“ワイヤ駆動型歩行訓練ロボットによる断続的な 介入による訓練効果の検証 ”，第 37 回日本ロボット学会学術講演会，3C3-03,，東京，9 月 4－7 日，2019 年.

[20] 三宅 太文，小林 洋，菅野 重樹，藤江 正克，"つまずき予防のためのワイヤ駆動型歩行訓練ロボットによる短期的トルク印加手法の構築"，第 56 回日本生体医工学会大会，仙台，2017 年.

[20] 三宅 太文，小林 洋，藤江 正克，菅野 重樹，“歩行訓練ロボット制御のための下肢関節間の協調性に着目した歩容の定量化手法の検討”， 第 32 回ライフサポート学会大会，第 16 回日本生活支援工学会大会，日本機械学会 福祉工学シンポジウム 2016，仙台，9 月 4－6 日 2016 年.

[21] 三宅 太文，築根 まり子，小林 洋，菅野 重樹，藤江 正克，"前遊脚期における膝関節に対する屈曲トルクのつま先高さに及ぼす効果の検証"，日本機械学会ロボティクス・メカトロニクス講演会，横浜，2016 年.（査読なし）

[22] 三宅 太文，築根 まり子，加藤 陽，小林 洋，菅野 重樹，藤江 正克，"高齢者の転倒予防に向けた前遊脚期の膝関節動作入力による歩容変化の関係導出"，バイオメカニズム学会 バイオメカニズム学術講演会 2015，1A-4-3，信州大学上田キャンパス，上田，11 月 28－29 日，2015 年.

Research grant

[23] 日本学術振興会特別研究員　DC2　研究奨励費 2019.04-現在
[24] 公益財団法人立石科学技術振興財団研究助成(C)“高齢者の躓き予防に向けた関節間協調性を高めるワイヤ駆動型歩行訓練ロボットの開発”, 代表, 2017.04-現在